THE PROTECTIVE AND PATHOLOGIC ROLES OF TOLL-LIKE RECEPTORS IN ARTHRITOGENIC ALPHAVIRUS INFECTION

Lauren Michelle Neighbours

A dissertation submitted to the faculty of the University of North Carolina at Chapel Hill in partial fulfillment of the requirements for the degree of Doctor of Philosophy in the Department of Microbiology and Immunology.

Chapel Hill
2013

Approved by:

Mark T. Heise, Ph.D.

Blossom Damania, Ph.D.

Stanley Lemon, M.D.

Steven Bachenheimer, Ph.D.

Nathaniel Moorman, Ph.D.

ABSTRACT

LAUREN NEIGHBOURS: The Protective and Pathologic Roles of Toll-like Receptors in Arthritogenic Alphavirus Infection
(Under the direction of Mark T. Heise)

Arthritogenic alphaviruses, including Chikungunya virus and Ross River virus (RRV), are mosquito-borne pathogens responsible for epidemics of debilitating polyarthritis in humans. The host inflammatory response plays an important role in the pathogenesis of arthritic alphaviruses, where some pathways, such as the complement cascade, exacerbate virus-induced disease, while type I IFN and other immune signaling pathways mediate protection from disease. Using a mouse model of alphavirus-induced arthritis/myositis, we demonstrated that toll-like receptor (TLR) signaling contributes to protection from and enhancement of alphavirus-induced disease. Myd88-dependent TLR7 signaling was critical for protection from severe RRV-induced morbidity and mortality. Additionally, TLR7 deficiency resulted in the production of low affinity, non-neutralizing RRV-specific antibodies that exacerbated virus-induced disease through systemic antibody- and complement-mediated mechanisms. Furthermore, TLR4 promoted RRV-induced morbidity and tissue damage in a complement-dependent manner, and complement-associated macrophage activation was dependent on TLR4 expression during RRV infection. Taken together, these studies establish the integral role that TLR pathways play in arthritic alphavirus pathogenesis.

To my parents, who always encouraged me to pursue my dreams

And provided me every opportunity to do so.

And to Stuart and Evan, who make every day a blessing,

Who remind me what is most important,

And whose love and support are my sanctuary.

ACKNOWLEDGMENTS

I would like to thank all of the individuals who have aided in my professional development and accomplishments during my graduate experience. Firstly to my mentor, Mark Heise, I am so thankful for his continued support and encouragement. In addition to providing valuable advice and guidance during the course of my research, Mark has celebrated every professional success and motivated me through every tribulation that I have encountered throughout my graduate career. I am grateful for the freedom that I was allotted in the laboratory to manage my research project and develop as an independent scientist, but I am also thankful for the constructive criticisms that were necessary for me to reach my full scientific potential.

I would also like to recognize Kristin Long, whose initial observations set the foundation for my dissertation research. Marty Ferris, who taught me several experimental techniques early in my graduate career that were instrumental in my research project, has become a good friend and consultant as a fellow new parent in the lab. Additionally, I am very thankful for the critical feedback that Marty lent on a grant proposal that ultimately led to my successful attainment of a graduate research fellowship. I would like to thank Alan Whitmore for his generous contributions to our lab through his immunological expertise, keen intellect and friendly demeanor. I am also grateful to former laboratory members, including Bonnie Gunn, Alina Lotstein, Jason Simmons, Cathy Cruz, and Lance Blevins, who were valuable resources for experimental input and protocols but also helped to foster an enjoyable work environment. I also have

to thank Bianca Trollinger, Charlie McGee, Adam Cockrell, Charissa Kam, Desi Matthews, Clancy Mullan, Clayton Morrison, and Doug Widman, who have each contributed to the success of our laboratory and have been wonderful colleagues.

Finally, I would like to thank my committee members: Blossom Damania, Steve Bachenheimer, Stan Lemon, and Nat Moorman. I appreciate all of the experimental ideas that they offered me at meetings and seminars to strengthen my research, and I am grateful for their positive feedback and encouragement throughout my graduate tenure. I have had the privilege of looking forward to committee meetings and have scheduled them as often as possible because of their crucial importance to my graduate training and success. I also acknowledge the ASEE and the Department of Defense for funding the National Defense Science & Engineering Graduate Fellowship, which supported three years of my dissertation research.

TABLE OF CONTENTS

LIST OF TABLES

LIST OF FIGURES

LIST OF ABBREVIATIONS

BFV	Barmah Forest virus
CHIKV	Chikungunya virus
CNS	Central nervous system
CPE	Cytopathic effect
DAMP	Damage-associated molecular pattern
DC	Dendritic cell
dsRNA	Double-stranded RNA
EEE	Eastern equine encephalitis
ER	Endoplasmic reticulum
HSP	Heat-shock protein
IFN	Interferon
IkB	Inhibitor of NFκB
IKK	IκB kinase
IPS-1	Interferon promotor stimulator-1
IRF	Interferon regulatory factor
ISRE	Interferon-stimulated response element
ISG	Interferon-stimulated gene
MBL	Mannose-binding lectin

Myd88	Myeloid differentiation primary response gene 88
NF-κB	Nuclear factor kappa B
NSP	Nonstructural protein
PAMP	Pathogen-associated molecular pattern
pDC	Plasmacytoid dendritic cell
PRR	Pattern recognition receptor
RdRp	RNA-dependent RNA polymerase
RLR	Rig-I-like receptor
RRV	Ross River virus
SFV	Semliki Forest virus
SINV	Sindbis virus
ssRNA	Single-stranded RNA
TICAM-1	TIR-domain-containing adaptor molecule 1
TIRAP	TIR-domain-containing adaptor protein
TLR	Toll-like receptor
TRAM	TRIF-related adaptor molecule
TRIF	TIR-containing-adaptor inducing interferon-b
VEEV	Venezuelan equine encephalitis virus
WEE	Western equine encephalitis

CHAPTER ONE:

INTRODUCTION

Overview of alphaviruses

Alphavirus taxonomy

Alphaviruses are positive-sense single-stranded RNA (ssRNA) arboviruses and are members of the family *Togaviridae* (1). The *Togaviridae* family consists of two genera, *Alphavirus* and *Rubivirus*, and 29 of the 30 species of togaviruses are alphaviruses, with Rubella virus being the only identified rubivirus (1). Alphaviruses and other arboviruses were originally grouped according to their antigenicity as determined using various serological and biochemical assays (2). Modern technological advances have expanded the classification of alphaviruses into distinct clades by comparing the genomic sequences of the viral species, which adds a complex genetic and evolutionary dimension to the taxonomy (3).

Alphaviruses are categorized into two groups, Old World and New World, which distinguish the viruses based on their geographic distribution and epidemiological characteristics (3). The Old World alphaviruses, including Ross River virus (RRV), chikungunya virus (CHIKV), and Sindbis virus (SINV), are associated with debilitating arthralgia and myalgia, while New World alphaviruses such as Venezuelan equine encephalitis virus (VEEV), eastern equine encephalitis (EEE) virus, and western equine

encephalitis (WEE) virus induce encephalitis (4, 5). Old World and New World alphaviruses are further segregated into seven distinct antigenic complexes or clades, including the Barmah Forest, Semliki Forest, Venezuelan equine encephalitis (VEE), EEE, WEE, Trocara, Middelburg, and Ndumu clades (1). An overview of alphavirus classification and epidemiology is included in Table 1, which focuses on Old World

Alphavirus taxonomy

Alphaviruses are positive-sense single-stranded RNA (ssRNA) arboviruses and are members of the family *Togaviridae* (1). The *Togaviridae* family consists of two genera, *Alphavirus* and *Rubivirus*, and 29 of the 30 species of togaviruses are alphaviruses, with Rubella virus being the only identified rubivirus (1). Alphaviruses and other arboviruses were originally grouped according to their antigenicity as determined using various serological and biochemical assays (2). Modern technological advances have expanded the classification of alphaviruses into distinct clades by comparing the genomic sequences of the viral species, which adds a complex genetic and evolutionary dimension to the taxonomy (3).

Alphaviruses are categorized into two groups, Old World and New World, which distinguish the viruses based on their geographic distribution and epidemiological characteristics (3). The Old World alphaviruses, including Ross River virus (RRV), chikungunya virus (CHIKV), and Sindbis virus (SINV), are associated with debilitating arthralgia and myalgia, while New World alphaviruses such as Venezuelan equine encephalitis virus (VEEV), eastern equine encephalitis (EEE) virus, and western equine encephalitis (WEE) virus induce encephalitis (4, 5). Old World and New World alphaviruses are further segregated into seven distinct antigenic complexes or clades,

including the Barmah Forest, Semliki Forest, Venezuelan equine encephalitis (VEE), EEE, WEE, Trocara, Middelburg, and Ndumu clades (1). An overview of alphavirus classification and epidemiology is included in Table 1, which focuses on Old World arthritogenic alphaviruses for the purposes of this work and was adapted with permission from Weaver and colleagues (1).

Alphavirus emergence and transmission

Alphaviruses are vector-borne viruses that cause a variety of diseases in humans, other vertebrates, and fish (1). Most alphaviruses are transmitted to their vertebrate hosts by mosquito vectors, and viral transmission is primarily maintained within an enzootic cycle via *Culex* and *Aedes* mosquito species that inhabit humid, marshy regions (1). As depicted in Figure 1.1, the enzootic transmission cycle of alphaviruses allows for maintenance of viral infection in zoonotic reservoir hosts with endemic disease occurring in certain geographic areas (Figure 1.1, which was adapted with permission from Weaver and colleagues)(1). However, alphaviruses also cause sporadic epidemics that can lead to widespread morbidity and mortality in humans (Figure 1.1) (4). Most epidemics involving New World alphaviruses, including VEE, EEE, and WEE viruses, have occurred in South, Central, and North America (5). Alternatively, Old World alphavirus epidemics have occurred in Africa, Asia, and Australia, with cases recently spreading to Europe and the United States after infected individuals traveled to endemic regions (6-8).

Because of the pronounced morbidity and explosive epidemics associated with infections, CHIKV is considered a high-risk emerging pathogen that poses significant global threats to public health (9). The first cases of CHIKV were identified in the 1950s

in Africa, where the virus is believed to have originated, and the virus caused multiple outbreaks through the 1980s in Africa and Southeast Asia (10). However, CHIKV outbreaks have re-emerged and expanded with widespread distribution since 2004, with thousands to millions of infections presenting with persistent debilitating arthraligia and a case fatality rate estimated at approximately 0.1% (1, 11). Additionally, the regions where CHIKV outbreaks tend to occur are also endemic for tropical diseases with similar symptomatic presentations such as dengue virus fever and malaria, and CHIKV infections are thus believed to be grossly underreported (12). Epidemics of CHIKV-like disease, which were characterized as dengue outbreaks but were likely caused by CHIKV, have been traced back as far as the 19th century (13). Moreover, genotyping of viral isolates from the La Réunion outbreak of 2005-2007 identified a mutation in the CHIKV strain that allowed more efficient transmission by *Aedes Albopictus* mosquitoes and resulted in rapid dissemination of the virus (11).

Increasing cases of endemic and epidemic disease induced by other arthritogenic alphaviruses such as RRV and Barmah Forest virus (BFV) have also spurred recent concerns (14). RRV, which results in over 4,000 cases of disease in Australia every year, is considered the most substantial arboviral threat to public health in the Australasian region because of the long-lasting morbidities associated with infections (14, 15). RRV was first isolated in 1959 from mosquitoes found near the Australian Ross River, and it was the causative agent of a 1979 epidemic in the South Pacific that resulted in over 60,000 cases of disease (16). BFV results in approximately 1,000 human cases of disease in Australia each year, with symptoms typically less severe and shorter than those induced by RRV or CHIKV (17). However, the recent rise in BFV infections have

concerned Australian public health authorities, and the growing number of arthritogenic alphavirus cases in the Australasian region results in a considerable economic burden as well (14). Moreover, models of climate change in alphavirus-endemic regions have predicted that alterations in environmental conditions, such as increasing rainfall and temperatures, may result in enhanced alphavirus activity and thus escalate the risk of human infections (14, 18).

Virus organization and life cycle

Alphaviruses are enveloped viruses of approximately 70 nm in diameter and contain an ssRNA genome of approximately 12 Kb in length (19-21). The virion contains a host-derived lipid membrane, which is embedded with heterodimeric trimer spikes formed by the highly glycosylated E1 and E2 viral glycoproteins (22). Within the membrane-bound virion is an icosahedral nucleocapsid, which is formed by the viral capsid proteins. The alphavirus genome encodes two open reading frames, from which the four nonstructural proteins (NSPs) are encoded from the genomic RNA and the five structural proteins are encoded from the 26S subgenomic strand (23). The genomic and subgenomic RNA species contain a 5' methylguanosine cap and 3' polyadenylated tail, and each strand is initially translated into polyproteins before being cleaved posttranslationally by viral and host proteases. A simplified schematic of the alphavirus genome, which was adapted with permission from Weaver and colleagues, can be found in Figure 1.2 (1).

Entry of alphaviruses is generally considered to occur via clathrin- and receptor-mediated endocytosis, although reports of entry via direct viral fusion with the plasma

membrane have also been reported (23). Upon receptor-mediated endocytosis of the virion, viral uncoating occurs to allow for the release of alphavirus ssRNA into the cytoplasm. The initial translation of the viral RNA, which is infectious upon entry, results in the formation of the NSP polyprotein, NSP1234 and structural polyproteins (24). Cleavage of NSP1234 into NSP123 and NSP4 allow for the formation of the replication complex, which synthesizes the negative strand RNA, and complete cleavage of the nonstructural proteins allows for the complete stable replication complex to be formed and initiates positive full-length and subgenomic RNA synthesis (23). Cleavage of the structural polyprotein releases the capsid protein, which associates with the newly transcribed viral RNA and facilitates packaging of the RNA into nucleocapsid vesicles (25). A signaling sequence on the E3 protein facilitates the relocation of the remaining structural polyprotein to relocate and bud into the endoplasmic reticulum (ER) for further processing by host proteases, while 6K facilitates downstream processing of the E1 glycoprotein and aids in viral budding (23). E1 and E2 interact shortly after synthesis to form dimers, which are transported from the ER-Golgi complex to the host plasma membrane (26). The nucleocapsids formed in the cytoplasm can then bud into the host membrane containing E1-E2 spikes and release envelope-containing particles (22).

In addition to their roles in replication and structural formation, alphavirus proteins are also involved in viral pathogenesis. NSP1, which mediates capping and methylation of viral RNA, regulates host inflammatory responses to alphavirus infection (22, 27, 28). Mutations in NSP1 of RRV resulted in reduced tissue damage in infected mice, and a virulence determinant within RRV and SINV was demonstrated to modulate type I interferon (IFN) responses and disrupt JAK/STAT signaling (27-29). NSP2, which

has numerous enzymatic activities and functions, performs multiple roles during replication and packaging but also mediates cellular cytopathic effects (CPE), induces host shut-off and antagonizes type I/II type I IFN induction during infection (30-33). Additionally, the use of NSP2 as an adjuvant in a CHIKV DNA vaccine enhanced protection of mice challenged with CHIKV when compared to mice immunized with the vaccine alone (34). Little is known about the functions of NSP3, which is required for RNA synthesis (22). However, NSP3 plays a role in neurovirulence and in the suppression of stress granule formation, and it may also influence vector specificity (35-38). The viral RNA-dependent RNA polymerase, NSP4, is proposed to have multiple functions during RNA replication and was recently reported to modulate the host translational machinery to enable more efficient replication during CHIKV infection (22, 39). Aside from their roles in virus entry and assembly, the structural proteins are also important mediators of viral pathogenesis. The precursor E2 protein is involved in RRV-induced inflammatory disease, while the glycans on the E1 and E2 glycoproteins modulate type I IFN production and mediate pathogenesis during RRV infection [(27, 40), Gunn and Heise, unpublished].

1.1 Human infection and animal models of disease

Pathogenesis of human arthritogenic alphavirus infection

Most human infections with Old World alphaviruses such as CHIKV and RRV result in mild "flu-like" symptoms of fever, headache, rash and malaise that usually dissipate within a week (15). However, a significant subset of infected individuals

develop a debilitating polyarthralgia and myalgia that can last for several months and in rare cases can induce chronic disease or mortality (41, 42). Chikungunya virus, which is named for the Makonde Tanzanian term for "that which bends up," is considered the most threating arthritogenic alphavirus to global public health because of its capacity to induce catastrophic epidemics and persistent disease (43). Severe cases of arthritogenic disease tend to occur in individuals with chronic underlying conditions such as diabetes or impaired kidney function or in patients that have adverse reactions to therapeutic drug treatment (43). Chronic pain associated with arthritogenic alphavirus infection can significantly impact the quality of life of infected individuals and results in a substantial economic burden in affected regions because of prolonged care and decreased productivity (14, 44, 45).

The incubation period of the virus is usually between 2-14 days prior to the onset of symptoms, with a viremia that lasts approximately 5-7 days (1, 15). The virus replicates in skeletal muscle and joint tissues during the acute infection, although RNA and viral proteins were found in various tissues and synovial macrophages for several weeks to months following the resolution of viral replication (41, 46). The pathology induced by arthritogenic alphavirus infection is believed to be mediated by host inflammatory responses induced by viral replication or viral products, although these are not considered autoimmune responses (15).

Although relatively rare, mother-to-child transmission can occur with CHIKV infection (42). A prospective study, which was conducted to determine the prevalence of CHIKV vertical transmission following the La Réunion outbreak in 2005, found that approximately 10% of the neonates were exposed to CHIKV during pregnancy, and 2.5%

of the exposed neonates became infected with CHIKV (47). All of the infected neonates developed symptoms of infection shortly after birth, and more than half of the infected neonates developed severe neurological disease including encephalopathy and persistent neurodevelopmental disabilities. Transmission rates of CHIKV were highest in mothers that were infected very late during pregnancy, although infection may have contributed to early fetal deaths that were also observed.

There are currently no effective treatments or vaccines available for arthritogenic alphavirus infections. The current treatment regimen typically consists of treatment with non-steroidal anti-inflammatory drugs (NSAIDs) and/or steroids (41, 42). Anti-rheumatic drugs, including methotrexate, salazopyrine, leflunomide, and hydoxychloroquine, and tumor necrosis factor alpha (TNFα) inhibitors, have shown varying efficacy in patients with chronic disease following CHIKV infection (48). Additionally, long-term and combinatorial drug treatments for severe or persistent arthritogenic alphavirus infections can lead to adverse side effects such as gastrointestinal bleeding and bone deterioration in affected patients (15, 41, 42).

Animal models of arthritogenic alphavirus-induced disease

To better understand the mechanisms of arthritogenic alphavirus pathogenesis, several animal models were generated to study the effects of infection in the laboratory. Intracranial infections of neonatal mice were used to study mortality and brain pathology following CHIKV and Semliki Forest virus (SFV) infections, while intranasal infections of CHIKV were used to study the effects of localized histological damage and viremia in mice (49). Some mouse models of SINV pathogenesis aimed to study the arthritic effect of the virus, although most SINV studies utilize the encephalitic model to study the

effects of SINV infection on neurological pathogenesis (50). More common models to study viral pathogenesis include subcutaneous infections into the footpads of C57BL/6 mice to study RRV- and CHIKV-induced inflammation and tissue damage (51-54).

The mouse model of RRV pathogenesis utilized by Morrison and colleagues was the model used in the studies described in this work (53). This model of alphavirus-induced arthritis/myositis involves a subcutaneous infection of 1000 PFU of RR64, an infectious clone of the T48 mouse-adapted strain of RRV, into the left-rear footpad of a twenty-four day old C57BL/6 mouse (53, 55). Over the course of infection, RRV-infected mice show transient weight loss and develop disease characterized by hind limb weakness and altered gait (depicted in Figure 1.3, which is modified from Morrison and colleagues)(53). The clinical disease in these mice peaks in severity between 7-10 days post-infection, after which mice recover their hind limb function and are indistinguishable from mock-infected animals by 30 days post-infection.

The disease induced by this RRV model can be further segregated into three distinct phases by histologically examining the skeletal muscle of RRV-infected animals over the course of infection because skeletal muscle is a target tissue for replication and pathology during infection (Figure 1.3) (53). The first phase of infection between 3-5 days post-infection is the initiation/recruitment phase, during which time the initial recruitment of inflammatory cells into the tissue is visible, but the skeletal muscle fibers remain intact. The second phase of the disease is the tissue destruction phase, wherein there is substantial inflammatory infiltration and destruction of the skeletal muscle tissue. The inflammatory infiltrate is primarily monocytic, consisting mainly of monocytes, macrophages, and NK cells (53). The final phase of the disease is the resolution/repair

phase, wherein the inflammation resolves, and the muscle fibers repair. Notably, peak viral replication in the tissues occurs between 24-48 hours post-infection, suggesting that the disease correlates with inflammatory infiltration and not with viral replication (53). Additionally, numerous studies using the RRV mouse model have demonstrated the roles of innate immune components, including macrophages and complement, in mediating RRV-induced disease (51, 56-60).

Several treatment therapies and vaccine approaches are efficacious in animal models. Because macrophages are critical mediators of RRV-induced disease, some therapies focused on targeting this cellular population to ameliorate the disease (51, 56, 57). Treatment of RRV-infected mice with bindarit, an inhibitor of monocyte chemotactic protein synthesis, resulted in significantly reduced tissue inflammation and damage compared to untreated mice (61). Additionally, a recent study showed complete protection from CHIKV challenge in mice immunized with a recombinant adenoviral vaccine, while another report demonstrated that a synthetic DNA vaccine protected mice and non-human primates from CHIKV-induced disease and elicited protective neutralizing antibody responses (62, 63). Mouse models of arthritogenic alphavirus-induced disease provide important insights into the pathogenesis of Old World alphavirus infection and remain important tools for testing and discovering potential therapeutics for the associated diseases.

1.2 Toll-like receptor signaling

Overview of toll-like receptors

Toll-like receptors (TLRs) are innate immune receptors that recognize conserved microbial patterns on the surface of pathogens such as viruses, fungi, parasites, and bacteria (64). TLRs are a class of pattern recognition receptors (PRRs), which are classified as such because they recognize specific pathogen-associated molecular patterns (PAMPs) that enable the receptor to identify the microbe as foreign and initiate an immune response. Other PRRs include the RIG-I-like receptors (RLRs) and Nod-like receptors (NLRs), and these PRRs signal exclusively from the cytosol. PRRs are expressed on a variety of immune cells, including phagocytic macrophages and dendritic cells (DCs), which use these receptors as a first line of defense against invading pathogens (65).

The basic structure of TLRs consists of a leucine-rich repeat extracellular domain, a membrane-spanning region and an intracellular region containing a Toll/interleukin-1 receptor (TIR) domain (66). The binding of the horseshoe-shaped extracellular domains of TLRs by their specific PAMP-containing ligands induces a conformational change in the receptors and the accompanying dimerization of their extracellular domains. Interactions between the TIR domains of the intracellular regions of the TLRs are then believed to recruit specific TIR domain-containing adaptors to the activated receptors. It is postulated that activated TLRs may undergo higher order clustering with other TLRs, which would presumably allow for more efficient downstream signaling and activation (67, 68). X-ray structures reveal the TLR extracellular and intracellular domains of the

receptors in their monomeric forms, although multimeric and clustered forms of TLRs in their native transmembrane conformation are not available (66).

Upon recognition of a PAMP via receptor complex engagement, TLRs signal to their downstream adaptor molecules to activate a downstream signaling cascade that will lead to the appropriate immune response to the invading pathogen (64). The TLR-induced signaling cascade leads to the activation of specific transcription factors, which can then induce the expression of various genes, such as pro-inflammatory cytokines, type I IFN, and IFN-stimulated genes (ISGs) (65). An overview of TLR signaling is depicted in Figure 1.4, which was adapted from Kawai and Akira with permission (69).

TLR signaling is modulated by the specificity of the TLR ligands and by the cellular localization of the receptors, which can affect ligand accessibility and downstream signal transduction. Based on these specific criteria, TLRs can be segregated into two groups: group A consists of TLRs 1, 2, 4, 5, 6 and 11, while group B consists of TLRs 3, 7, 8 and 9 (64). Group A TLRs are primarily localized to the plasma membrane except for TLR4, which can also be localized to endosomal compartments. Group B TLRs are localized to intracellular vesicles such as endosomes, lysosomes, endolysosomes, and the ER. With regards to PAMP sensing, Group A TLRs recognize a range of lipids and other microbial membrane components, while Group B TLRs recognize nucleic acids. This section will provide more in-depth background on TLR4 and TLR7 because of their relevance to the studies discussed in this work. A description of the known human and murine TLRs, along with their ligands and adaptors, was adapted with permission from Li et al. and can be found in Table 1.2 (70-74).

TLR4, which recognizes bacterial lipopolysaccharide (LPS), fungal mannans, and other microbial components, the chemotherapeutic drug, Taxol, and several endogenous molecules, is localized to both the cellular plasma membrane and to endocytic vesicles (64, 75-77). At the plasma membrane, TLR4, in complex with MD-2, signals through the adaptor molecule myeloid differentiation primary response gene 88 (Myd88), as well as the adaptor Mal/ TIR-domain-containing adaptor protein (TIRAP), within the Myd88-dependent pathway. However, TLR4 also signals through a Myd88-independent pathway in endocytic vesicles, and this pathway recruits the adaptor molecules, TRIF-related adaptor molecule (TRAM) and TIR-containing-adaptor inducing interferon-b (TRIF)/TIR-domain-containing adaptor molecule 1 (TICAM-1). The Myd88-dependent TLR4 pathway leads to the activation of nuclear factor kappa B (NF-κB) through the phosphorylation and release of its inhibitory factor, IκB, by IκB kinases (IKKs) (78). The liberated NF-κB can then translocate into the nucleus and initiate pro-inflammatory cytokine gene expression. The TRAM/TRIF-dependent TLR4 pathway leads to NF-κB activation and interferon regulatory factor (IRF)3 serine phosphorylation, after which both transcription factors can transverse the nucleus to bind their respective promoters and commence gene transcription (64, 79). The activation of NF-κB and IRF3 signaling pathways lead to pro-inflammatory cytokine and type I IFN induction, respectively (65). TLR4 is expressed on a variety of immune cells, including macrophages, DCs, neutrophils, eosinophils, mast cells, B and T lymphocytes, and can be induced in a variety of non-professional tissues (75, 80-84).

TLR7, which is located on the X chromosome, is found exclusively within intracellular compartments and interacts with the membrane protein UNC93B to facilitate

signaling (64, 85). TLR7 recognizes viral ssRNA and synthetic ligands such as the imidazoquinoline derivatives, imiquimod and R848/resiquimod (86). Recognition of TLR7-specific PAMPs leads to the activation of Myd88-dependent signaling pathways, resulting in IRF7 and NF-κB activation. Serine phosphorylation of IRF7 leads to its translocation into the nucleus wherein it can bind to IFN-α and -β gene promoters and initiate the expression of Type I IFN genes, while NF-κB activation initiates pro-inflammatory cytokine induction (64, 79). Plasmacytoid DCs (pDCs) preferentially express high levels of TLR7 and secrete type I IFN, particularly IFN-α, following TLR7 activation (87). However, TLR7 signaling plays important and distinct roles in other immune cells such as myeloid DCs, eosinophils, macrophages, and B and T lymphocytes (75, 80, 82, 83).

Toll-like receptor signaling during viral infection

The role of toll-like receptors in antiviral immunity is well-documented and established in the literature (88). One of the most important roles of TLRs during viral infection is to induce type I IFNs and other pro-inflammatory cytokines to stimulate an antiviral response in the host. Stimulation of TRIF-dependent signaling cascades via TLR3 or TLR4 activation lead to IRF3 phosphorylation and early IFN-β production during viral infection (79). Myd88-dependent TLR signaling leads to type I IFN production via IRFs and leads to pro-inflammatory cytokine production via NF-κB (65). One of the earliest producers of type I IFN during viral infection are pDCs, which express high levels of TLRs 7 and 9 and mediate IFN production through these TLR sensing pathways (87, 88).

Intracellular nucleic acid-sensing TLRs, including TLRs 3, 9 and 7, may recognize viral nucleic acids through multiple mechanisms during infection (65). The first mechanism through which intracellular TLRs may recognize viral nucleic acids is through direct recognition following endocytosis of the virion. Because of the highly acidic and enzymatic environment within endocytic compartments (such as lysosomes), the endocytosed viral particle may become damaged within the endosome, which could lead to the release of nucleic acid into the vesicle and result in TLR engagement. An alternative mechanism of intracellular TLR activation could be through the uptake of virally infected cells by phagocytes. Nucleic acid-containing viral capsids from apoptotic cells may be trafficked to lysosomal compartments in the phagocytes wherein the capsids can be degraded to release the viral RNA or DNA for TLR activation (65).

TLR3 and TLR9, which recognize double-stranded RNA (dsRNA) and DNA respectively, have been reported to recognize a variety of RNA and DNA viruses (88). Activation of TLR7 signaling has been observed during infections with multiple RNA viruses, including influenza virus, West Nile virus, HIV, Friend virus, vesicular stomatitis virus, yellow fever virus, lymphocytic choriomeningitis virus, and murine pneumonia virus (89-95). In addition to mediating antiviral immunity via type I IFN induction, TLR7 has recently been shown to play an important role in adaptive immune responses to viral infection (88). Indirect effects of TLR7 signaling via type I IFN and cytokine production influences T cell differentiation, and TLR7 expression in B cells is critical for generating protective antibody responses to multiple viral infections (80, 82, 96). Moreover, the TLR7 agonist imiquimod, which induces IFN-α and pro-inflammatory cytokine production through TLR7 signaling, has shown efficacy in the treatment of human

papillomavirus-induced genital warts by enhancing antigen presentation and promoting antigen-specific T helper type 1 (Th1) cell-mediated immune responses (97).

The mechanisms through which plasma membrane-expressed TLRs are activated during viral infection are not well defined. Evidence suggests that certain viral proteins, including viral envelope glycoproteins, can serve as TLR ligands during infection (88). TLR2 has been implicated to recognize a variety of viral proteins, and TLR4 has been implicated to recognize mouse mammary tumor virus (MMTV) and respiratory syncytial virus (RSV) envelope proteins (88, 98-102). MMTV-mediated activation of TLR4 leads to IL-10 production, which promotes an anti-inflammatory response during infection and prevents viral clearance (100). TLR4 signaling also plays protective and pathologic roles in a variety of viral infections, including KSHV, hepatitis C virus, influenza virus, hantaan virus, and Chandipura virus, although the mechanism of TLR4 recognition of these viruses has not been reported (103-108). TLR4-mediated cytokine induction mediates inflammatory cell infiltration and activation at the sites of infection, and TLR4 agonists have shown efficacy in promoting protective antibody responses to viral vaccines (64, 96).

The role of toll-like receptors in autoimmunity and arthritis

In addition to mediating immune responses to microbial pathogens, TLRs recognize and become activated in response to a range of host molecules, which can lead to the development of autoimmune disorders (109). The expression of TLRs 2, 4, and 9 correlate with the development of type I diabetes mellitus, while multiple studies demonstrate that TLR7 and TLR9 mediate systemic lupus erythematosus through the

production of autoantibodies (109, 110). Moreover, the expression of multiple TLRs is elevated in rheumatoid arthritis patients (109).

Because of its ubiquitous expression in immune cells and non-professional tissues and its ability to recognize a wide range of ligands, TLR4 is implicated in the development of multiple autoimmune conditions (75, 109). In addition to recognizing bacterial LPS and other PAMPs, TLR4 has been shown to recognize several endogenous molecules that can trigger immune responses in the presence or absence of infection (75). TLR4 recognizes several damage-associated molecular patterns (DAMPs) such as heat-shock proteins (HSPs), which are produced following exposure to various environmental stress conditions (111-113). Heparan sulfate proteoglycans, hyaluronic acid oligosaccharides, fibrinogen, oxidized lipoproteins, and saturated fatty acids also induce TLR4 activation in mice and macrophages (114-118).

Besides its potential roles in diabetes, inflammatory bowel disease, multiple sclerosis, and cancer, multiple studies demonstrate that TLR4 signaling plays a pathologic role in human and mouse models of arthritis (109, 119-127). The predominant mechanism of TLR4-mediated disease in arthritis and other autoimmune disorders is through its role in exacerbating local and systemic inflammation, which has led to the development of several TLR4 antagonists that are currently undergoing clinical trial evaluation (128). Additionally, TLR4 is stimulated by the myeloid inflammatory calgranulins, s100A8 and s100A9, which can promote autoreactive CD8+ T cell activity and are expressed in a TLR4-dependent manner in osteoarthritis patients and juvenile idiopathic arthritis (129-133). Moreover, the expression of TLRs 2, 3, 4 and 7 were

enhanced in the synovial fluid of rheumatoid arthritis patients, suggesting that multiple TLRs may function in the development of arthritic diseases (109, 134).

1.3 Host response to alphavirus infection

Type I/II IFN responses to infection

Several immune pathways are implicated in the host response to alphavirus infection. Because of their critical roles in antiviral immunity, the type I and II IFN pathways are widely studied in the context of alphaviruses (135-139). The induction of type I IFN is critical for early control of viral replication following Old World and New World alphavirus infection in mice, while type I (IFN-α and –β) and type II (IFN-γ) IFN responses influence adaptive immune responses to infection (135). Type I IFN receptor (IFN-α/βR)-deficient mice, which are unable to respond to type I IFN, rapidly succumb to infection with mutant SINV, VEEV, and SFV strains that are avirulent in wild-type (WT) mice (137, 138, 140). Moreover, IFN-α/βR-deficient mice show an inability to control viremia following CHIKV infection and also succumb rapidly to virus-induced disease (139, 141). Treatment with IFN-α or IFN-γ also demonstrates potent antiviral activity against alphavirus-induced CPE in cell culture, and antibody-mediated inhibition of type I IFN results in enhanced VEEV replication in macrophages (142, 143). Signal transducer and activator of transcription 1 (STAT1)-deficient mice, which are unable to mount positive feedback amplification of type I IFN, show diminished type I IFN responses and enhanced lethality following alphavirus infection (141, 144, 145). Regarding the adaptive arm of the immune response, type I IFN is required for efficient lymphocyte activation

during SFV infection, and the induction of type I IFN is dependent on viral replication (140, 146). Furthermore, IFN-γ-deficient mice show increased susceptibility to SFV-induced mortality and succumb to infection between 7-10 days post-infection, suggesting that IFN-γ is necessary for stimulating protective adaptive immune responses to alphavirus infection (147).

Because IRFs mediate type I IFN and inflammatory gene induction, IRF-dependent gene transcription is essential for protective antiviral responses during alphavirus infection. Both IRF3 and IRF7 are required for efficient type I IFN signaling during viral infection, with IRF3 responsible for initial type I IFN responses and IRF7 required for late IFN-α/β transcription (148). IFN induction via IRF3 and IRF7 activation pathways are required for protection against CHIV-induced mortality in mice, and mice deficient in both IRF3 and IRF7 succumb to fatal CHIKV infection despite robust IFN-γ responses (149, 150). IFN-α induction is mediated by IRF7 following neurovirulent SINV infection in microglial cultures (149, 151). Furthermore, protection from WEEV cytopathology is dependent on IRF3-mediated type I IFN responses in mice. (152). Other IRFs such as IRF-1 and IRF-2 may also be important in protection from alphavirus-induced disease because mice deficient in these IRFs showed increased susceptibility to VEEV replication and virus-induced pathology (143).

Alphavirus infection induces the expression of an array of antiviral genes, including interferon-stimulated genes (ISGs) (135, 142, 153-156). ISG15 is critical for controlling SINV and CHIKV infections, and virus-induced expression of ISG15 protects IFN-α/βR-deficient mice from lethal SINV infection (157-159) Furthermore, mice lacking RSAD2, which encodes the ISG viperin, showed increased viremia and virus-

induced pathology during CHIKV infection compared to WT mice (160). Expression of the human MxA protein confers resistance to SFV replication *in vitro*, and bone marrow stromal antigen 2 (BST-2) reportedly functions to antagonize CHIKV infection by retaining progeny viral particles on the surface of the host cell (161, 162). Additionally, the ISG PARP inhibited the replication of multiple alphaviruses, including VEEV, SINV, and CHIKV, and expression of the IFN-induced 2', 5'-Oligoadenylate Synthetase (OAS)3 inhibited CHIKV replication in cell culture (163, 164). Moreover, data suggests that the zinc finger antiviral protein (ZAP), which attenuates SINV virulence in neonatal mice, synergizes with multiple ISGs to mediate alphavirus inhibition (156, 165).

Because of the important roles of IFN in controlling viral replication and modulating adaptive immune responses during alphavirus infection, Old World and New World alphaviruses have developed mechanisms of IFN inhibition to allow for the establishment and dissemination of infection (31, 166). Old World alphaviruses, including SFV, CHIK, and SINV, utilize mechanisms of transcriptional and translational shutoff to block IFN induction during infection (31-33). The NSP2 proteins of CHIKV, SFV, and SINV induce transcriptional shutoff by mediating ubiquitination of Rbp1, a catalytic subunit of the RNA polymerase II complex (167). Alphaviruses also mediate shutoff-independent mechanisms of IFN inhibition by blocking STAT phosphorylation, thereby preventing amplification of type I and II IFN responses (29, 32, 135, 168, 169). Moreover, alphaviruses may target the downstream effects of IFN by inhibiting ISGs. The NSP1 of CHIKV has been shown to actively antagonize the antiviral function of BST-2 by downregulating BST-2 expression, and there may be other ISGs targeted by alphaviruses as well (161).

Immunopathology associated with alphavirus infection

The immune-mediated pathology associated with alphavirus infection is well-characterized (15, 136, 170). Arthritogenic alphaviruses such as RRV and CHIKV induce severe myositis and arthritis in humans that correlate with host inflammatory responses and persist in the absence of active viral replication (15, 46). Gene profiling reveals that CHIKV-induced arthritis generates a similar gene expression signature to rheumatoid arthritis and collagen-induced arthritis, indicating that the host inflammatory pathways induced by these arthritides overlap (171). Additionally, the host complement pathway promotes RRV-induced morbidity and tissue damage in mice, although complement reportedly functions to limit neuropathology during encephalitic alphavirus infection (53, 59, 60, 172-174). Evidence also suggests that macrophages contribute to arthritogenic alphavirus pathogenesis (15). Depletion of macrophages or macrophage-dependent factors results in significantly reduced inflammation and tissue destruction following RRV infection, and mice treated with Bindarit, an inhibitor of monocyte chemotactic protein-1 (MCP-1), show significantly reduced disease following RRV or CHIKV infection (51, 57, 61, 175, 176). Alphavirus-associated immunopathology is not limited to arthritogenic alphaviruses, however, because depletion of NK cells resulted in a delayed mean time to death following SFV infection, and NK cell-induced immunopathology is mediated by the granule-exocytosis and Fas cytotoxic pathways (147).

The role of pattern-recognition receptors during infection

PRRs, which recognize and respond to viral PAMPs through the induction of IFN and pro-inflammatory cytokines, also mediate antiviral signaling during alphavirus infection. The RLR helicases, RIG-I and MDA5, are implicated in mediating antiviral

responses to alphavirus infection (165, 177, 178). MDA-deficient macrophages show slightly impaired IFN-α production following SINV infection, and both RIG-I and MDA5 can mediate a synergistic effect with the ISG ZAP to induce antiviral activity against SINV *in vitro* (165, 179). However, because RIG-I-deficient mice are embryonic lethal or die shortly after birth, it is unclear whether the antiviral activity of RIG-I during alphavirus infection is biologically relevant *in vivo* (180). IPS-1, which is an adaptor for MDA5 and RIG-I, mediates IRF-dependent type I IFN and antiviral gene transcription during CHIKV infection (150, 181). Additionally, mice deficient in IPS-1 succumb to avirulent SINV infection, and CHIKV-infected IPS-1-deficient mice show increased viremia and increased foot swelling compared to WT mice (150, 182). Another cytoplasmic RNA sensor, the double-stranded RNA-binding protein kinase R (PKR), induces type I IFN and regulates IFN-α/β mRNA stability during SFV infection (183). Moreover, SINV infection induces translational shutoff via PKR-dependent and PKR-independent mechanism *in vitro*, suggesting a role for multiple PRRs in the host response to alphavirus infection (184).

There is also evidence that host c-type lectin receptors (CLRs), which recognize viral glycans, also regulate the host response to alphavirus infection. Alphavirus glycoproteins, E1 and E2, are N-linked glycosylated, and the viral glycosylation patterns are dependent on the species within which the virus is propagated (1). Type I IFN expression during alphavirus infection is modulated by differential glycosylation patterns between mosquito- and mammalian-derived viruses, and mutations in SINV N-linked glycans results in altered viral infectivity and virulence in mice (40, 185, 186). Additionally, human monocytic THP-1 cells become permissive to SINV replication

when they express the CLRs DC-SIGN or L-SIGN, suggesting that DC-SIGN or L-SIGN may facilitate SINV entry into host cells (187). The complement-dependent activity of the soluble CLR, mannose binding lectin (MBL), promotes RRV-induced disease in mice and correlates with severe RRV-induced disease in humans (60). Furthermore, mice deficient in the dendritic cell immune receptor (DCIR), a CLR that negatively regulates the host inflammatory response, showed increased morbidity and tissue damage following CHIKV infection, suggesting that DCIR plays a protective role in regulating the inflammatory response to CHIKV (188).

There is limited data regarding the role of TLRs in alphavirus infection. The TLR adaptor, Myd88, protects CHIKV-infected mice from significant viral dissemination during infection (141). Although Myd88-deficient mice do not show enhanced disease as indicated by foot swelling during CHIKV infection, TRIF-deficient mice show increased serum viremia and enhanced foot swelling compared to WT mice, suggesting that a TRIF-dependent, Myd88-independent TLR pathway may contribute to protection from severe CHIKV-induced disease (150). Treating cells with the TLR3 agonist, Poly (I:C), inhibits CHIKV replication through TLR3-dependent antiviral responses (189). Although TLR3- and Myd88-deficient mice show similar phenotypes to WT mice following neurovirulent SINV infection, TRIF-deficient mice show increased susceptibility to SINV-induced mortality, suggesting that perhaps TRIF-dependent TLR signaling may contribute to protection from SINV-induced neurologic disease (144, 151, 182).

1.4 Dissertation objectives

Despite significant contributions to the understanding of the host response to alphavirus infection, many of the signaling pathways and mechanisms underlying alphavirus pathogenesis remain poorly defined. As mentioned in the previous discussion, IRF-mediated IFN induction is required for protection from alphavirus-induced disease, and some studies have reported that IPS-1 contributes to IRF activation. However, it is unclear which PRRs are required for effective antiviral responses during alphavirus infection *in vivo*, and the mechanisms by which PRRs mediate inflammatory responses to alphavirus infection have not been reported. In particular, the role of TLRs during alphavirus infection is largely undefined. Furthermore, the host pathways that contribute to immune-mediated pathology during arthritogenic alphavirus infection are poorly understood. Although macrophages and complement activation mediate RRV-induced disease, it is unclear whether other cell types or pathways contribute to arthritogenic alphavirus pathogenesis.

Our primary goal in these studies was to further elucidate the host pathways underlying arthritogenic alphavirus infection. Specifically, we aimed to 1) determine whether TLRs were important host factors in the response to arthritogenic alphavirus infection and if so, 2) determine the mechanism(s) of TLR-mediated protection or enhancement of arthritogenic alphavirus-induced disease. We initially tested whether the central TLR signaling adaptor, Myd88, played any role in the host response to RRV infection and found that Myd88 mediated protection from severe RRV-induced morbidity and mortality. We also found that Myd88-dependent protection from severe RRV-

induced disease was dependent on TLR7, and we demonstrated that Myd88-dependent TLR7 deficiency resulted in a failure to control viral replication late during infection that correlated with a loss in protective virus-specific antibody responses. Moreover, we found that mice deficient in TLR7 or Myd88 showed antibody- and complement-dependent disease in both skeletal and cardiac muscle tissue. Because of its demonstrated roles in viral infections and arthritic diseases, we also tested whether TLR4 contributed to arthritogenic alphavirus-induced disease in a mouse model of RRV arthritis/myositis and found that TLR4 promoted RRV-induced morbidity and tissue damage in a complement-dependent manner. Additionally, we demonstrated that complement-dependent macrophage activation during RRV infection was dependent on TLR4 expression. Taken together, these findings demonstrate that TLRs contribute to protection from and enhancement of arthritogenic alphavirus infection. The aims addressed herein are:

Aim 1: To determine the cell types involved in mediating TLR-induced pathogenesis during RRV infection.

Aim 2: To determine whether TLRs and complement activate the same signaling pathways to induce pathogenesis during RRV infection.

Aim 3: To determine the signaling pathways upstream and downstream of TLR7 activation involved in protection from RRV-induced disease.

Table 1.1: Alphavirus classification and epidemiology

	ANTIGENIC COMPLEX	SPECIES	CLINICAL SYNDROME	DISTRIBUTION
OLD WORLD	Barmah forest	Barmah Forest (BFV)	Febrile illness, rash, arthritis	Australia
	Middelburg	Middelburg (MIDV)	None recognized	Africa
	Ndumu	Ndumu virus (NDUV)	None recognized	Africa
	Semliki forest	Semliki Forest (SFV)	Febrile illness	Africa
		Chikungunya (CHIKV)	Febrile illness, arthralgia, rash	Africa, Asia
		O'nyong-nyong (ONNV)	Febrile illness, arthralgia, rash	Africa
		Getah (GETV)	None recognized	Asia
		Bebaru (BEBV)	None recognized	Malaysia
		Ross River (RRV)	Febrile illness, arthralgia, rash	Australia, Oceania
		Mayaro (MAYV)	Febrile illness, arthralgia, rash	South America, Trinidad
		Una (UNAV)	None recognized	South America
	Western equine encephalitis (WEE)	Sindbis (SINV)	Febrile illness, arthralgia, rash	Africa, Europe, Asia, Australia
NEW WORLD		WEEV	Febrile illness, encephalitis	Western North, South America
	Venezuelan equine encephalitis (VEE)	VEEV	Febrile illness, encephalitis	North, Central, South America
	Eastern equine encephalitis (EEE)	EEEV	Febrile illness, encephalitis	North, Central, South America
	Trocara	Trocara (TROV)		South America
OTHER	Salmon pancreas disease	Salmon pancreas disease (SPDV)	Pancreatic disease (salmon), sleeping disease (trout)	Atlantic Ocean and tributaries, Europe
	Southern elephant seal	Southern elephant seal (SESV)	None recognized	Australia

Table 1.2: TLR overview

TLRs	Exogenous ligands	Potential endogenous ligands	TLR adaptor(s)
TLR1	Tri-acyl lipopeptide (Bacteria and mycobacteria)		Myd88 & TIRAP
TLR2	PGN, Lipoteichoic acid (Gram-positive bacteria)	HSPs	Myd88 & TIRAP
	Lipoarabinomannan (Mycobacteria)	HMGB1	
	Glycoinositolphospholipids (Trypanosomes)	Biglycan	
	Glycolipids (Treponema)	EDN	
	Porins (Neisseria)		
	Zymogen (Fungi)		
	Atypical LPS (Gram-negative bacteria)		
	Lipoprotein/Lipopeptides		
TLR3	Double-stranded RNA (Virus)	mRMA	TRIF
TLR4	LPS (Gram-negative bacteria)	HMGB1	Myd88 & TIRAP; TRAM & TRIF
	Taxol (Plant)	HSPs	
	Fusion protein (RSV)	Fibronectin extra domain A	
	Envelope proteins (MMTV)	Minimally modified-low-density-lipoprotein	
	Hsp60 (Chlamydia pneumoniae)	Hyaluronan fragments	
	Hyphae (Aspergillus)	Heparan sulfate	
	Pertussis toxin	Fibrinogen	
		Lung surfactant protein A	
TLR5	Flagellin (Bacteria)		Myd88
TLR6	Di-acyl lipopeptides (Mycoplasma)		Myd88 & TIRAP
TLR7	Imidazoquinoline, Loxoribine, Bropirimine (Synthetic compounds)	U1snRNP RNA	Myd88
	Single-stranded RNA (Virus)		
TLR8	Imidazoquinoline (Synthetic compounds)		Myd88
	Single-stranded RNA (Virus)		
TLR9	CpG ODN (Bacteria and viruses)	Hypomethylated CpG-DNA	Myd88
	Pigment hemozoin (Malaria)		
TLR10^	Triacylated lipopeptides		Myd88, TIRAP?
TLR11*	Profilin-like protein (Toxoplasma gondii)		Myd88
TLR12*	Profilin-like protein (Toxoplasma gondii)		Myd88
TLR13*	Bacterial rRNA		Myd88

HSP: Heat Shock Protein; LPS: Lipopolysaccharides; ND: Not determined; PGN: Peptidoglycan

^Not functional in mice.

*Functional gene only found in mice.

Figure 1.1

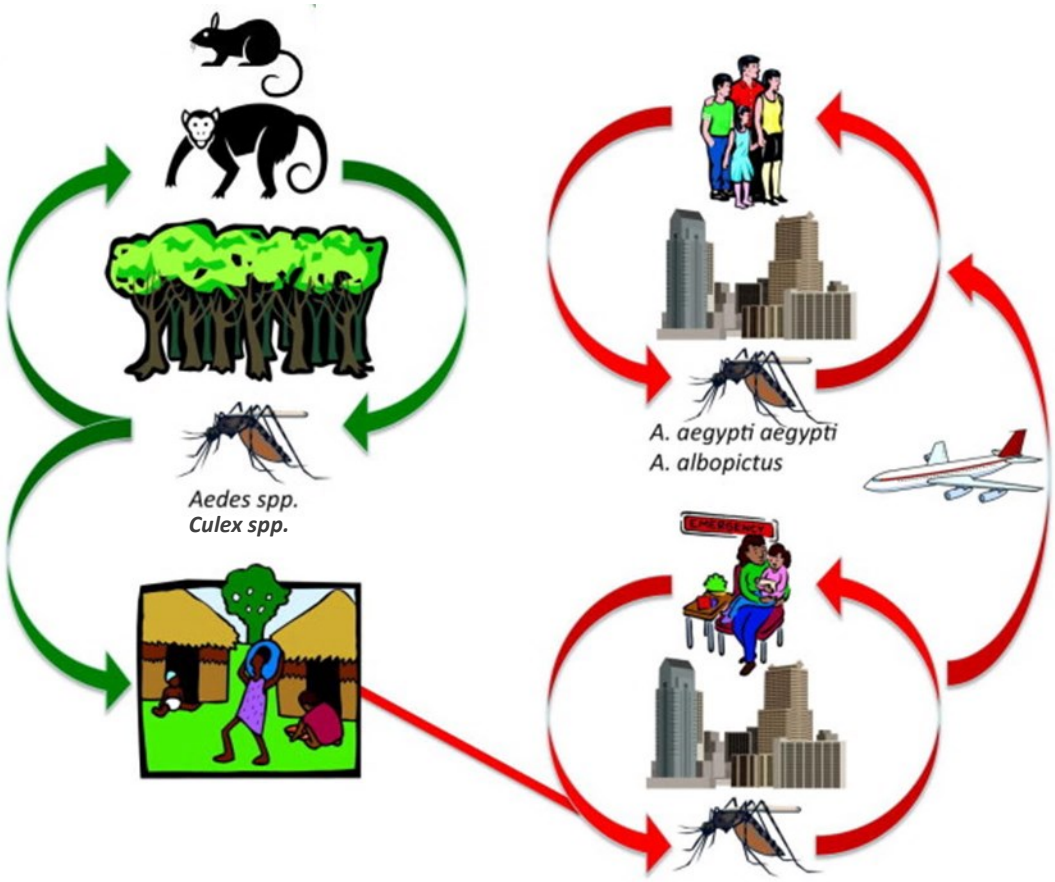

Figure 1.1: Alphavirus transmission cycles

Enzootic and epidemic/endemic transmission cycles of alphaviruses.

Figure 1.2

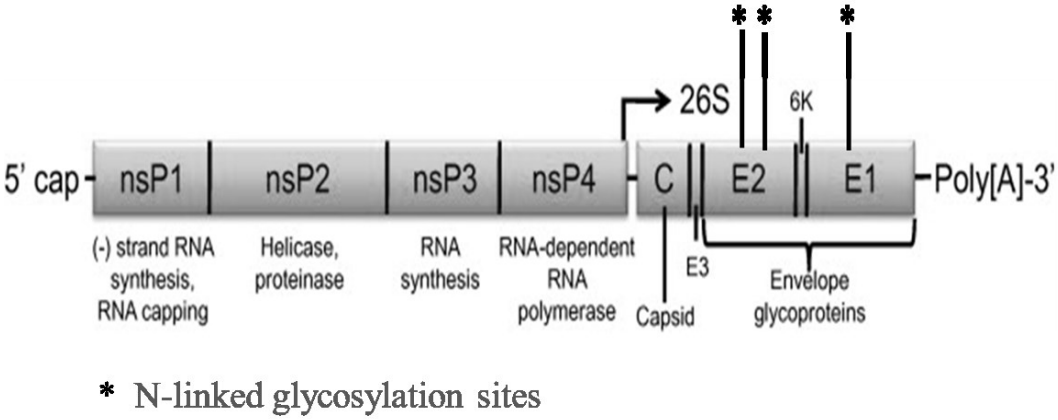

Figure 1.2: Alphavirus genome

Simplified schematic of the alphavirus genome, with major protein functions and locations of N-linked glycosylation sites indicated.

Figure 1.3

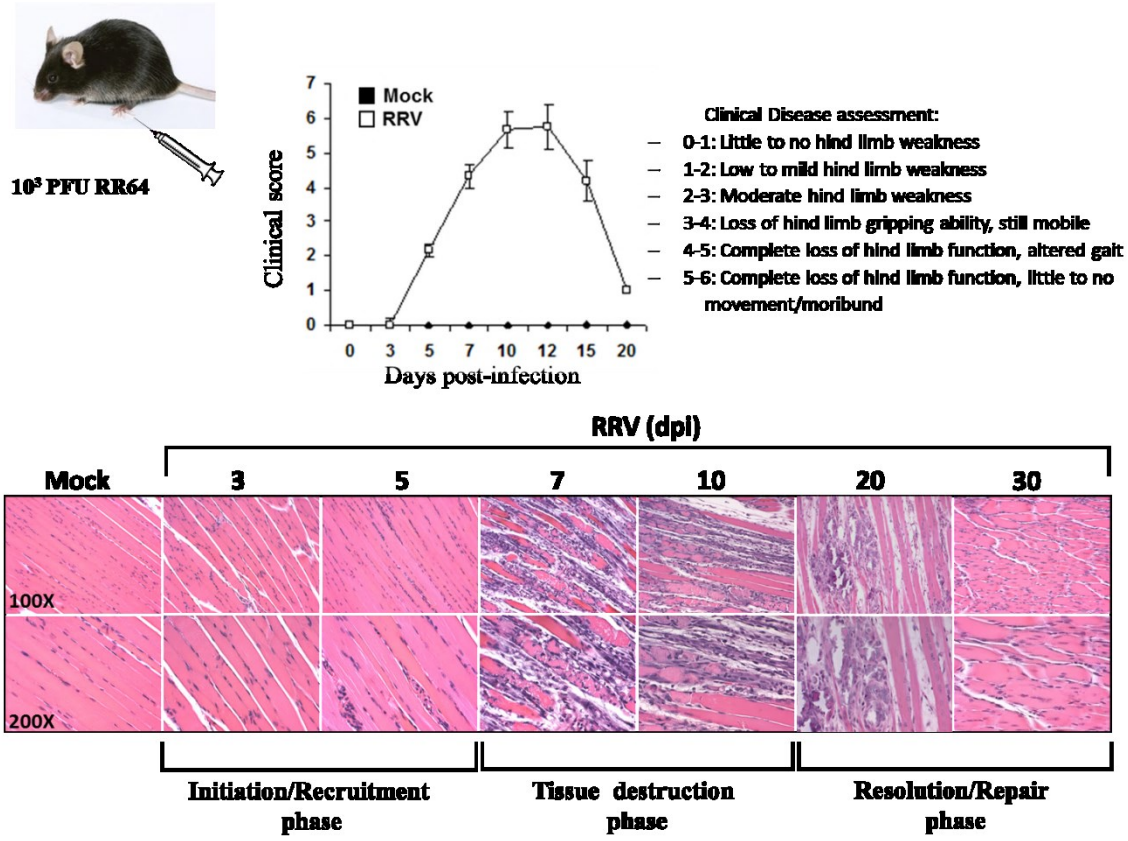

Figure 1.3: Mouse model of RRV infection

In this model of alphavirus-induced arthritis/myositis, 24 day-old C57BL/6 mice are subcutaneously infected in the left-rear footpad with 10^3 PFU of RR64, the molecular clone of RRV. Over the course of infection, mice show transient weight loss (not pictured) and develop disease signs that are characterized by hind limb weakness. Peak disease, which occurs between 10 and 12 days post-infection, correlates with skeletal muscle damage and inflammation.

Figure 1.4

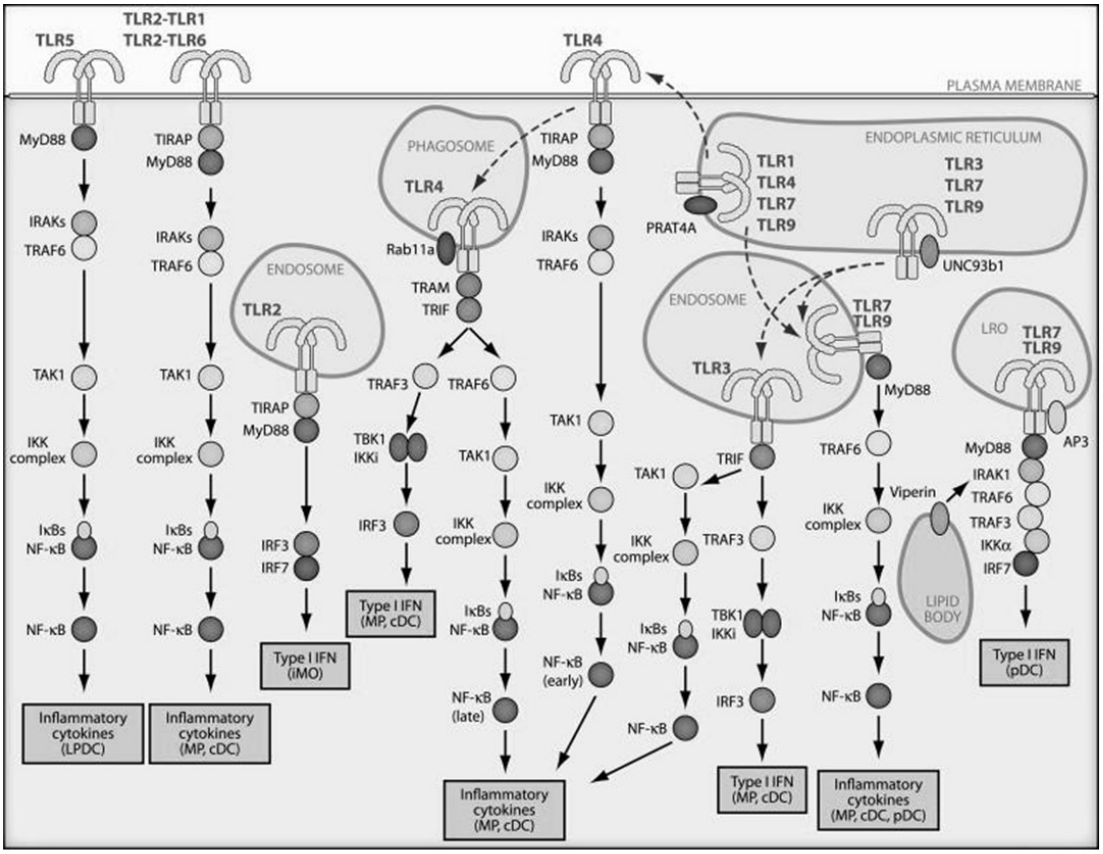

LPDC: Lamina propria DC; MP: macrophages; cDC: Conventional DC; pDC: plasmacytoid DC; iMO: Inflammatory monocyte

Figure 1.4: Overview of TLR signaling

TLRs initiate signal transduction in various cell types to mediate immune responses to infections. Upon stimulation by specific pathogenic (or endogenous) ligands, TLRs recruit their respective downstream adaptor(s) to activate signaling pathways that lead to type I IFN and inflammatory cytokine induction.

CHAPTER TWO:

MYD88-DEPENDENT TLR7 SIGNALING MEDIATES PROTECTION FROM SEVERE ROSS RIVER VIRUS-INDUCED DISEASE IN MICE[†]

2.1 Overview

Arthralgia-associated alphaviruses, including chikungunya virus (CHIKV) and Ross River virus (RRV), pose significant public health threats because they cause explosive outbreaks of debilitating arthralgia and myalgia in human populations. Although the host inflammatory response is known to contribute to the pathogenesis of alphavirus-induced arthritis and myositis, the role that toll-like receptors (TLRs), which are major regulators of host antiviral and inflammatory responses, play in the pathogenesis of alphavirus-induced arthritis and myositis has not been extensively studied. Using a mouse model of RRV-induced myositis/arthritis, we found that myeloid differentiation primary response gene 88 (Myd88)-dependent TLR7 signaling is involved in protection from severe Ross River Virus (RRV)-associated disease. Infections of Myd88- and TLR7-deficient mouse strains with RRV revealed that both Myd88 and TLR7 significantly contributed to protection from RRV-induced mortality, and both mouse strains exhibited more severe tissue damage than wild-type (WT) mice following RRV infection. Additionally, while viral loads were unchanged in either knockout when

[†]Lauren M. Neighbours, Kristin Long, Alan C. Whitmore, and Mark T. Heise.
Departments of Microbiology & Immunology and Genetics, UNC-Chapel Hill.
First published in *Journal of Virology*, October 2012, Vol. 86, No. 19: p. 10675-85.
DOI:10.1128/JVI.00601-12.

compared to WT mice at early times post-infection, both Myd88 and TLR7 knockout mice exhibited higher viral loads than WT mice at late times post-infection. Furthermore, while high levels of RRV-specific antibody were produced in TLR7-deficient mice, this antibody had very little neutralizing activity and had lower affinity compared to WT antibody. Additionally, TLR7- and Myd88-deficient mice showed defects in germinal center activity, and the passive transfer of antisera from TLR7-deficient mice failed to protect WT mice from RRV-induced disease, suggesting that TLR7-dependent signaling is critical for the development of protective antibody responses against RRV.

2.2 Introduction

Mosquito-transmitted alphaviruses cause a variety of disease states in animals and humans, ranging from joint and muscle pain to severe neuropathology and encephalitis (4, 5, 45). Because of the wide distribution of their viral vectors and their ability to cause explosive outbreaks of debilitating arthralgia and myalgia, arthralgia-associated viruses such as chikungunya virus (CHIKV) and Ross River virus (RRV) are considered to be significant emerging disease threats (42, 190-192). Though rarely fatal, alphavirus-induced arthritis can be quite debilitating and can progress to chronic disease in a significant subset of individuals, thereby significantly affecting the patients' quality of life and placing substantial burdens on health care systems (16).

Several studies have demonstrated that immune pathology contributes to alphavirus-induced arthritis and myositis (51, 56-59, 175). Mouse models of arthritogenic

alphavirus infection have implicated inflammatory macrophages and complement in the development of alphavirus-induced disease (51, 53, 56, 57, 59, 175, 193). However, the signaling pathways underlying alphavirus pathogenesis remain poorly understood, and further characterization of the pathways contributing to alphavirus-induced arthritis and myositis may lead to the development of more effective antiviral therapies to treat affected individuals (192).

Toll-like receptors (TLRs) are pattern-recognition receptors that recognize conserved microbial patterns on pathogens, including bacteria, fungi and viruses (64). Following TLR engagement and stimulation by invading microbes, specific adaptor molecules interact with the activated TLRs and then initiate downstream signaling cascades to promote innate immune responses and target the associated infection (194). Although TLRs have been found to play a role in many virally-induced diseases, usually functioning in a protective capacity, and certain TLRs, including TLRs 1, 2, 3, 7, 8 and 9, and the TLR adaptor molecule myeloid differentiation primary response gene 88 (Myd88), have been found to be upregulated during alphavirus infection (144, 195, 196), the importance of TLRs in the pathogenesis of alphavirus-induced arthritis/myositis has not been elucidated.

To determine whether TLRs influence alphavirus pathogenesis, we evaluated the role of Myd88 in a mouse model of RRV-induced arthritis/myositis. Because Myd88 is essential for signaling by all TLRs except for TLR3 and partial TLR4 signaling, we chose first to focus our studies on Myd88 to determine whether RRV-induced disease is impacted by the absence of this central TLR signaling molecule (194, 197-199). Here we report that mice deficient in Myd88 developed more severe disease and RRV-induced

mortality compared to RRV-infected wild-type C57BL/6J (WT) mice, and that TLR7-deficient animals exhibited an almost identical phenotype to the Myd88-deficient mice during RRV infection. Moreover, mice deficient in TLR7 produced less neutralizing antibodies following RRV infection when compared with WT animals, suggesting that Myd88-dependent TLR7 signaling is required for the control of RRV replication and for protection from severe RRV-induced disease.

2.3 Materials and Methods

Virus stocks and cells. Viral stocks of the mouse-virulent T48 strain of Ross River Virus (RRV) were generated from the full-length T48 cDNA clone (generously provided by Richard Kuhn, Purdue University) as previously described (55). Viral titrations were determined by plaque assay on Vero cells as described below. Fresh and confluent Vero cell monolayer, grown in DMEM/F12 (Gibco) with 10% Hyclone FBS, 1% non-essential amino acids, 1% Pen/Strep, 2.5% $NaHCO_3$ (Gibco) and 1% L-glutamine, were used for all plaque assay and PRNT assay experiments.

Mouse experiments. C57BL/6J wild-type (WT), TLR7-deficient ($TLR7^{-/-}$), and Myd88-deficient ($Myd88^{-/-}$) mice were obtained from The Jackson Laboratory (Bar Harbor, ME) and bred in-house. $TLR7^{-/-}$ and $Myd88^{-/-}$ mice were both maintained on a C57BL/6 background. Animal husbandry and experiments were performed in accordance with all UNC-CH Institutional Animal Care and Use Committee guidelines. All mouse studies were performed in a biosafety level 3 laboratory. Twenty-four day old mice were used for

all *in vivo* studies. Mice were anesthetized with isoflurane (Halocarbon Laboratories) prior to subcutaneous inoculation in the left rear footpad with 10^3 PFU of virus in phosphate-buffered saline (PBS) diluent in a 10 μl volume. Mock-infected animals were inoculated with PBS diluent alone. Mice were weighed and monitored daily for clinical disease signs. Disease scores were determined by assessing grip strength, hind-limb weakness and altered gait as described previously (53). Briefly, mice were scored on a scale from 0 to 5, wherein 0 indicated no disease signs, 1-2 indicated ruffled fur and mild hind limb weakness, 3-4 indicated moderate hind limb weakness and altered gait, 5 indicated severe hind limb weakness and dragging of hind limbs, and 6 indicated that the mice were moribund and thus unable to consume adequate amounts of food and water, thus meeting euthanasia criteria.

Viral titers. To determine viral titers in RRV-infected murine tissues, mice were anesthetized and sacrificed by exsanguination. Quadriceps tissues were excised and homogenized and serum was extracted prior to freezing at -80°C until viral titers were assessed. Viral tissues were thawed on ice and subsequently diluted in PBS diluent in 10-fold dilutions. After dilution, 200 μl of infected tissue samples were pipetted into each well of 70% confluent Vero cells in duplicate for each dilution. The samples were incubated on the cells for 1 hour at 37°C in a CO_2 incubator and gently agitated every 15 minutes to ensure a uniform distribution of the inoculum on the cell monolayer. After incubation, the cells were overlayed with an agar overlay solution consisting of 50% of 2.5% CMC (Sigma), 50% 2X Modified Eagles Media, 3% FBS, 1% Pen/Strep, 1% L-glutamine and 1% 1M HEPES buffer (Mediatech), and incubated for 48-72 hours at 37°C in a CO_2 incubator. Cells were then fixed with 4% Paraformaldehyde for 24 hours,

counterstained with a 0.25% Crystal Violet solution in water, and viral plaques were counted.

Histological analysis. At 10 days post-infection, mice were sacrificed and perfused with 4% paraformaldehyde, pH 7.3. Excised tissues were embedded in paraffin, and 5-µm sections were prepared. To determine the extent of inflammation and tissue pathology, tissues were stained with hematoxylin and eosin (H & E) (53). Stained sections were blinded and scored for overall inflammatory cell infiltration and tissue damage as described (53). Both scoring systems utilized a 10-point scale where a score of 0-3 represents no to mild inflammation or damage, 4-6 represents moderate inflammation or damage, and 7-10 represents severe inflammation or damage. For the analysis of germinal center formation, spleen tissue from WT and TLR7$^{-/-}$ mice were stained with H & E, and stained sections were blinded and scored for the number of germinal centers (GCs) and the number of total follicles within the section. GCs were identified within each follicle by their characteristic staining pattern of a pale, circular region surrounded by a darker region containing the mantle and marginal zones.

Flow cytometry. Mice were inoculated as described above, sacrificed by exsanguination at indicated times post-infection and perfused with 1X PBS. Quadriceps muscles or spleens were dissected, minced, and incubated for 1.5-2 hours with vigorous shaking at 37°C in digestion buffer (RPMI, 10% fetal bovine serum, 15 mM HEPES, 2.5 mg/ml collagenase A [Worthington Biochemical Co.], 17 µg/ml DNase I [Roche]). Digested tissues were pelleted, resuspended in HFA buffer (Hanks balanced salt solution [Gibco], 1% fetal bovine serum, 0.1% sodium azide), passed through a 70 µm cell strainer, and centrifuged for 8 min at 1,000 rpm. Cells were resuspended in HFA buffer, and viable cell

totals were determined by trypan blue exclusion. Isolated cells were incubated with various antibodies, according to the associated staining panel, for 30 min to an hour at 4°C in fluorescence-activated cell sorter staining buffer (1x Hanks balanced salt solution, 1% fetal bovine serum, 2% normal rabbit serum). Cells were washed, fixed overnight in 2% paraformaldehyde and analyzed on a Cyan cytometer (Becton Dickinson) using Summit software. Isolated splenocytes from mock-infected animals were prepared similarly and used for single-color staining controls. The lymphocyte staining panel included the following antibodies: anti-NK1.1-phycoerythrin (PE) (eBioscience), anti-CD3-fluorescein isothiocyanate (FITC) (eBioscience), anti-B220-PE Texas Red (PETR) (Invitrogen), anti-LCA-PECy5 (eBioscience), anti-F4/80-PECy7 (eBioscience), anti-CD4-pacific blue (PB) (Caltag Laboratories), anti-CD8-pacific orange (PO) (Invitrogen), anti-CD49b-allophycocyanin (APC) (eBioscience), and anti-GL7-Alexa88 (eBioscience). The monocyte staining panel included the following antibodies: anti-Ly6G-FITC (BD Pharmingen), anti-SigLecF-PE (BD Pharmingen), anti-CD11c-PETR (Invitrogen), anti-LCA-PECy5 (eBioscience), anti-F4/80-PECy7 (eBioscience), anti-CD11b-eF450 (eBioscience), anti-MHC class II-APC (eBioscience), and anti-B220-eF780 (eBioscience).

The gating strategies were as follows: For the inflammatory leukocytes, CD11c+, LCA+ viable cells were displayed on a histogram of Gr-1 plotted *versus* SigLecF. Neutrophils appear as a distinct Gr-1 high population and SigLecF+ cells appear on the other side of the diagonal. The SigLecF+ subpopulation is displayed on a histogram of CD11b *versus* CD11c, where eosinophils appear as a CD11b high, CD11c low group, while resident macrophages are CD11b low, CD11c high. With neutrophils and SigLecF

high groups gated out, the remaining CD11c positive cells are displayed on a plot of MHC class II *versus* B220. The B220 high, MHC class II low pDCs are gated out and the remaining cells are displayed on a plot of MHC class II *versus* CD11b; the MHC class II low cells are enumerated as monocyte-derived DCs (also referred to as TIP-DCs in some publications), and MHC class II high, CD11b hi cells are classified as inflammatory DCs (or CD11b high DCs). For lymphocyte populations, viable lymphocytes (selected by forward/side scatter characteristics) are plotted on a histogram of CD3 *versus* autofluorescence, and the CD3+ cells are further displayed on a plot of CD4 versus CD8. Lymphocytes that are both CD19+ and B220+ are counted as B cells and those that are both CD49b+ and NK1.1+ are counted as NK cells.

Type I IFN (IFN-α/β) bioassay. IFN-α/β levels in cell culture supernatants were measured by an IFN bioassay as described previously (40, 185). Briefly, L929 mouse fibroblasts (ATCC CCL-1) were seeded into 96-well plates and grown in αMEM media. Samples were diluted 1:5 in αMEM media, acidified to a pH of 2.0 for 24 hours and then neutralized to pH 7.4. Samples were then subjected to UV light for 15 minutes to inactivate any remaining virus, followed by titration of the samples by two-fold serial dilutions across the seeded 96-well plate. Twenty-four hours later, encephalomyocarditis virus was added to each well at an MOI of 5. At 18 to 24 hpi, 3-(4,5-dimethyl-2-thiazolyl)-2,5-diphenyl-2H-tetrazolium bromide (MTT; Sigma) was added to the plate to assess the viability in each well. The MTT product produced by viable cells was dissolved in isopropanol containing 0.4% hydrochloric acid and quantified by absorbance readings on a microplate reader at 570 nm. Each plate contained an IFN-β standard

(Chemicon or R&D Systems) that was used to determine the number of international units of IFN-α/β per milliliter of the unknown samples.

Plaque reduction neutralization test (PRNT) assay. Neutralizing antibody titers were determined by PRNT assay on Vero cell monolayers. Briefly, mice sera were heat-inactivated at 56°C for 30 minutes in a water bath and then placed on ice. Identical volumes (200 µl) of two-fold mice sera dilutions (1:2) and wild-type RRV (10^3 PFU virus/ml of PBS diluent) were mixed together and incubated at 37°C for 30 minutes in a water bath. After incubation, 200 µl of serum/virus sample mixture were pipetted into each well of 70% confluent Vero cells in duplicate for each dilution. The samples were incubated on the cells for 1 hour at 37°C in a CO_2 incubator and gently agitated every 15 minutes to ensure a uniform distribution of the inoculum on the cell monolayer. After incubation, the cells were overlayed with an agar overlay solution consisting of 50% of 2.5% CMC (Sigma), 50% 2X Modified Eagles Media, 3% FBS, 1% Pen/Strep, 1% L-glutamine and 1% 1M HEPES buffer (Mediatech), and incubated for 48-72 hours at 37°C in a CO_2 incubator. Cells were then fixed with 4% Paraformaldehyde for 24 hours, counterstained with a 0.25% Crystal Violet solution in water, and viral plaques were counted. Neutralizing antibody titers are expressed as $PRNT_{50}$, which is the reciprocal dilution wherein 50% of the total number of viral plaques in the virus/PBS diluent samples was reduced.

Enzyme-linked immunosorbent assay (ELISA). RRV-specific antibody titers in sera of infected mice were determined by ELISA with inactivated RRV (1µg/ml) on high-binding 96-well plates. The serum was first diluted 20-fold and then further diluted in two-fold serial dilutions. The ELISA antibody titer expressed is the estimated dilution

factor that gave an $OD_{450} = 0.2$ and is derived from nonlinear regression analysis of the serial dilution curve. Detection of bound antibody is obtained using an HRP-conjugated goat anti-mouse secondary antibody (Abcam, Cambridge, MA) and ABTS substrate (Invitrogen).

Antibody Affinity ELISA. RRV-specific antibody titers in sera of WT and $TLR7^{-/-}$ infected mice were first determined by ELISA as described above. Inactivated RRV (1μg/ml) was then plated on high-binding 96-well plates for 12-24 hours, and sera was diluted in antibody diluent (PBS containing 0.05% Tween-20 and 10% Sigma Block) and then plated at a known dilution across the plate to obtain maximum antibody-antigen binding and then incubated at 4ºC for 2 hours. Following the sera incubation, increasing concentrations of sodium thiocyanate (NaSCN) were added to the plate to serially dissociate the antibody-antigen complexes, followed by incubation with a conjugated secondary IgG antibody and substrate incubation as described in the ELISA protocol above. Values were reported as the percent maximum total IgG binding at each NaSCN concentration.

Passive serum transfer. Twenty-four day old WT and $TLR7^{-/-}$ mice were subcutaneously infected in the left rear footpad with 10^3 PFU of RRV and subsequently harvested at day 10 post-infection by exsanguination. Serum from each strain of infected mice was collected, pooled according to strain, and heat-inactivated at 56ºC for 1 hour. Twenty-four day old naïve WT mice were then inoculated with 50 μl of the heat-inactivated WT or $TLR7^{-/-}$ antisera. At one hour post-serum transfer, the mice were subcutaneously infected in the left rear footpad with 10^3 PFU of RRV and monitored daily for weight loss and disease signs as described above.

Statistical analyses. Data were analyzed using Prism software (GraphPad Software, Inc.). Comparisons of one-variable data were performed using a two-tailed unpaired Student's *t* test. Percent starting weight for WT, TLR7$^{-/-}$ and Myd88$^{-/-}$ mice was analyzed using a one-way ANOVA with multiple comparisons corrections ($P<0.01$ is considered significant). Clinical scores for WT, TLR7$^{-/-}$ and Myd88$^{-/-}$ mice were analyzed by Mann-Whitney analysis with Bonferroni's correction ($P<0.01$ is considered significant). Bar graphs represent mean values ± standard deviation. Significant differences are represented by comparison (*) with the following legend: *$P\leq0.05$, **$P\leq0.01$, ***$P\leq0.001$, ****$P\leq0.0001$, unless otherwise indicated.

2.4 Results

Myd88 mediates protection from RRV-induced disease.

Previous studies have shown that the host inflammatory response plays a major role in the pathogenesis of alphavirus-induced arthritis and myositis (51, 56-59, 175). To further define the host pathways that contribute to alphavirus-induced pathology, we evaluated the role of toll-like receptors (TLRs) in a mouse model of RRV-induced arthritis/myositis. Because Myd88 is an essential adaptor for signaling through multiple TLRs, we evaluated mice deficient in Myd88 for their susceptibility to RRV-induced inflammatory disease (194, 197-199). Myd88-deficient (Myd88$^{-/-}$) mice were highly susceptible to RRV-induced disease, with Myd88$^{-/-}$ mice developing more severe disease signs, as measured by weight loss and clinical disease scores, than wild-type (WT)

C57BL/6J animals over the course of infection (Figure 2.1A and 2.1B). Consistent with previous studies, RRV-infected WT mice lost weight between days 6 and 10 post-infection and reached peak disease scores between day 9 and 10 post-infection (Figure 2.1A and 2.1B). Although Myd88$^{-/-}$ mice showed a similar disease progression, they lost more weight and exhibited more severe disease than WT animals over the course of RRV infection (Figure 2.1A and 2.1B). Furthermore, while RRV-induced disease is self-limited in WT animals, with the animals completely recovering from RRV-induced disease, 100% of Myd88$^{-/-}$ mice were moribund by day 10 post-infection and had to be euthanized. These results suggest that rather than contributing to disease pathogenesis, Myd88-dependent signaling plays an essential protective role during RRV infection.

TLR7-deficient mice exhibit an identical phenotype to Myd88-deficient animals.

While Myd88 operates as an essential adaptor molecule for most TLRs, it can also serve as an adaptor for IL-1 and IL-18 receptor signaling (200, 201). Therefore, it was unclear whether Myd88's protective effect during RRV infection reflected a role for a specific TLR or possibly signaling through the IL-1/IL-18 receptors. To address this question, we sought to evaluate the role of specific TLRs in the pathogenesis of RRV-induced disease. These studies initially focused on TLR7, a Myd88-dependent TLR that is known to play a role in the antiviral response against multiple viruses, including single-stranded RNA viruses (90, 194, 202-206). When TLR7$^{-/-}$ mice were infected with RRV, they exhibited an identical phenotype to Myd88-deficient animals, with TLR7$^{-/-}$ mice losing more weight and developing more severe disease signs than WT mice (Figure 2.1C and 2.1D). RRV-infected WT and TLR7$^{-/-}$ mice lost weight between 7 and 10 days post-infection, with TLR7-/- mice losing weight at a faster rate than WT animals (Figure

2.1C). WT and TLR7$^{-/-}$ mice reached peak clinical disease scores between days 9 and 10 post-RRV infection (Figure 2.1D). However, mice deficient in TLR7 developed disease more rapidly than WT animals following RRV infection, and peak disease was more severe, with peak disease scores in TLR7$^{-/-}$ mice (5.7 ± 0.4) significantly higher than disease scores in WT animals (4.3 ± 0.2) (Figure 2.1D). Similar to Myd88$^{-/-}$ mice, TLR7$^{-/-}$ mice became moribund by day 10 post-infection and had to be euthanized. Therefore, although we cannot rule out a role for other Myd88-dependent TLRs, such as TLR2 or IL-1/IL-18 receptor signaling in the pathogenesis of RRV infection, these results indicate that TLR7-dependent signaling through Myd88 plays a major protective role during RRV infection.

Tissue damage is enhanced in Myd88- and TLR7-deficient mice following RRV infection.

Because skeletal muscle is a targeted tissue for viral replication, inflammation and tissue destruction following RRV infection (53, 58, 59), we evaluated the role of TLR7 and Myd88 in protecting from RRV-induced tissue damage and inflammation. WT, TLR7$^{-/-}$ and Myd88$^{-/-}$ mice were sacrificed at 10 days post-infection, which represents the time of peak disease in the animals (58, 59, 193), and quadriceps tissues were excised and prepared for histological analysis. As shown in Figure 2.2, TLR7$^{-/-}$ and Myd88$^{-/-}$ mice showed enhanced tissue damage in skeletal muscle tissue when compared with WT mice following RRV infection. While mock-infected animals of all strains showed similar levels of resident inflammatory cells and intact muscle fibers in skeletal muscle tissue, muscle tissue from TLR7$^{-/-}$ and Myd88$^{-/-}$ mice showed less intact muscle fibers and more overall tissue destruction following RRV infection relative to WT mice, despite similar levels of inflammation (Figure 2.2A).

To quantify the extent of inflammation and damage present in the muscle tissues at 10 days post-infection, histological slides were blinded and scored using a blind scoring method that assigns scores based on the presence of inflammatory cell infiltrates and overall damage in the muscle tissue (Figure 2.2B and 2.2C). The results of the blind scoring analyses showed that while WT and TLR7$^{-/-}$ mice showed similar levels of inflammatory cell infiltration in skeletal muscle tissue following RRV infection, there was significantly more damage in the quadriceps tissue of TLR7$^{-/-}$ mice relative to WT mice (Figure 2.2B), and this was also observed following histological scoring of WT and Myd88$^{-/-}$ skeletal muscle tissues (Figure 2.2C). However, no differences were observed following histological analyses of non-target tissues such as the brain and spinal cord of WT, TLR7$^{-/-}$ and Myd88$^{-/-}$ mice at day 10 post-infection (data not shown), suggesting that the enhanced tissue damage observed in TLR7- and Myd88-deficient mice is specific to RRV-targeted skeletal muscle. These data suggest that TLR7 and Myd88 play a critical role in protection from severe skeletal muscle damage following RRV infection.

TLR7 deficiency does not affect macrophage recruitment but does affect T cell recruitment into RRV-infected muscle tissue.

Previous studies have shown that inflammatory macrophages play a major role in promoting RRV-induced disease (51, 57, 175). Although the histological scoring analyses revealed similar degrees of inflammation in the skeletal muscle tissue of WT and TLR7$^{-/-}$ mice following RRV infection, we sought to more rigorously quantify the overall number and composition of inflammatory cells within the skeletal muscle of RRV-infected TLR7$^{-/-}$ and WT mice. At 5 and 7 days post-infection, WT and TLR7$^{-/-}$ mice showed similar numbers of inflammatory leukocyte cell populations, including

inflammatory macrophages, in RRV-infected quadriceps tissues as determined by flow cytometry (Figure 2.3A and 2.3C). Moreover, total numbers of LCA-positive cells isolated from RRV-infected muscle tissues were not different between WT and TLR7$^{-/-}$ mice at both 5 and 7 days post-infection (data not shown). Analyses of infiltrating lymphocytes in the quadriceps muscle tissues revealed a slight decrease in the total numbers of lymphocyte cell populations, including B cells and CD4+ T cells, in TLR7$^{-/-}$ mice when compared to WT mice at 5 and 7 days post-RRV infection (Figure 2.3B and 2.3D). Additionally, CD3-positive and CD4-positive T cell populations were significantly decreased in TLR7$^{-/-}$ mice relative to WT mice at 7 days post-infection (Figure 2.3D). Therefore, although TLR7 deficiency did not have a general effect on inflammatory cell recruitment, it appears that TLR7 is required for the full recruitment of T cells into the inflamed muscle tissue during RRV infection.

Type I IFN production in sera of TLR7- and Myd88-deficient mice is similar to WT mice at early times post-RRV infection.

TLR7 is known to play an important role in the antiviral response against a wide range of viral pathogens, in large part through its ability to regulate type I IFN responses (89, 90, 207-211). Because type I IFN receptor signaling is essential for the control of a number of alphaviruses (137-139, 212, 213), including RRV (R. Shabman and M.T. Heise, unpublished), we evaluated whether TLR7 was required for the early regulation of type I IFN responses *in vivo*. As shown in Figure 2.4, there were no differences in type I IFN production between WT and TLR7-deficient animals at 12, 24 and 48 hours post-infection as measured by Type I IFN bioassay (Figure 2.4A). Moreover, type I IFN production was similar between WT and Myd88$^{-/-}$ mice at 24 and 48 hours post-infection

(Figure 2.4B), suggesting that the early type I IFN response does not contribute to the enhanced disease phenotype observed in TLR7- and Myd88-deficient mice following RRV infection.

Viral titers are elevated in mice lacking TLR7 or Myd88 at late times post-infection.

To determine whether viral burden was altered in mice deficient in TLR7 or Myd88, we quantified the amount of virus present in the quadriceps and serum of WT, TLR7$^{-/-}$ and Myd88$^{-/-}$ mice at various times post-RRV infection. No significant differences in viral titer were detected in the quadriceps muscles or serum of WT, TLR7$^{-/-}$ and Myd88$^{-/-}$ mice at early times post-infection (Figure 2.5). WT and TLR7$^{-/-}$ mice did not show significant differences in viral titer in the quadriceps muscles by plaque assay at days 0.5, 1, 2 and 3 post-infection (Figure 2.5A). However, viral titers in the serum of TLR7$^{-/-}$ mice were significantly enhanced over WT mice at day 3 post-infection (Figure 5B), and analysis of viral burden in infected quadriceps tissues at later times post-infection revealed that TLR7$^{-/-}$ mice had significantly higher viral titers than WT mice at days 5 and 7 post-infection (Figure 2.5A). Similar results were found in Myd88-deficient mice (Fig. 2.5C and 2.5D). Although viral titers in the quadriceps were similar at day 10 post-infection in WT, TLR7$^{-/-}$ and Myd88$^{-/-}$ mice (Figure 2.5A and 2.5C), these titers were close to or below the limit of viral detection by plaque assay and any differences between the strains would thus be difficult to ascertain at this timepoint. Therefore, these findings suggest that RRV is able to infect and spread within target tissues of TLR7$^{-/-}$ and Myd88$^{-/-}$ mice with kinetics similar to WT animals early during infection, but mice lacking TLR7 or Myd88 cannot effectively control viral replication within the muscle tissue at later times post-infection. Although RRV-induced disease is characterized by

high levels of viral replication within joint and muscle tissues, with subsequent overactive inflammatory responses in these tissues contributing to disease pathogenesis (51, 53, 58, 59), the inability of TLR7- or Myd88-deficient mice to control viral replication at late times post-infection raised the possibility that the enhanced disease/mortality in these mice might be due to enhanced viral replication in other tissues, such as the central nervous system (CNS). However, we observed no differences in viral load within the brain and spinal cord of WT and TLR7$^{-/-}$ mice at 1 and 2 days post-infection, and viral titers in these tissues were below the limit of detection for both mouse strains by day 7 post-infection (data not shown). We also observed no differences in viral titer between WT and TLR7$^{-/-}$ mice in the kidney, liver, spleen and draining lymph node at 1 and 2 days post-infection (data not shown), suggesting that excess viral replication within the CNS or other non-target tissues of RRV infection does not explain the enhanced disease observed in TLR7-deficient mice.

TLR7$^{-/-}$ mice show reduced neutralizing antibody production and decreased antibody affinity following RRV infection.

Because TLR7$^{-/-}$ mice showed enhanced viral titers when compared to WT mice at late times post-infection, we hypothesized that deficiency in TLR7 signaling may result in an ineffective antibody response that leads to an inability to control viral replication during RRV infection. To determine whether deficiency in TLR7 affected antibody production following RRV infection, RRV-specific antibody levels were quantified in the sera of WT and TLR7$^{-/-}$ mice by ELISA at 7 and 10 days post-infection (Figure 2.6A and 2.6B). TLR7$^{-/-}$ mice showed increased RRV-specific total IgG production at 7 and 10 days post-infection when compared with WT animals (Figure

2.6A and 2.6B), with TLR7$^{-/-}$ mice having significantly increased total RRV-specific IgG at day 7 post-infection (Figure 2.6A). Additionally, analysis of RRV-specific IgG subtypes revealed that TLR7$^{-/-}$ mice showed significantly increased IgG1 and IgG2c antibody production at 7 days post-infection, as well as increased IgG2c antibody levels at day 10 post-infection, relative to WT mice (Figure 2.6A and 2.6B). These results suggest that RRV-specific antibody production is elevated in TLR7$^{-/-}$ mice following RRV infection. Furthermore, because IgG1 is indicative of T-helper 2 (Th2) immune responses and IgG2c is indicative of T-helper 1 (Th1) immunity, analysis of RRV-specific IgG subtypes reveals that TLR7$^{-/-}$ mice have a skewed Th1/Th2 antibody response following RRV infection relative to WT mice (Figure 2.6A and 2.6B) (214-216).

To determine whether the quality of RRV-specific antibody was altered in TLR7-deficient mice, we first tested the neutralization capacity of WT and TLR7$^{-/-}$ antisera from 7 and 10 days post-RRV infection by PRNT assay (Figure 2.5C). Antisera from TLR7$^{-/-}$ mice had significantly less neutralization activity when compare to WT antisera at both 7 and 10 days post-infection, suggesting that the quality of RRV-specific antibody produced by TLR7-deficient mice is defective and less neutralizing relative to WT antibody responses following RRV infection (Figure 2.6C). To further assess the quality of RRV-specific antibody in TLR7$^{-/-}$ mice, we determined whether TLR7-deficiency altered the affinity of RRV-specific antibody using an Affinity ELISA (Figure 2.7). As shown in Figure 2.7, RRV-specific IgG from infected TLR7$^{-/-}$ mice displayed less affinity for RRV than WT IgG, suggesting that TLR7-deficiency affects the affinity maturation of virus-specific antibody during RRV infection.

Lastly, we directly tested whether sera from TLR7$^{-/-}$ mice showed a reduced capacity to protect from RRV-induced disease in adoptive transfer studies. We passively transferred heat-inactivated sera obtained from WT or TLR7$^{-/-}$ mice at day 10 post-infection to naïve WT mice prior to RRV infection. As shown in Figure 2.7, the transfer of TLR7-deficient antisera failed to protect WT mice from RRV infection (Figure 2.7B and C). WT mice that received sera from RRV-infected TLR7$^{-/-}$ mice showed significantly reduced weight gain and enhanced disease signs between days 5 and 10 post-infection compared to mice that received WT antisera, which were protected from RRV-induced disease (Figure 2.7B and C). Taken together, these results indicate that TLR7 is critically important in the establishment of an effective antibody response following RRV infection.

Myd88- and TLR7-deficiency alters germinal center development following RRV infection.

Germinal center (GC) B cells have been shown to be critical for antibody affinity maturation and for the development of class-switched neutralizing antibodies (217). Because RRV-specific antibody responses were defective in TLR7-deficient mice, we investigated whether GC development was altered in TLR7$^{-/-}$ mice during RRV infection. As shown in Figure 2.8, histological analysis of spleens from WT and TLR7$^{-/-}$ mice at day 10 post-infection revealed that TLR7$^{-/-}$ mice show reduced GC formation following RRV infection. While RRV-infected WT mice exhibited abundant GC structures at 10 days post-infection, GC formation was visibly reduced in TLR7$^{-/-}$ mouse spleens (Figure 2.8A). Blind scoring analysis of GC formation also revealed a reduced percentage of GCs per follicle in TLR7-deficient mice (Figure 2.8B). To determine whether Myd88-

dependent TLR7 signaling is important in GC B cell development, we quantified the total numbers of GC B cells present in the spleens of WT and Myd88$^{-/-}$ mice at day 9 post-RRV infection by flow cytometry. As shown in Figure 2.8C, Myd88-deficient mice showed significantly reduced GL7+ GC B cells compared to WT mice. These results demonstrate that Myd88-dependent TLR7 signaling is critical for germinal center development following RRV infection. Furthermore, these findings implicate the importance of TLR7 in generating an effective adaptive immune response during RRV infection.

2.5 Discussion

The host inflammatory response is known to play a major role in the pathogenesis of alphavirus-induced arthritis and myositis, yet the role of specific host sensing pathways in regulating these processes has not been investigated in detail. The studies presented here demonstrate that TLR7 and its essential adaptor molecule, Myd88, mediate protection against severe RRV-induced disease and mortality. Furthermore, both TLR7- and Myd88-deficient mice exhibited a defect in viral clearance, and TLR7$^{-/-}$ mice failed to mount effective antibody responses against RRV, showing both reduced antibody neutralizing activity and reduced RRV-specific antibody affinity. Moreover, TLR7$^{-/-}$ mice show reduced germinal center formation, and Myd88-deficient mice show reduced germinal center (GL7+) B cells compared to WT animals following RRV infection. These results suggest that TLR7-dependent interactions with the adaptive immune response play a crucial role in regulating the development of protective immune

responses against RRV. Although we cannot rule out a role for other Myd88-dependent TLRs, such as TLR2 or IL-1/IL-18 receptor signaling in RRV-induced disease, these findings provide new insights into the role that TLR7 plays in alphavirus pathogenesis by highlighting the importance of this pathway in regulating antiviral adaptive immunity, and by identifying TLR7 as a possible target for enhancing vaccine-induced immune responses against alphaviruses.

To our knowledge, TLR7's role in alphavirus pathogenesis has not previously been investigated. Because type I IFN receptor signaling is important for the control of a number of alphaviruses (137-139, 212, 213), we initially focused our analysis on evaluating whether TLR7 was required for the early control of RRV infection or regulation of the type I IFN response *in vivo*. Somewhat surprisingly, we found no evidence for altered viral loads either in the serum or skeletal muscle at very early to intermediate times in the infection process (Figure 2.5), nor did we find evidence for enhanced viral replication in other sites, such as the CNS and other non-target tissues, that might contribute to exacerbated RRV-induced disease and mortality (data not shown). Furthermore, we found no evidence that systemic type I IFN responses were decreased in TLR7-and Myd88-deficient animals at early times post-infection as measured by Type I IFN bioassay (Figure 2.4), suggesting that other innate sensing pathways, such as RIG-I and PKR that are known to be involved in the type I IFN response to alphaviruses (166, 218-220), rather than TLR7, may contribute to the early antiviral response against RRV.

In contrast to our findings that TLR7 was not required for the early control of RRV replication, we did see significant defects in the ability of both TLR7- and Myd88-

deficient animals to control RRV replication at late times post-infection. Moreover, although TLR7$^{-/-}$ mice were able to mount RRV-specific antibody responses, the virus-specific antibody produced demonstrated little neutralizing activity and showed less affinity for RRV than WT antibody. Moreover, the passive transfer of TLR7-deficient antisera failed to protect naïve WT mice from *de novo* RRV infection, suggesting that TLR7 plays a major role in driving the development of protective antibody in response to RRV. Because Myd88-dependent TLR7 signaling in B cells has been shown to be important in the development of neutralizing antibodies during retrovirus infection (93), it is possible that TLR7 signaling is necessary for an effective antibody response to multiple viral pathogens. In addition to the impact on neutralizing antibody responses, we also found that TLR7-deficiency resulted in a reduction in the number of CD4+ T cells recruited into the inflamed muscle tissue (Figure 2.3). This observed decrease in T cell recruitment was not due to a general defect in inflammatory cell infiltration in the TLR7$^{-/-}$ mice because macrophage recruitment was unaffected. Moreover, both TLR7- and Myd88-deficient mice showed defects in germinal center formation following RRV infection. Because germinal center B cells have been shown to be regulated by CD4+ follicular T cells, it is possible that the defect in CD4+ T cell recruitment that we observe in TLR7-deficient mice is modulating germinal center formation and B cell function in these mice during RRV infection (221). Taken together, these findings provide further evidence that Myd88-dependent TLR7 signaling plays a role in regulating multiple aspects of the host adaptive immune response Although it remains to be determined exactly how TLR7 and Myd88 are modulating RRV-induced adaptive immune responses, Myd88 has been shown to be required for efficient cross-presentation of viral antigens by

dendritic cells, wherein Myd88-deficiency leads to decreased priming and activation of CD8-positive T cells during infection (222). Likewise, stimulation of TLR7 signaling during vaccination can improve neutralizing antibody production, and it is possible that TLR7 deficiency may also affect neutralizing activity and affinity maturation of antibodies during alphavirus infection (96). Importantly, given TLR7's importance in regulating the development of protective anti-RRV responses, these studies suggest that enhancing TLR7-mediated responses may be beneficial during vaccination against RRV or other alphaviruses.

TLR7 is expressed on a wide variety of cell types, including macrophages and dendritic cell subsets. Although type I IFN responses in many cell types, including myeloid dendritic cells, are independent of Myd88 and therefore TLR7 (223), TLR7 is the major driver of type I IFN production by plasmacytoid dendritic cell (pDCs) in response to viral infection or RNA ligands (224). Because pDCs are known to express high levels of TLR7 and have been shown to recognize ssRNA viruses through TLR7 and Myd88, one potential mechanism for the enhanced RRV-induced disease seen in TLR7-deficient mice is through dysfunctional pDC activity (202, 222, 224, 225). We found no defect in the ability of pDCs isolated from TLR7-deficient mice to produce type I IFN in response to RRV infection *in vitro* (data not shown), although it is possible that pDCs lacking TLR7 may have other functional defects during RRV infection that we have not yet uncovered with our studies. Moreover, a recent study demonstrated the importance of Myd88-dependent TLR7 signaling in B cells for the development of effective neutralizing antibody production during Friend virus infection (93), and it is possible that Myd88 and TLR7 deficiency in B cells may affect neutralizing antibody production

during alphavirus infection as well. Studies are ongoing in our lab to assess whether TLR7 expression is required for the functional activity of pDCs, B cells and other immune cell types to RRV infection.

These studies clearly demonstrate that TLR7 is required for protection from lethal RRV-induced disease and that TLR7 modulated the development of RRV-specific adaptive immune responses. However, it is not clear whether the failure to clear RRV infection in TLR7-deficient mice can be directly linked to the enhanced disease and virus-induced mortality. We have previously shown that RAG-1-deficient (RAG-$1^{-/-}$) mice, which lack functional T and B cells, are susceptible to RRV-induced disease (53). However, unlike TLR7-deficient animals, RAG-$1^{-/-}$ mice do not die from RRV-induced disease (53). This suggests that the lack of a protective adaptive immune response does not pre-dispose mice to RRV-induced mortality. This raises two major possibilities, where the first is that TLR7 is regulating some aspect of early virus control, such as type I IFN responses, that we were unable to detect in our studies. While we cannot rule this possibility out, the fact that we did not observe any major changes in viral load at early times post-infection argues against this possibility. It is also possible that some aspect of the non-protective adaptive immune response in $TLR7^{-/-}$ animals acts to exacerbate RRV-induced disease. A similar outcome has been found with respiratory syncytial virus (RSV) vaccination, where the lack of Myd88 signaling in response to RSV vaccination results in the lack of a protective anti-RSV response within the lungs and leads to the development of vaccine-induced immune pathology (226). This may be particularly important for RRV because accumulation of immune complexes comprised of antibody-bound viral particles in TLR7-deficient animals could lead to enhanced complement

activation via the classical pathway (227, 228). RRV-mediated inflammatory disease has previously been shown to be mediated by complement activation in a mouse model of infection, and other arthritic diseases are associated with complement activation as well (58, 59, 229, 230). Alternatively, the high titers of non-neutralizing, RRV-specific antibodies present in TLR7-deficient mice could enhance RRV infection through an antibody-dependent enhancement (ADE) mechanism, resulting in increased Fc-mediated uptake of antibody-bound viral particles by phagocytic cells (231). ADE has previously been reported to enhance RRV infection of macrophages *in vitro*, and this mechanism could explain the increased viral titers observed in TLR7- and Myd88-deficient animals at late times post-RRV infection, correlating with the onset of adaptive immune responses (56). Studies are currently underway to determine whether either of these possible mechanisms is contributing to the enhanced disease and mortality observed in RRV-infected TLR7$^{-/-}$ mice.

In conclusion, the results of this study identify an essential protective role for the Myd88-dependent TLR7 signaling pathway during RRV infection and further define the impact of host factors in the pathogenesis of alphavirus-induced arthritis/myositis. Given the impact of TLR7 signaling on viral control and on the generation of protective adaptive immunity following RRV infection, it may be beneficial to design vaccination and treatment strategies for alphavirus infections that enhance Myd88-dependent TLR7 signaling, such as through the delivery of TLR7 agonists or through stimulation of downstream signaling molecules, to ensure optimal protection from alphavirus-induced disease. Further studies will be necessary to elucidate the mechanism of TLR7-mediated protection from severe RRV-induced disease.

Figure 2.1

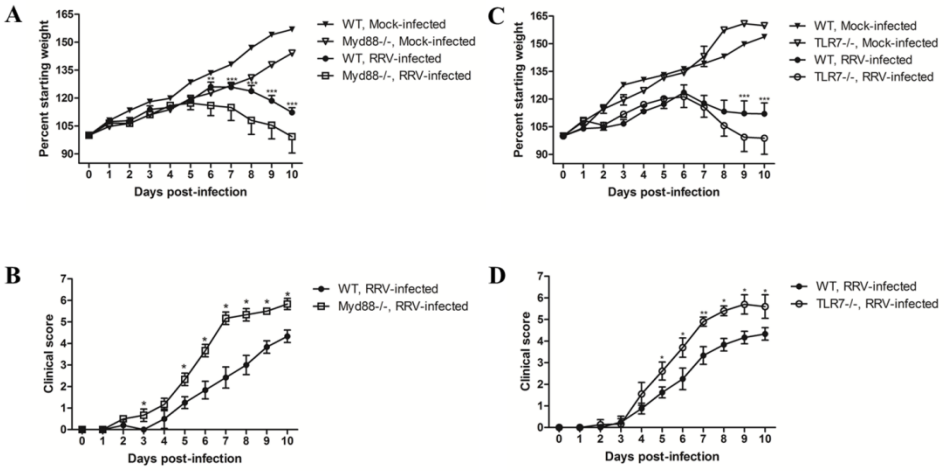

Figure 2.1: TLR7 and Myd88 contribute to protection from RRV-induced disease *in vivo*.

Twenty-four day old C57BL/6J wild-type (WT), TLR7$^{-/-}$ and Myd88$^{-/-}$ mice were subcutaneously infected in the left rear footpad with either PBS diluent (Mock) or 10^3 PFU of RRV and monitored for (A) & (B) weight loss and (C) & (D) clinical disease. N = 5-15 mice/strain/timepoint. *P<0.01, **P≤0.001 and *** P≤0.0001.

Figure 2.2

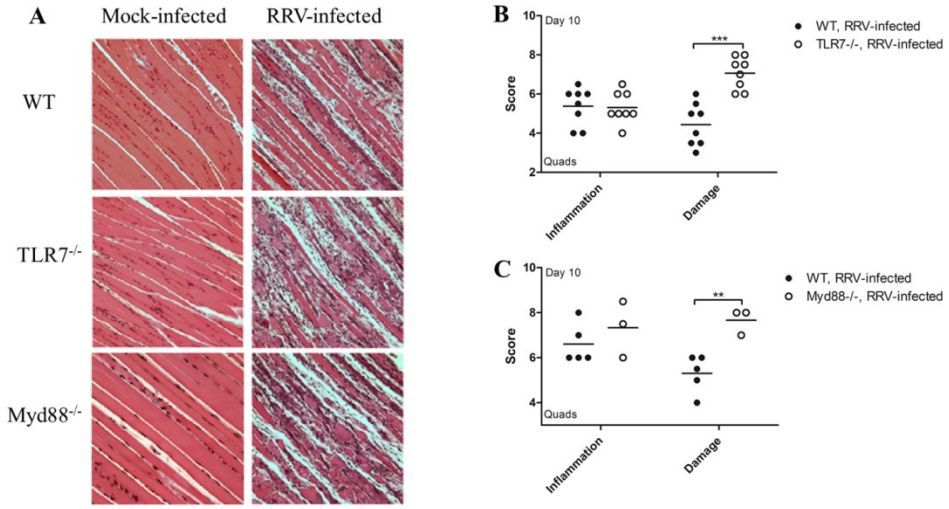

Figure 2.2: TLR7- and Myd88-deficient mice show enhanced tissue damage following RRV infection.

Twenty-four day old WT, TLR7$^{-/-}$ and Myd88$^{-/-}$ mice were subcutaneously infected in the left rear footpad with either PBS diluent or 10^3 PFU of RRV. Mice were sacrificed and perfused with 4% paraformaldehyde at 10 days post-infection. Quadriceps muscles were excised and paraffin-embedded, and 5 µm tissue sections were stained with H&E. (A) Histological analysis of mock-infected and RRV-infected quadriceps muscles from WT, TLR7$^{-/-}$ and Myd88$^{-/-}$ mice at day 10 post-infection. Representative images are shown. (B) Blind scoring of overall inflammatory cell infiltration and damage observed in RRV-infected WT and TLR7$^{-/-}$ muscle tissue. N = 8 (WT and TLR7$^{-/-}$). (C) Blind scoring of overall inflammatory cell infiltration and damage observed in RRV-infected WT and Myd88$^{-/-}$ muscle tissue. N = 5 (WT) or 3 (Myd88$^{-/-}$). **P≤0.01, ***P≤0.001.

Figure 2.3

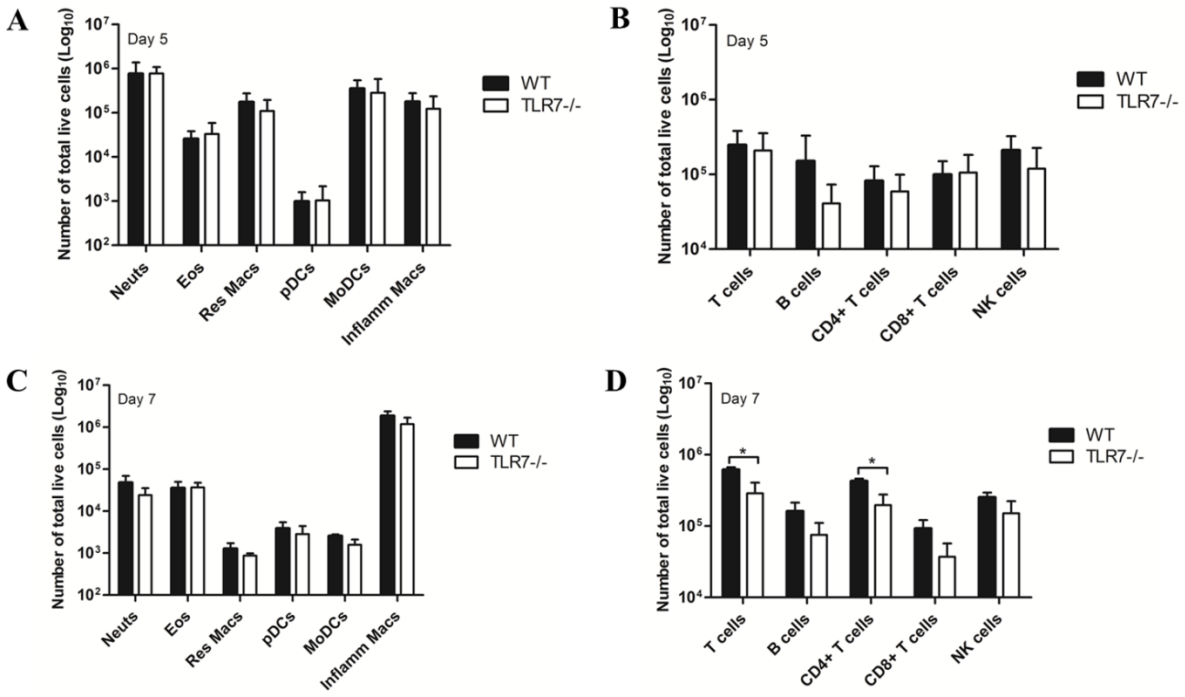

Figure 2.3: Inflammatory cell recruitment is similar in WT and TLR7$^{-/-}$ mice following RRV infection.

Twenty-four day old WT and TLR7$^{-/-}$ mice were subcutaneously infected in the left rear footpad with 10^3 PFU of RRV. At 5 and 7 days post-infection, mice were sacrificed and perfused with 1X PBS. Quadriceps muscles were excised, digested and prepared for flow cytometric analysis as described in Materials and Methods. (A) & (C) Total numbers of infiltrating inflammatory leukocyte cell populations isolated from RRV-infected WT and TLR7$^{-/-}$ quadriceps muscle tissue. (B) & (D) Total numbers of infiltrating lymphocyte cell populations isolated from RRV-infected quadriceps muscle tissue. N = 4-7 mice/strain/timepoint. *P≤0.01.

Figure 2.4

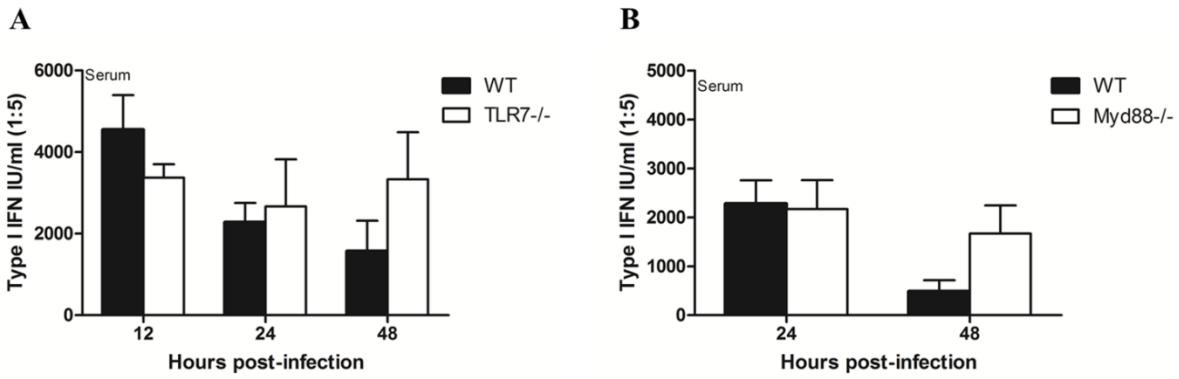

Figure 2.4: Type I IFN production in sera of TLR7$^{-/-}$ and Myd88$^{-/-}$ mice is similar to WT mice early during infection.

Twenty-four day old WT, TLR7$^{-/-}$ and Myd88$^{-/-}$ mice were subcutaneously infected in the left rear footpad with 10^3 PFU of RRV. At the indicated timepoints, mice were sacrificed by exsanguination and serum was collected. Serum was diluted 1:5 in media and analyzed for the presence of Type I IFN (IFN-α/β) by IFN Bioassay as described in Materials and Methods. (A) Type I IFN production in sera of WT and TLR7$^{-/-}$ mice. (B) Type I IFN production in sera of WT and Myd88$^{-/-}$ mice. N = 3-5 mice/strain/timepoint.

Figure 2.5

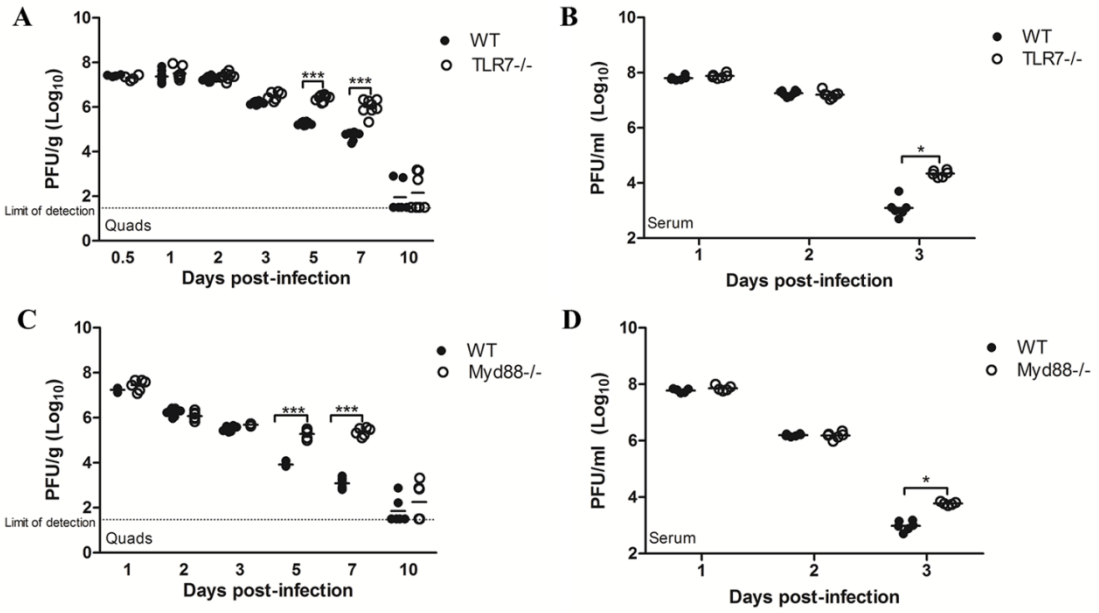

Figure 2.5: Mice lacking TLR7 or Myd88 show an inability to control viral titer at late times post-infection.

Twenty-four day old WT, TLR7$^{-/-}$ and Myd88$^{-/-}$ mice were subcutaneously infected in the left rear footpad with 10^3 PFU of RRV. At the indicated timepoints, mice were sacrificed by exsanguination and quadriceps tissues were dissected. Infectious virus present in (A) & (C) homogenized ipsilateral quadriceps tissue and (B) & (D) serum was quantified by plaque assay on Vero cells. N = 4-8 mice/strain/timepoint. *P≤0.05, **P≤0.01, ***P≤0.001.

Figure 2.6

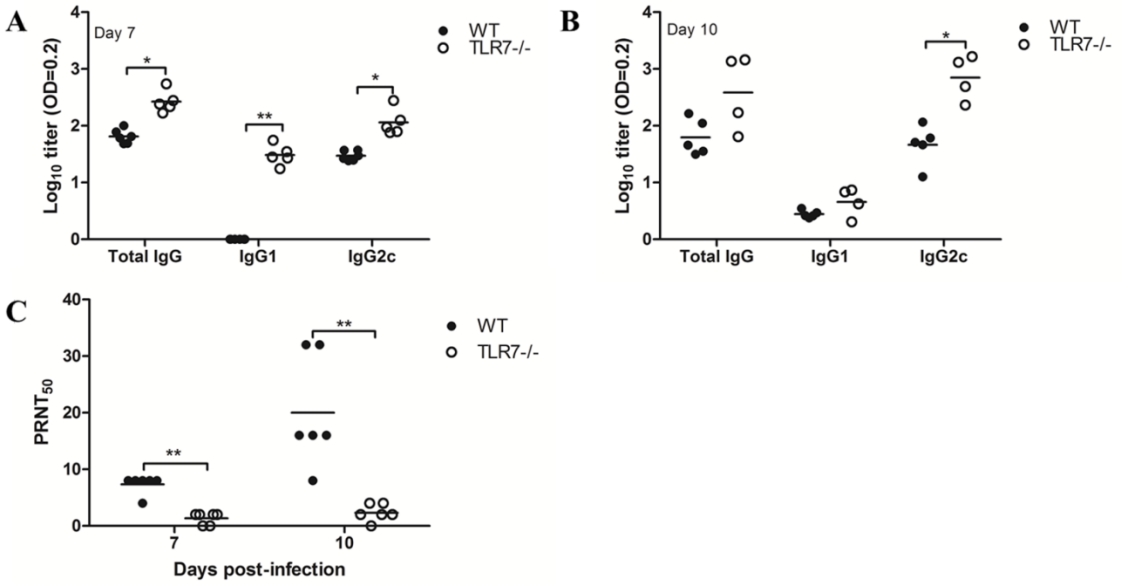

Figure 2.6: TLR7$^{-/-}$ mice show reduced neutralizing antibody production following RRV infection.

Twenty-four day old WT and TLR7$^{-/-}$ mice were subcutaneously infected in the left rear footpad with 10^3 PFU of RRV. (A) At 7 and 10 days post-infection, mice were sacrificed by exsanguination and serum antibody levels were measured by ELISA as described in Materials and Methods. Levels of total RRV-specific IgG, IgG1 and IgG2c antibodies in RRV-infected WT and TLR7$^{-/-}$ mice at day 7 (A) and day 10 (B) are shown. (C) At 7 and 10 days post-infection, mice were sacrificed by exsanguination and sera from RRV-infected WT and TLR7$^{-/-}$ mice was tested for RRV neutralization activity using PRNT assay as described in Materials and Methods. Neutralizing antibody titers are expressed as the inverse of the dilution wherein 50% of the virus present was neutralized ($PRNT_{50}$) for a given sample. N = 6 mice/strain/timepoint. *P≤0.05, **P≤0.01, and ***P≤0.001.

Figure 2.7

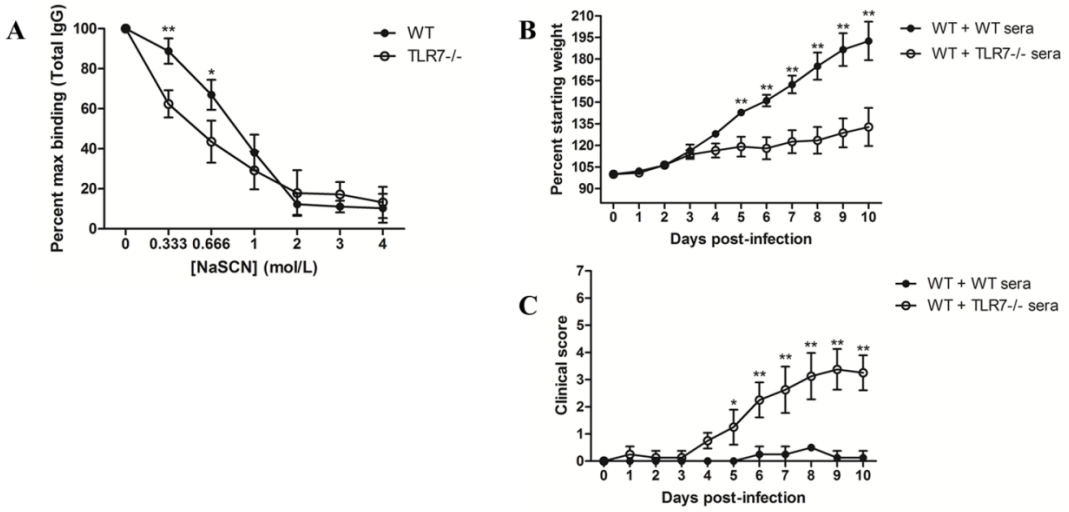

Figure 2.7: TLR7$^{-/-}$ mice shows decreased antibody affinity and fails to protect from RRV-induced disease.

Twenty-four day old WT and TLR7$^{-/-}$ mice were subcutaneously infected in the left rear footpad with 10^3 PFU of RRV. At 10 days post-infection, mice were sacrificed by exsanguination and serum antibody levels were measured by ELISA as described in Materials and Methods. (A) To measure antibody affinity, inactivated RRV was plated on ELISA plates and sera were added at a 1:40 dilution across the plate. Levels of total IgG were measured in the presence of increasing concentrations of NaSCN as described in the Materials and Methods. Representative data is shown, where n = 4 (WT) or 6 (TLR7$^{-/-}$) mice. (B and C) Twenty-four day old WT mice were intraperitoneally inoculated with 50 µl of heat-inactivated sera from RRV-infected WT or TLR7$^{-/-}$ mice harvested at day 10 post-infection. At one hour post-serum transfer, mice were subcutaneously infected in the left rear footpad with 10^3 PFU of RRV and monitored for (B) weight loss and (C) clinical disease. N = 4 mice/group/timepoint. *P≤ 0.001, **P≤0.0001.

Figure 2.8

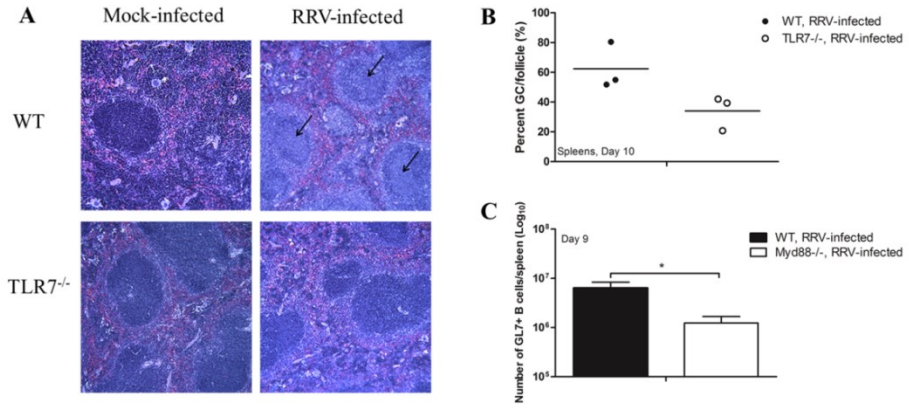

Figure 2.8: TLR7$^{-/-}$ mice show reduced germinal center formation following RRV infection.

Twenty-four day old WT and TLR7$^{-/-}$ mice were subcutaneously infected in the left rear footpad with 10^3 PFU of RRV. Mice were sacrificed and perfused with 4% paraformaldehyde at 10 days post-infection. Spleens were excised and paraffin-embedded, and 5 μm tissue sections were stained with H&E. (A) Histological analysis of mock-infected and RRV-infected spleens from WT and TLR7$^{-/-}$ mice at day 10 post-infection. Representative images are shown. (B) Blind scoring of germinal centers (GC) per follicle observed in WT and TLR7$^{-/-}$ spleens. GCs are indicated by arrows. N = 3 mice/strain. (C) Twenty-four day old WT and Myd88$^{-/-}$ mice were subcutaneously infected in the left rear footpad with 10^3 PFU of RRV At 9 days post-infection, mice were sacrificed and perfused with 1X PBS. Spleens were excised and prepared for flow cytometric analysis as described in Materials and Methods. Total numbers of GL7+ B cells isolated from RRV-infected WT and Myd88$^{-/-}$ mouse spleens are shown. N = 5 mice/strain. *P≤0.01.

CHAPTER THREE:

MYD88-DEPENDENT TLR7 SIGNALING PROTECTS MICE FROM SYSTEMIC COMPLEMENT- AND ANTIBODY-MEDIATED DISEASE FOLLOWING ROSS RIVER VIRUS INFECTION

3.1 Overview

Chikungunya virus and Ross River virus (RRV) are mosquito-borne alphaviruses responsible for epidemics of severe acute and chronic musculoskeletal disease in humans. The host innate immune system plays an integral role in the pathogenesis of arthritic alphaviruses, where some pathways, such as the host complement cascade, exacerbate the virus-induced disease process, while other innate signaling pathways protect from virus-induced disease. We have previously shown that Myd88-dependent signaling through TLR7 mediates protection from severe RRV-induced morbidity and mortality, and that TLR7 deficiency results in the production of low affinity, non-neutralizing RRV-specific antibodies. Here we report that these low affinity antibodies exacerbate the virus-induced disease process. TLR7- and Myd88-deficient mice exhibited enhanced antibody and complement deposition in skeletal muscle, cardiac, and renal tissues compared to WT mice, and Myd88-dependent TLR7 signaling was required for protection from myocardial injury and complement-associated pro-inflammatory marker expression. Passive transfer experiments demonstrated that RRV-specific antisera from Myd88- or

[†]Lauren M. Neighbours, Alan C. Whitmore, and Mark T. Heise.
Departments of Microbiology & Immunology and Genetics, UNC-Chapel Hill.

TLR7-deficient mice induced increased morbidity and tissue damage in B cell-deficient mice during *de novo* RRV infection. Furthermore, mice deficient in TLR7 and C1q (TLRxC1q DKO), which are unable to trigger antibody-dependent complement pathways, did not show enhanced disease following RRV infection, suggesting that Myd88-dependent TLR7 signaling protects mice from developing systemic complement-dependent immune complex disease during RRV infection.

3.2 Introduction

Alphaviruses are single-stranded, positive-sense RNA pathogens that are transmitted by mosquitos. These arboviruses cause unpredictable and destructive epidemics of human disease, and the global distribution of their arthropod vectors continues to pose considerable risks to public health (1). Infections with Old World alphaviruses such as chikungunya virus (CHIKV) and Ross River virus (RRV) are associated with debilitating symptoms of polyarthritis and myositis, which can persist in a subset of individuals for months and in rare cases cause fatalities (15). The chronic morbidities generated by arthritogenic alphavirus-induced diseases produce a significant health care burden, and better insight into the mechanisms of alphavirus pathogenesis are necessary for the development of more effective therapeutics to treat and prevent infections.

Evidence suggests that the arthropathy associated with CHIKV and RRV infections is immune-mediated, resulting from the activation of host inflammatory

pathways (51, 53, 54, 57, 172, 175, 232, 233). Human cases and mouse models of RRV-induced arthritis/myositis have demonstrated that complement activation correlates with an enhancement in disease (58-60). The complement pathway that is implicated in mediating RRV pathogenesis is the lectin pathway, which utilizes the soluble mannose-biding lectin (MBL) protein to bind carbohydrate moieties on the surface of pathogens and mediate activation of the downstream complement cascade (60, 234). Mice deficient in the central complement component 3 (C3), complement receptor 3 (CR3), or MBL are resistant to RRV-induced morbidity and tissue damage, while mice deficient in components of the classical pathway (C1q) or the alternative pathway (Factor B) of complement activation develop disease similar to wild-type (WT) mice (58-60). Moreover, serum MBL concentrations are enhanced in RRV-infected individuals and directly correlate with severity of RRV-induced polyarthritis (60).

Additionally, toll-like receptors (TLRs), which are innate immune receptors that recognize pathogen-associated molecular patterns on microbes, also play a role in the development of RRV-induced disease (64, 235). Upon stimulation by foreign pathogens or other TLR ligands, TLRs mediate signal transduction to promote antiviral responses such as type I interferon and pro-inflammatory cytokine signaling (64). We recently demonstrated that TLR7, which recognizes ssRNA, and its sole adaptor molecule, myeloid differentiation primary response gene 88 (Myd88), mediate protection from severe RRV-induced morbidity and mortality (64, 235). Furthermore, despite showing high titers of virus-specific antibodies, $TLR7^{-/-}$ mice produced lower affinity and less neutralizing RRV-specific antibodies, indicating that Myd88-dependent TLR7 signaling is critical for the development of protective adaptive immune responses to RRV infection

(235). However, the mechanism(s) of exacerbated RRV-induced disease in TLR7-deficient mice have not been reported.

To determine the mechanism of enhanced disease in the absence of Myd88-dependent TLR7 signaling, we evaluated whether the defective antibody responses in TLR7-deficient mice were directly inducing pathology during RRV infection. Because mice that lack functional B cells (μMT) show a similar disease progression as WT mice during RRV infection, we first assessed whether passive transfer of RRV-specific antisera from TLR7- or Myd88-deficient mice was protective or pathologic in infected μMT mice. The data reported here demonstrate that RRV-specific antisera from TLR7$^{-/-}$ mice induced increased morbidity and tissue destruction than WT antisera in μMT mice during *de novo* RRV infection. Additionally, TLR7- and Myd88-deficient mice exhibited enhanced antibody and complement deposition in RRV-infected skeletal muscle tissue, while infected WT mice failed to show antibody deposition. Moreover, mice deficient in TLR7 showed substantial focal cardiac pathology, which was also associated with antibody deposition and complement-dependent inflammatory activation. Furthermore, kidney pathology consistent with complement-dependent immune complex disease was evident in RRV-infected Myd88$^{-/-}$ mice, and mice deficient in both TLR7 and C1q (TLR7xC1q DKO), which are unable to activate the antibody-dependent classical complement pathway, developed disease similar to WT mice following RRV infection. Taken together, these data suggest that the Myd88-dependent TLR7 signaling pathway protects mice from systemic antibody- and complement-dependent exacerbation of RRV-induced disease.

3.3 Materials and Methods

Virus stocks and cells. Viral infections were performed using the mouse-adapted T48 strain of Ross River virus (RRV), which were generated from the T48 cDNA infectious clone (generously provided by Richard Kuhn, Purdue University) as (55)previously described . Titrations of viral stocks were determined by plaque assay on Vero cell monolayers, grown in DMEM/F12 (Gibco) with 10% Hyclone FBS, 1% non-essential amino acids, 1% Pen/Strep, 2.5% $NaHCO_3$ (Gibco) and 1% L-glutamine, as described previously (53).

Mouse experiments. C57BL/6J wild-type (WT), TLR7-deficient ($TLR7^{-/-}$), Myd88-deficient ($Myd88^{-/-}$), and μMT mice were obtained from The Jackson Laboratory (Bar Harbor, ME). C1q-deficient ($C1q^{-/-}$) mice were obtained from Michael Diamond at Washington University. Mice deficient in both TLR7 and C1q (TLR7xC1q DKO) were generated by our laboratory. All of the mice were maintained on a C57BL/6 background and bred in-house. All of the mouse studies were performed in a biosafety level 3 laboratory in accordance with UNC-CH Institutional Animal Care and Use Committee guidelines. Twenty-four day old mice were used for all *in vivo* RRV infection studies and infections were performed as described previously (235). Briefly, mice were anesthetized with isoflurane (Halocarbon Laboratories) prior to subcutaneous footpad inoculation with 10 μl of 10^3 PFU of RRV in phosphate-buffered saline (PBS) diluent or mock-infected with PBS diluent alone. Mice were monitored daily for weight loss and clinical disease signs. Clinical disease was scored on a scale from 0-5 by assessing grip strength, hind-limb weakness and altered gait as described previously (53, 235).

Passive serum transfer. Twenty-four day old WT, TLR7$^{-/-}$ and Myd88$^{-/-}$ mice were subcutaneously infected in the left rear footpad with 10^3 PFU of RRV and subsequently harvested at day 10 post-infection by exsanguination. Serum from each strain of infected mice was collected, pooled according to strain, and heat-inactivated at 56ºC for 1 hour. Twenty-four day old naïve μMT mice were then subcutaneously infected in the left rear footpad with 10^3 PFU of RRV and received intraperitoneal inoculations at 4, 6, and 8 days post-RRV infection with 50 μl of the heat-inactivated WT, TLR7$^{-/-}$ or Myd88$^{-/-}$ antisera. All of the infected mice were monitored daily for weight loss and disease signs as described above.

Histological analysis. At 10 days post-infection, mice were sacrificed and perfused with 4% paraformaldehyde, pH 7.3, and tissues were excised for histology. Excised tissues were paraffin-embedded, and 5-μm sections were prepared and stained with hematoxylin and eosin (H & E) (53).

Immunohistochemistry (IHC) staining. Mock- and RRV-infected animals were sacrificed at 10 days post-infection and perfused with 4% paraformaldehyde, pH 7.3. Excised tissues were paraffin-embedded, and 5-μm unstained sections were prepared. To determine the extent of complement or antibody deposition in RRV-infected tissues, the sections were deparaffinized in xylene, rehydrated through an ethanol gradient, and then probed with a goat anti-mouse complement component 3 (C3) polyclonal antibody (1:500, Cappel) or a goat anti-mouse immunoglobulin (IgG) antibody (1:500, Southern Biotech) using the Vectastain ABC-AP kit (Vector Labs, CA) and the Vector Blue alkaline phosphatase substrate kit (Vector Labs, CA) according to the manufacturers'

instructions. Sections were then counterstained with Gill's hematoxylin. C3 or IgG deposition is indicated by a dark blue/violet stain within the tissues.

DNP-KLH Immunizations. 8-10 week old WT and TLR7$^{-/-}$ mice were anesthetized with isoflurane and immunized subcutaneously with a formulation of dinitrophenyl (DNP) conjugated to keyhole limpet hemocyanin (KLH) (DNP-KLH, Calbiochem) with alum at 1 μg of DNP/mouse. Immunized mice were boosted at 3 weeks post-prime (wpp) with 1 μg/mouse DNP-KLH only. Sera was collected from the mice via tail bleeding at 1 wpp, 3 wpp, 1 week post-boost (wpb), and 3 wpb, heat-inactivated at 56 ºC for 1 hour, and then stored at 4°C until used for subsequent analyses.

Enzyme-linked immunosorbent assay (ELISA). Quantitation of antibody titers was performed by ELISA as described previously, with minor modifications (235). Briefly, DNP-specific antibody titers in the sera of WT and TLR7$^{-/-}$ DNP-KLH immunized mice were determined by ELISA using DNP-coated (1μg/ml) high-binding 96-well plates. The serum was first diluted 50 to 100-fold and then further diluted by two-fold serial dilutions. ELISA antibody titers are expressed as the estimated dilution factor that gave an $OD_{450} = 0.2$, which is obtained following nonlinear regression analysis of the serial dilution curve. Antigen-bound antibody is detected using an HRP-conjugated goat anti-mouse secondary antibody (Abcam, Cambridge, MA) and ABTS substrate (Invitrogen).

Antibody Affinity ELISA. Antibody affinity ELISAs were performed as previously described, with minor modifications (235). In brief, DNP-specific antibody titers in the sera of WT and TLR7$^{-/-}$ DNP-KLH immunized mice were first determined by ELISA as described above. To determine antibody affinity, sera was diluted in antibody diluent (PBS containing 0.05% Tween-20 and 10% Sigma Block), plated on DNP-coated

(1μg/ml) high-binding 96 well plates at an optimal dilution to obtain maximum antibody-antigen binding, and then incubated at 4ºC for 2 hours. Following the incubation period, the plates were washed and increasing concentrations of sodium thiocyanate (NaSCN) were added to the plate to serially dissociate the antibody-antigen complexes. The plates were washed and then incubated with an HRP-conjugated secondary IgG antibody, washed, and then incubated with the substrate as described in the ELISA protocol above. Values were reported as the percent maximum total IgG binding at each NaSCN concentration.

Statistical analyses. Data were analyzed using Prism software (GraphPad Software, Inc.). Comparisons of one-variable data were performed using a two-tailed unpaired Student's *t* test. Percent starting weight was analyzed using a one-way ANOVA with multiple comparisons corrections ($P<0.01$ is considered significant). Clinical scores were analyzed by Mann-Whitney analysis with Bonferroni's correction ($P<0.01$ is considered significant). Bar graphs represent mean values ± standard deviation. Significant differences are represented by comparison (*) with the following legend: *$P\leq0.01$, **$P\leq0.001$, unless otherwise indicated.

3.4 Results

Passive transfer of antisera from TLR7- and Myd88-deficient mice is pathologic in B cell-deficient mice during de novo RRV infection.

Host innate immune pathways are critical mediators of arthritogenic alphavirus-induced disease (51, 56-59, 175). We have previously shown that the Myd88-dependent TLR7 signaling pathway protects mice from severe RRV-induced disease and mortality, and TLR7 signaling is required for the development of protective, neutralizing virus-specific antibody responses (235). We have also shown that μMT mice, which lack functional B cells, do not show enhanced disease following RRV infection (53). Because Myd88- and TLR7-deficient mice showed enhanced non-neutralizing virus-specific antibody responses, we hypothesized that perhaps the low affinity, non-neutralizing antibody produced by the knockout mice was resulting in antibody-mediated immunopathogy (236). To determine whether the RRV-specific antibody induced in the absence of Myd88-dependent TLR7 signaling was pathologic in the context of infection, we evaluated the effects of passively transferred RRV-specific antisera from C57BL/6J wild-type (WT), Myd88-deficient ($Myd88^{-/-}$) and TLR7-deficient ($TLR7^{-/-}$) mice into μMT mice during *de novo* RRV infection. As shown in Figure 3.1, passive transfer of RRV-specific antisera from TLR7- or Myd88-deficient mice to RRV-infected μMT mice resulted in increased weight loss and clinical disease scores compared to mice that received WT antisera (Figure 3.1A-D). Although the antisera from all of the strains induced disease signs in the μMT mice, mice that receive antisera from $Myd88^{-/-}$ mice

showed significantly enhanced disease compared to the mice that received WT antisera (Figure 3.1D).

Moreover, histological analysis of the quadriceps tissues from the RRV-infected μMT at day 10 post-infected revealed that the mice that received antisera from TLR7$^{-/-}$ mice showed profoundly more skeletal muscle damage compared to the mice that received WT antisera (Figure 3.1E). The μMT mice that received antisera from TLR7-deficient mice showed significant skeletal muscle destruction and pronounced tissue necrosis, which was absent in the mice that received WT antisera (Figure 3.1E). Furthermore, because antibody-antigen complexes can deposit in renal tissues and induce kidney pathology, we analyzed the kidneys from RRV-infected μMT mice that received WT or Myd88-deficient antisera (237). While mice that received WT antisera showed normal kidney morphology, with round intact glomeruli and ordered interstitial spaces, mice that received antisera from Myd88-deficient mice showed collapsed, deformed glomeruli and dysregulated interstitial spaces with evidence of tissue necrosis (Figure 3.1F). Taken together, these data indicate that the antisera from Myd88- and TLR7-deficient mice induced increased weight loss and tissue damage in μMT mice during *de novo* RRV infection. Furthermore, because the sera was heat-inactivated prior to performing the passive transfer experiments, these findings suggest that the antibody present in the RRV-specific antisera from Myd88- and TLR7-deficient mice was responsible for the enhanced pathology observed in μMT mice.

TLR7- and Myd88-deficient mice show enhanced IgG and C3 deposition in RRV-infected muscle tissue.

It is known that antibody generated during viral infection can bind to infected cells and exert several functions to mediate cell death (236). Additionally, we have previously demonstrated that Myd88- and TLR7-deficient mice show significantly enhanced RRV-induced tissue damage compared to WT mice (235). Because antisera from Myd88- and TLR7-deficient mice was pathologic in RRV-infected μMT mice, we hypothesized that the pathologic antibody was forming immunoglobulin (IgG) complexes and depositing on RRV-infected tissue, leading to exacerbated antibody-induced cellular cytotoxicity. To address whether antibody deposition was occurring in the tissues of Myd88- and TLR7-deficient mice during RRV infection, we performed immunohistochemistry (IHC) staining for IgG on RRV-targeted skeletal muscle tissues from WT, $Myd88^{-/-}$, and $TLR7^{-/-}$ mice at day 10 post-RRV infection. The IHC analyses demonstrated that Myd88- and TLR7-deficient mice showed substantial IgG deposition in quadriceps tissues following RRV infection, while WT-infected skeletal muscle tissue failed to show IgG deposition (Figure 3.2).

Complement activation is known to play an important role in RRV pathogenesis (58-60). Additionally, antibody complex formation can result in complement fixation and activation, a reaction known as serum sickness, which leads to inflammatory responses that typically result in cellular cytotoxicity (238-240). Because antibody deposition can induce complement-dependent cytotoxicity (CDC), we sought to determine whether complement deposition was enhanced in Myd88- and TLR7-deficient mice during RRV infection (236). Therefore, we performed IHC analyses on RRV-infected quadriceps

tissues from WT, Myd88$^{-/-}$, and TLR7$^{-/-}$ mice to determine the extent of complement deposition as indicated by the presence of the central complement component 3 (C3). As shown in Figure 3.2, RRV-infected skeletal muscle tissue from Myd88- and TLR7-deficient mice showed considerably more C3 deposition than RRV-infected tissues from WT mice (Figure 3.2). Taken together, these results indicate that both antibody and complement deposition is enhanced in the skeletal muscle tissue of Myd88- and TLR7-deficient mice following RRV infection. Moreover, the increased antibody and complement deposition observed directly correlates with the enhanced skeletal muscle damage incurred in Myd88- and TLR7-deficient mice, suggesting that Myd88-dependent TLR7 signaling protects mice from antibody-mediated CDC during RRV infection.

Myd88- and TLR7-deficient mice show severe cardiac muscle damage following RRV infection.

Following RRV infection, mice deficient in Myd88 or TLR7 succumb to virus-induced disease by 10 days post-infection, while WT mice recover from the infection and are indistinguishable from mock-infected animals by 30 days post-infection (53, 235). Additionally, Myd88- and TLR7-deficient mice show aberrant adaptive immune responses to RRV infection, and dysregulated immune responses to viral infection can reportedly result in cardiomyopathy and cardiac arrest (235, 241, 242). Therefore, we examined cardiac tissues from RRV-infected WT, Myd88$^{-/-}$, and TLR7$^{-/-}$ mice to determine whether RRV infection resulted in myocardial damage in the absence of Myd88-dependent TLR7 signaling. Histological analyses of cardiac muscle tissue at 10 days post-infection from WT, Myd88$^{-/-}$, and TLR7$^{-/-}$ mice revealed that Myd88- and TLR7-deficient mice developed severe myocardial pathology during RRV infection,

which is absent in WT mice (Figure 3.3). While RRV-infected cardiac tissue from WT mice appeared similar to mock-infected tissues, the myocardial tissues from Myd88- and TLR7-deficient mice contained multiple focal lesions of necrotic tissue (Figure 3.3). Thus, these results demonstrated that Myd88-dependent TLR7 signaling prevents the development of myocardial damage during RRV infection.

Cardiac damage in TLR7-deficient mice is induced by antibody-mediated complement activation during RRV infection.

Non-neutralizing antibody induced by viral infection can promote tissue pathology and can lead to cardiac disease in the case of coxsackieviruses (243). Because Myd88- and TLR7-deficient mice exhibited cardiac pathology following RRV infection, we hypothesized that the high level of low-affinity, non-neutralizing antibody produced in the deficient animals could be depositing on RRV-infected cardiac muscle and inducing the observed pathology. As shown in Figure 3.4, the myocardial tissues from TLR7- and Myd88-deficient mice showed focal IgG deposition at 10 days post-RRV infection, while IgG deposition was not detected in WT cardiac tissues (Figure 3.4A). Moreover, because we detected both IgG and C3 deposition in the skeletal muscle tissue of RRV-infected TLR7- and Myd88-deficient mice, we further probed the cardiac tissues of Myd88- and TLR7-deficient mice for C3 deposition. Although C3 deposition was not present in WT cardiac tissues, mice deficient in Myd88 or TLR7 showed significant C3 deposition in myocardial tissues (Figure 3.4A). These findings indicate that deficiency in Myd88-dependent TLR7 signaling during RRV infection results in antibody and complement deposition in myocardial tissues, and antibody-mediated CDC may result in cardiac damage in the RRV-infected Myd88- and TLR7-deficient mice.

Complement and inflammatory cytokine activity in the heart has been linked to cardiac dysfunction and damage (244-249). Because C3 deposition was prominently detected in the cardiac tissues of Myd88- and TLR7-deficient mice following RRV infection, we sought to assess the expression levels of C3 and other inflammatory markers in RRV-infected myocardial tissues by quantitative real-time PCR (qRT-PCR). The qRT-PCR analyses revealed that TLR7$^{-/-}$ mice showed upregulation of C3 and multiple pro-inflammatory markers in cardiac tissues at 2 and 7 days post-RRV infection (Figure 3.4B). At 2 days post-infection, IL-6 and Arginase-1 (Arg1) expression was significantly upregulated in TLR7-deficient mice compared to WT mice (Figure 4B). Additionally, IL-1β, TNF, and the calgranulins, s100A8 and s100A9, were increased in the myocardial tissues of TLR7$^{-/-}$ mice relative to WT mice at 2 days post-RRV infection (Figure 3.4B). Furthermore, the expression levels of s100A8, s100A9, and Arg1 were enhanced in the cardiac tissues of TLR7-deficient mice at 7 days post-infection (Figure 3.4B). These results suggest that deficiency in Myd88-dependent TLR7 signaling results in pro-inflammatory responses that may damage or suppress cardiac function during RRV infection.

Myd88-deficient mice show IgG and C3 deposition in the kidneys following RRV infection.

Immune complex formation associated with serum sickness can generate kidney pathology (237). Additionally, C3 expression that is induced by antibody-associated complexes in the kidney is associated with renal injury (237, 250). To determine whether Myd88$^{-/-}$ mice developed immune complex-associated nephropathology following RRV infection, we performed IHC analyses on kidneys obtained from WT and Myd88-

deficient mice at 10 days post-RRV infection (Figure 3.5). While RRV-infected WT mice failed to show IgG or C3 deposition, the glomeruli and interstitial regions of the kidneys from Myd88-deficient mice showed both IgG and C3 deposition, indicative of immune complex deposition (Figure 3.5). Additionally, histological analyses of the kidneys revealed normal renal anatomy in the RRV-infected WT mice. However, several glomeruli in the Myd88-deficient mice appeared abnormally shaped and collapsed following RRV infection (Figure 3.5). Mock-infected kidneys showed normal renal anatomy and looked similar to RRV-infected WT kidneys (data not shown). Therefore, these results indicate that Myd88-deficient mice develop immune complex-induced renal disease during RRV infection.

C1q mediates enhanced disease in TLR7-deficient mice during RRV infection.

Because Myd88- and TLR7-deficient mice showed evidence of systemic complement- and antibody-mediated pathology during RRV infection, we hypothesized that the antibody-mediated CDC was resulting from the classical complement pathway, wherein C1q binds to antibody complexes to trigger downstream complement activation (234). Additionally, because C1q-deficient mice develop disease similar to WT mice following RRV infection, we hypothesized that in the absence of C1q, TLR7-deficient mice would not exhibit enhanced RRV-induced disease (60). Thus, we generated mice that were deficient in both TLR7 and C1q (TLR7xC1q DKO) and observed them over a 10-day timecourse of RRV infection. Following RRV infection, mice deficient in TLR7 and C1q developed a disease similar to WT mice, showing comparable weight loss and clinical scores (data not shown). Additionally, histological analyses of quadriceps muscles revealed that TLR7xC1q DKO mice did not show enhanced tissue destruction

compared to WT tissues at 10 days post-RRV infection (Figure 3.6). While Myd88$^{-/-}$ mice showed profound destruction of skeletal muscle tissue, the skeletal muscle tissues of TLR7xC1q DKO mice were less damaged than that of Myd88-deficient mice and showed a similar degree of damage to the skeletal muscle tissues of WT and C1q$^{-/-}$ mice (Figure 3.6).

These data indicate that C1q mediates antibody-mediated CDC in TLR7-deficient mice and further that Myd88-dependent TLR7 signaling is required for protection from systemic antibody-mediated CDC during RRV infection.

3.5 Discussion

We have previously shown that Myd88-dependent TLR7 signaling mediates protection from severe RRV-induced morbidity and mortality and that TLR7 is required for the development of a protective adaptive immune response to RRV infection (235). However, the mechanism of RRV-induced disease enhancement that occurs in the absence of Myd88-dependent TLR7 signaling had not yet been elucidated. The studies described herein demonstrate that Myd88-dependent TLR7 signaling is required for protection against systemic antibody- and complement-associated disease during RRV infection. The passive transfer of antisera from RRV-infected TLR7- and Myd88-deficient mice resulted in enhanced morbidity and tissue pathology in B cell-deficient mice, and both TLR7- and Myd88-deficient mice exhibited pronounced antibody-associated complement deposition in RRV-infected skeletal muscle tissues. Furthermore,

RRV-infected mice developed severe myocardial damage in the absence of TLR7 or Myd88, and both antibody and complement deposition was observed in the diseased cardiac tissues of TLR7- and Myd88-deficient animals following RRV infection. Additionally, the expression of complement and other pro-inflammatory markers such as IL-6, TNF-α, and IL-1β that are associated with myocardial suppression were significantly enhanced in the cardiac muscles of TLR7-deficient mice (245-248). Nephrological analyses revealed antibody and complement deposition in the kidneys of RRV-infected Myd88$^{-/-}$ mice, indicative of immune complex deposition, and Myd88$^{-/-}$ mice presented evidence of renal pathology following RRV infection. Moreover, mice deficient in both TLR7 and C1q (TLR7xC1q DKO) did not show enhanced RRV-induced morbidity, suggesting that the exacerbated disease exhibited in infected TLR7-deficient mice is directly attributed to complement activation via the classical pathway. Therefore, these findings suggest that Myd88-dependent TLR7 signaling protects against immune-mediated enhancement of RRV-induced disease, and deficiencies in TLR7 signaling may lead to systemic antibody-mediated CDC during RRV infection.

The role of complement in mediating RRV-induced disease is well established (58-60). Previous reports have indicated that RRV infection results in MBL-dependent complement activation via the lectin pathway, which is activated by pathogen-associated carbohydrate moieties and is an antibody-independent mechanism of complement activation (60). Our data suggests that in the absence of Myd88-dependent TLR7 signaling, RRV infection results in antibody-dependent complement activation via the C1q-mediated classical pathway of the complement cascade. Moreover, while complement-mediated disease is restricted to the skeletal muscle tissue in RRV-infected

WT mice, mice deficient in Myd88 or TLR7 showed systemic manifestations of antibody-dependent CDC following RRV infection, with cardiac- and kidney-associated pathology. Furthermore, the antibody and complement deposition observed in the kidneys of RRV-infected Myd88$^{-/-}$ mice suggests that Myd88 deficiency leads to immune complex-induced serum sickness during RRV infection. Although complement fixation associated with serum sickness can be mediated by cellular infiltrates such as macrophages or neutrophils, we did not observe extensive renal inflammation that could explain leukocyte-mediated C3 deposition in the kidneys of RRV-infected Myd88-deficient mice (240). However, the observed complement deposition in Myd88-deficient mice can be explained through local production of C3 by glomerular epithelial or mesangial cells in the kidney (237, 240). Because renal glomerular cells express Fc receptors, they are capable of binding IgG from immune complexes and mediating complement expression. Additionally, the role of local complement production in renal disease is well-documented, and immune complex-mediated kidney disease has been observed in the absence of cellular inflammation (240).

Although Myd88 signaling reportedly induces cardiac damage in animal models of myocardial injury, this is the first study that we are aware of to demonstrate the role of Myd88 in protecting from myocardial disease during viral infection. Interestingly, there is limited evidence from severe disease cases that arthritogenic alphaviruses may play a role in the development or exacerbation of myocardial damage (251, 252). In one study, a young child was diagnosed with myocarditis and congestive heart failure associated with a severe CHIKV infection (252). Additionally, multiple cases of severe CHIKV-induced disease and fatalities have been associated with cardiomyopathy and/or heart failure,

some of whom had no evidence of pre-existing heart conditions or other co-morbidities (251, 253). Therefore, severe cases of arthritogenic alphavirus infections may lead to systemic complications that induce or exacerbate cardiac disease, and Myd88-dependent TLR7 signaling may protect from cardiac injury associated with alphavirus infection. In contrast, Myd88-deficient mice show reduced susceptibility to coxackievirus-induced myocarditis, indicating that the role of Myd88-dependent signaling in virus-associated cardiac injury may be dependent on the infectious agent (254).

Because Myd88- and TLR7-deficient mice exhibit increased viral loads in skeletal muscle tissues late during RRV infection, we hypothesized that the cardiac muscle pathology observed in the absence of Myd88 or TLR7 was attributable to enhanced viral loads in myocardial tissues (235). However, plaque assay analyses revealed similar viral loads in the cardiac tissues of WT, Myd88$^{-/-}$, and TLR7$^{-/-}$ mice early during RRV infection, and virus was undetectable in by 5 days post-infection in all of the strains (data not shown). Cases of fatal virus-associated myocardiac disease have been reported in the absence of infectious virus, such as with B19 parvovirus, encephalomyocarditis virus coxackievirus infections (249, 255). Although we do not detect infectious virus in the cardiac tissue late during infection, it is possible that the viral RNA may persist in the cardiac tissue at low levels and is sufficient to induce antibody-mediated CDC. This phenomenon has been demonstrated with picornavirus infections, whereby persistent viral genomic material in cardiac tissue can induce inflammatory responses such as myocarditis (249, 256, 257). Further studies will be necessary to determine whether the myocardial injury observed in Myd88- and TLR7-deficient mice is dependent on persistent viral RNA expression.

Myd88-dependent TLR7 signaling has been demonstrated to be required for efficient neutralizing antibody production by B cells during multiple viral infections, including alphavirus infections (80, 93, 96, 235). Thus, one mechanism to explain antibody-mediated CDC in the cardiac tissues of Myd88- and TLR7-deficient mice in the absence of viral replication or RNA persistence could be through epitope spreading, whereby autoantibodies to host tissues are produced during viral infection and can cross react with other host tissues (249, 258). In this model, autoantibodies produced during RRV infection in the absence of TLR7 signaling could be directed towards skeletal muscle antigens such as myosin, and these muscle-directed antibodies may cross-react with cardiac muscle tissue and lead to cardiac tissue damage. Follow-up studies will be needed to determine whether autoantibodies are generated in TLR7- and Myd88-deficient mice during RRV infection.

Some reports suggest that TLR stimulation promotes B cell differentiation and germinal center responses, which enables activated B cells to undergo somatic hypermutation and class switch recombination to produce affinity-matured, antigen-specific antibodies (80). Additionally, TLR7 deficiency leads to defective germinal center formation during retrovirus and alphavirus infections in mice, resulting in the production of antibody with reduced affinity and neutralization capacities for viral antigens (93, 235). However, because the role of TLR7 in B cell antibody functionality has only been reported in response to viruses or TLR7 agonists, we sought to determine whether TLR7 deficiency could affect the quality of antibody produced in response to antigens that are not known to directly stimulate TLR7 (93, 96, 235, 259, 260). Thus, we immunized WT and TLR7-deficient mice with a hapten-protein conjugate formulation of DNP-KLH on a

prime-boost schedule and found that DNP-specific antibody from TLR7$^{-/-}$ mice showed significant defects in antigen affinity at 1 week post-prime compared to the antibody from WT mice, despite showing similar levels of total DNP-specific IgG throughout the experiment (3.7A and B). However, DNP-associated antibody affinity was improved in TLR7-deficient mice following a secondary immunization, and the antibody generated from immunized WT and TLR7-deficient mice showed similar degrees of affinity for the immunogen at 1 week post-boost (3.7C). These findings are supported by a study demonstrating that Myd88-deficient mice, which are susceptible to primary influenza virus infection, are resistant to secondary infection when primed with a non-lethal dose of influenza virus (261). These results provide additional evidence that TLR7 plays a broad role in regulating antibody efficiency and suggest that therapeutic approaches to improve TLR7 signaling may aid in the development of protective humoral responses to vaccines and viral infections.

In summary, the data reported in this study demonstrate that Myd88-dependent TLR7 signaling protects mice from systemic antibody- and complement-mediated disease during RRV infection. Given the significant role that TLR7 signaling plays in the development of effective antibody responses to viral and non-viral stimuli, therapeutic strategies aimed at enhancing antibody efficacy may benefit from TLR7-directed stimulation.

Figure 3.1

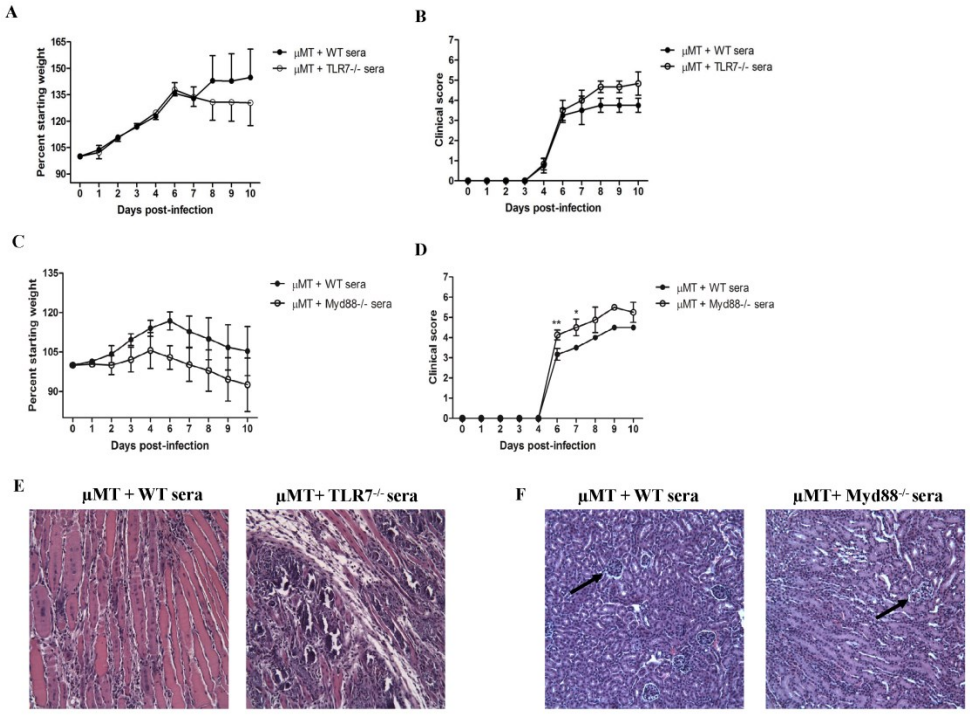

Figure 3.1: Passive transfer of antisera from TLR7- and Myd88-deficient mice is pathologic in B cell-deficient mice during *de novo* RRV infection.

Twenty-four day old B cell-deficient μMT mice were subcutaneously infected in the left rear footpad with 10^3 PFU of RRV and monitored for (A) & (C) weight loss and (B) & (D) clinical disease. At 4, 6, and 8 days post-infection, RRV-infected μMT mice received 50 μl intraperitoneal inoculations of RRV antisera from (A) & (B) day 10-infected C57BL/6J wild-type (WT) and $TLR7^{-/-}$ mice or (C) & (D) day 10-infected WT and $Myd88^{-/-}$ mice. N = 3-4 mice/strain/timepoint. *P ≤ 0.01 and **P≤0.001. (E) Mice were sacrificed and perfused with 4% paraformaldehyde at 10 days post-infection. Quadriceps (E) and kidney (F) tissues were excised and paraffin-embedded, and unstained 5 μm tissue sections were obtained for histological analyses. Arrows indicate glomeruli. Representative images are shown**.**

Figure 3.2

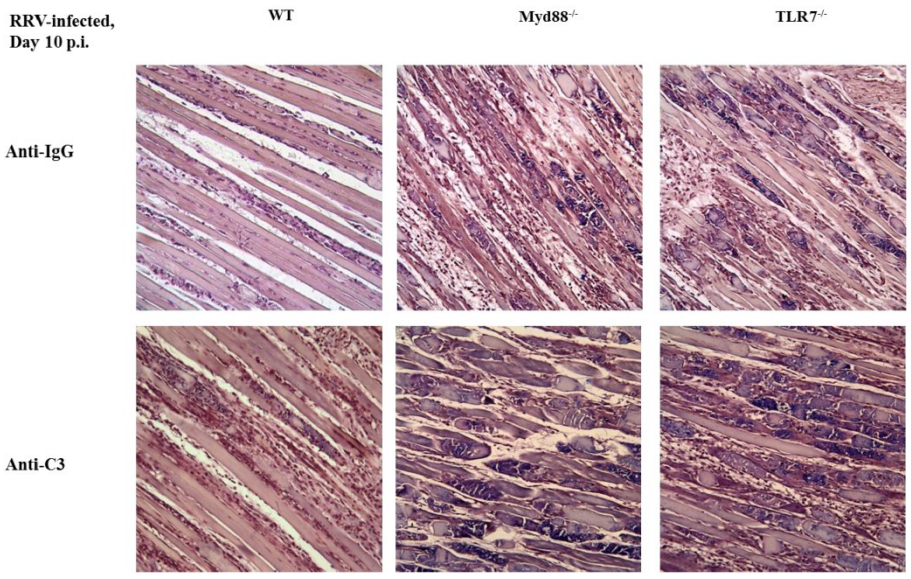

Figure 3.2: TLR7$^{-/-}$ mice show enhanced IgG and C3 deposition in RRV-infected muscle tissue.

Twenty-four day old WT, Myd88$^{-/-}$, and TLR7$^{-/-}$ mice were subcutaneously infected in the left rear footpad with either PBS diluent or 10^3 PFU of RRV. Mice were sacrificed and perfused with 4% paraformaldehyde at 10 days post-infection. Quadriceps muscles were excised and paraffin-embedded, and unstained 5 μm tissue sections were obtained for immunohistochemistry (IHC) and coutnerstained with Gill's hemotoxylin as described in Materials and Methods. IHC staining for murine immunoglobulin (IgG) and complement component 3 (C3) deposition in RRV-infected quadriceps muscle tissue is indicated by dark blue/violet staining at areas of tissue damage. Representative images are shown.

Figure 3.3

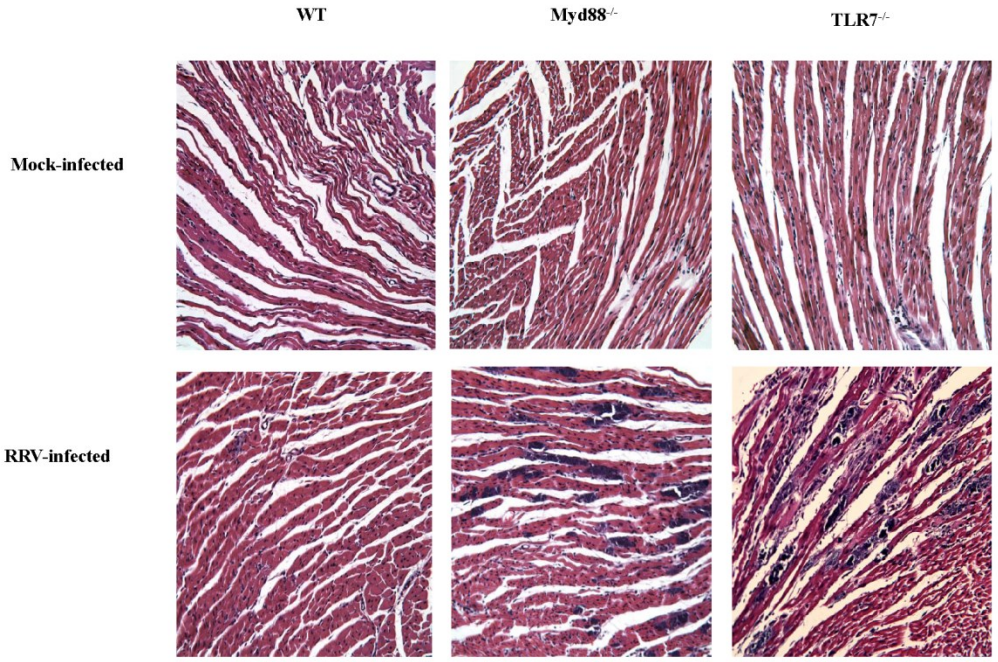

Figure 3.3: Myd88- and TLR7-deficient mice show severe cardiac muscle tissue damage following RRV infection.

Twenty-four day old WT, TLR7$^{-/-}$ and Myd88$^{-/-}$ mice were subcutaneously infected in the left rear footpad with either PBS diluent or 10^3 PFU of RRV. Mice were sacrificed and perfused with 4% paraformaldehyde at 10 days post-infection. Cardiac tissues were excised and paraffin-embedded, and unstained 5 µm tissue sections were obtained for histological analyses. Representative images are shown.

Figure 3.4

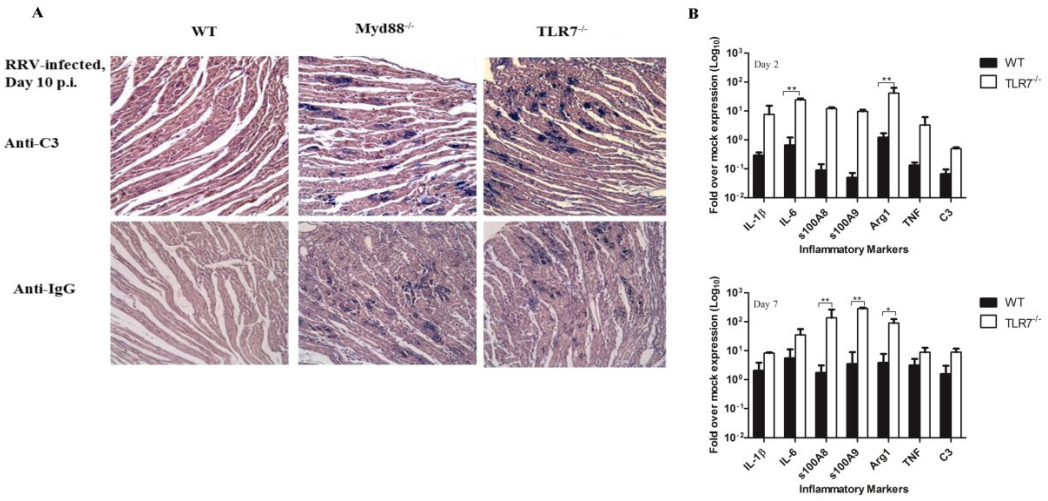

Figure 3.4: Myd88^{-} and TLR7-deficient mice show IgG and C3 deposition in cardiac muscle tissue following RRV infection.

Twenty-four day old WT, Myd88$^{-/-}$ and TLR7$^{-/-}$ mice were subcutaneously infected in the left rear footpad with either PBS diluent or 10^3 PFU of RRV. (A) Mice were sacrificed and perfused with 4% paraformaldehyde at 10 days post-infection. Cardiac tissue were excised and paraffin-embedded, and unstained 5 μm tissue sections were obtained for IHC and coutnerstained with Gill's hemotoxylin as described in Materials and Methods. IHC staining for IgG and C3 deposition in RRV-infected cardiac tissue from WT, Myd88$^{-/-}$ and TLR7$^{-/-}$ mice at day 10 post-infection is indicated by dark blue/violet staining at areas of tissue damage. Representative images are shown. (B) & (C) At 2 and 7 days post-infection, mice were sacrificed by exsanguination and cardiac tissues were dissected. Total RNA was isolated from cardiac tissues, reverse transcribed, and analyzed for cytokine expression by quantitative Real-time PCR as described in Materials and Methods. The inflammatory markers analyzed included IL-1β, IL-6., s100A8, s100A9, Arginase-1 (Arg1), TNF, and C3. *P≤0.01 and **P≤0.001.

Figure 3.5

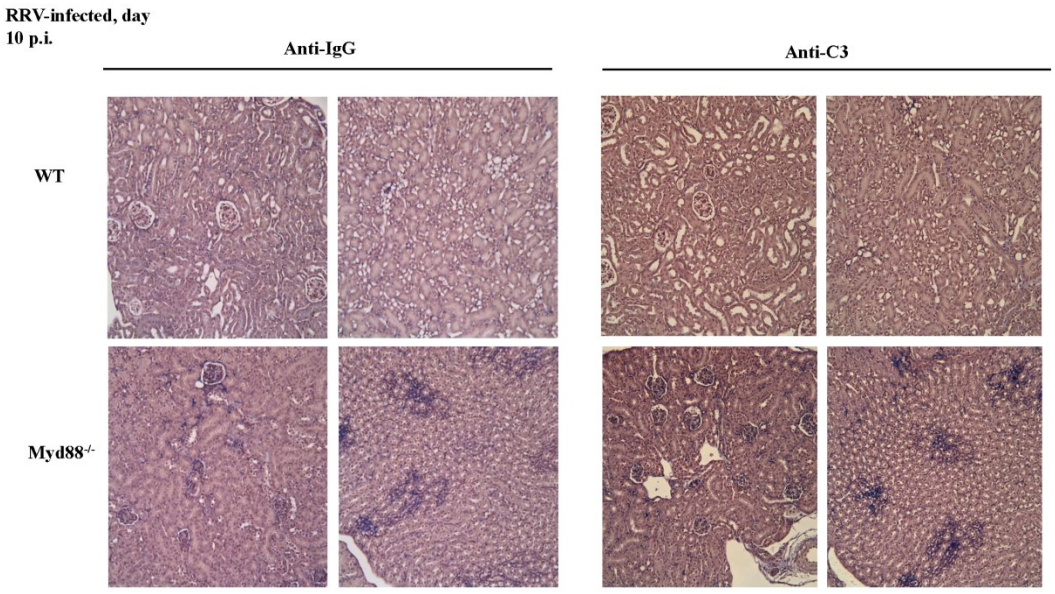

Figure 3.5: Myd88$^{-/-}$ mice show IgG and C3 deposition in the kidneys following RRV infection.

Twenty-four day old WT and Myd88$^{-/-}$ mice were subcutaneously infected in the left rear footpad with either PBS diluent or 10^3 PFU of RRV. Mice were sacrificed and perfused with 4% paraformaldehyde at 10 days post-infection. Kidneys were excised and paraffin-embedded, and unstained 5 µm tissue sections were obtained for IHC and coutnerstained with Gill's hemotoxylin as described in Materials and Methods. IHC staining for IgG and C3 deposition in RRV-infected kidneys from WT and Myd88$^{-/-}$ mice at day 10 post-infection is indicated by dark blue/violet staining. Representative images are shown.

Figure 3.6

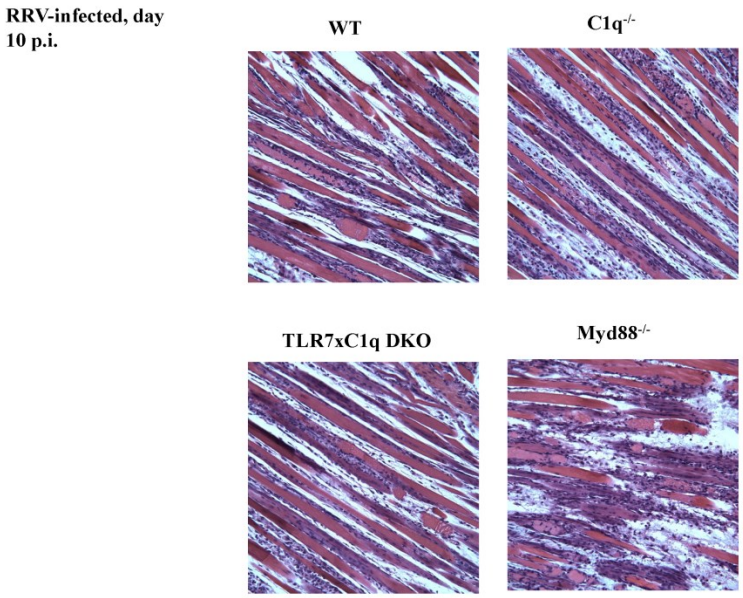

Figure 3.6: TLR7xC1q DKO mice do not show enhanced disease following RRV infection.

Twenty-four day old WT, $C1q^{-/-}$, TLR7xC1q DKO, and $Myd88^{-/-}$ mice were subcutaneously infected in the left rear footpad with 10^3 PFU of RRV. At day 10 post-infected, mice were sacrificed, and quadriceps tissues were excised and prepared for histological analyses as described in Materials and Methods. N = 3-4 mice/strain.

Figure 3.7

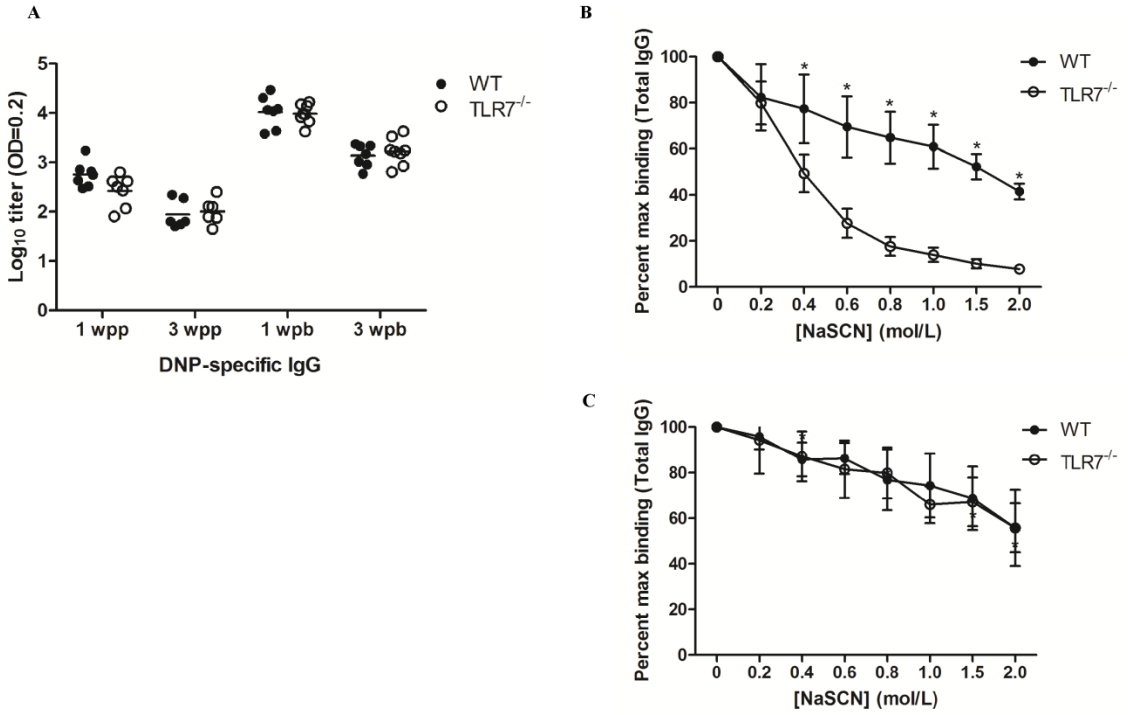

Figure 3.7: TLR7 regulates antibody affinity responses to non-RNA stimuli. 8-10 week old WT and TLR7$^{-/-}$ mice were immunized subcutaneously with a formulation of dinitrophenyl (DNP) conjugated to keyhole limpet hemocyanin (KLH) with alum at 1 µg of DNP/mouse. Immunized mice were boosted at 3 weeks post-prime (wpp) with 1 µg/mouse DNP-KLH only. Sera was collected from the mice via tail bleeding at 1 wpp, 3 wpp, 1 week post-boost (wpb), and 3 wpb.(A) Sera from immunized WT and TLR7$^{-/-}$ mice was analyzed at each indicated timepoint for total DNP-specific IgG titers by ELISA as described in Materials and Methods. (B) & (C) Antibody affinity of DNP-specific IgG was measured by affinity ELISA as described in Materials Methods at (B) 3 wpp and (C) 1 wpb. N = 6-8 mice/strain/timepoint. *P ≤0.0001.

CHAPTER FOUR:

TLR4 PROMOTES ROSS RIVER VIRUS-INDUCED DISEASE IN MICE

4.1 Overview

Arthritis-associated alphaviruses, such as chikungunya virus and Ross River virus (RRV) are mosquito-transmitted pathogens that cause severe arthritis and myositis in infected individuals. Host inflammatory pathways play a major role in regulating the alphavirus-induced disease process, with some pathways such as the complement cascade contributing to disease, while other pathways such as TLR7-dependent signaling mediating protection. To further investigate the role of TLRs in alphavirus-induced disease, we evaluated TLR4, which has been linked to other inflammatory diseases, for its role in RRV-induced arthritis and myositis. Using a mouse model of RRV-induced arthritis/myositis, we evaluated TLR4 deficient mice for disease susceptibility and demonstrated that TLR4 is essential for the development of RRV-induced disease and inflammatory tissue damage. Despite markedly different outcomes in disease, TLR4-deficient and WT mice showed similar viral loads throughout the course of infection, suggesting that the disease mediated by TLR4 is independent of RRV replication. Moreover, TLR4-deficient mice showed reduced complement deposition and activation in RRV-targeted skeletal muscle tissue compared to WT mice, and macrophages deficient

[†]Lauren M. Neighbours, Kristin Long, Alan C. Whitmore, and Mark T. Heise.
Departments of Microbiology & Immunology and Genetics, UNC-Chapel Hill.
Submitted to *PLoS Pathogens*, March 8, 2013.

in TLR4 exhibited reduced expression of complement component 3 (C3) following co-culture with RRV-infected myotubes. These results demonstrate a unique role for TLR4 in regulating complement production and subsequent disease development during alphavirus-induced arthritis and suggest that specifically targeting TLR4 dependent signaling pathways may provide therapeutic benefits in the treatment of alphavirus-induced arthritis.

4.2 Introduction

Arthropod-bourne alphaviruses are associated with significant outbreaks of infectious polyarthritis or encephalitis in humans (4, 5, 45). Furthermore, because of their broad vector distribution, many of these viruses, including chikungunya virus (CHIKV) and Ross River virus (RRV) are capable of emerging in new regions and causing disease outbreaks affecting thousands to millions of individuals (16, 262-265). Although arthritis-associated alphaviruses are a significant emerging disease threat, there are currently no approved vaccines or virus-specific therapies for these viruses.

Old world arthritogenic alphaviruses such as CHIKV and RRV cause debilitating joint and muscle pain, stiffness, and swelling that can result in a chronic disease in some individuals (16, 42, 190-192). Inflammatory cells and pro-inflammatory cytokines are a prominent feature of RRV and CHIKV infection in humans (15). Mouse models of alphavirus-induced arthritis and myositis have demonstrated that the host inflammatory response directly mediates alphavirus pathogenesis, with inflammatory macrophages and

complement being required for the development of severe disease (51, 56-60, 175). Additionally, toll-like receptors (TLRs), which are pattern-recognition receptors that recognize conserved pathogen-associated molecular patterns, have been shown to be upregulated during alphavirus infection, and TLR7 signaling is required for protection from severe arthritogenic alphavirus morbidity and mortality in mice (64, 144, 195, 196, 235). However, it is currently unclear whether other TLR pathways play a role in the pathogenesis of alphavirus infection, and the downstream mechanisms of alphavirus-induced diseases remain poorly understood. Further characterization of the roles that host inflammatory pathways, including TLR responses, play in alphavirus-induced disease may lead to the development of targeted therapeutic strategies to treat affected individuals (192).

TLRs are critical mediators of antiviral immunity and have essential roles during acute and chronic viral infections (88, 100, 105, 108, 235, 266-276). TLR4, which recognizes bacterial lipopolysaccharide and other microbial components, has been demonstrated to function in both protective and pathologic capacities during RNA and DNA virus infections (100, 103-108). In addition to its varying roles in viral infections, TLR4 has been shown to be pathologic in human and mouse models of arthritis, which is attributed in part to its role in promoting joint inflammation (119-126). Additionally, two complement component 3 (C3)-dependent calgranulins, s100A8 and s100A9, which are upregulated during arthritogenic alphavirus infection, have been shown to be upregulated in a TLR4-dependent manner in human osteoarthritic chondrocytes and in the synovial fluid of osteoarthritic patients (59, 60, 132, 133). Moreover, *in vitro* studies have demonstrated that TLR4 signaling is modulated in a monocyte/macrophage cell line

through a direct interaction between the TLR4 signaling complex and mannose binding lectin (MBL), which is a critical mediator of complement-dependent alphavirus disease (60, 277, 278).

The aim of this study was to further evaluate the roles of host sensing pathways in the development of arthritogenic alphavirus-induced disease. Because TLR4 plays a significant role in multiple viral infections and is known to regulate a number of inflammatory disease processes, we hypothesized that TLR4 signaling may play a role in alphavirus-induced arthritis and myositis. To determine whether TLR4 contributes to RRV-induced disease, we evaluated the role of TLR4 in a mouse model of arthritis/myositis and found that mice deficient in TLR4 were resistant to RRV-induced morbidity. TLR4-deficient mice showed decreased clinical disease and tissue destruction compared to RRV-infected wild-type C57BL/6J (WT) mice, despite showing similar levels of viral replication in target tissues. Mice deficient in TLR4 also showed reduced complement deposition and activation in RRV-infected skeletal muscle tissue, suggesting that TLR4 is required for complement-mediated RRV pathogenesis. This was supported by results from a novel *in vitro* co-culture model, whereby we demonstrated that TLR4-deficient macrophages exhibited decreased complement production following co-culture with RRV-infected myotubes. Therefore, these studies indicate that TLR4 plays a major role in the pathogenesis of RRV induced disease by regulating the production of complement in response to viral infection.

4.3 Materials and Methods

Ethics Statement. Mouse studies were performed at University of North Carolina at Chapel Hill using protocols approved by the Institutional Animal Care and Use Committee (IACUC) in accordance with the recommendations in the Guide for the Care and Use of Laboratory Animals of the National Institutes of Health.

Virus stocks and cells. Ross River virus (RRV) stocks were generated from the mouse-virulent, full-length T48 cDNA clone (generously provided by Richard Kuhn, Purdue University) as previously described (55). Viral titrations were determined by plaque assay on Vero cells as described previously (235). Vero cells were grown in DMEM/F12 (Gibco) supplemented with 10% Hyclone FBS, 1% non-essential amino acids, 1% Pen/Strep, 2.5% $NaHCO_3$ (Gibco) and 1% L-glutamine.

Mouse experiments. C57BL/6J wild-type (WT) and TLR4-deficient ($TLR4^{-/-}$) mice were obtained from The Jackson Laboratory (Bar Harbor, ME), and breeding was maintained in-house. $TLR4^{-/-}$ mice were maintained on a C57BL/6 background and backcrossed onto the C57BL/6 background for an additional five generations (to obtain ten-generation backcrossed mice) prior to experimentation. Animal husbandry and experiments were conducted according to UNC-CH Institutional Animal Care and Use Committee guidelines. All of the *in vivo* mouse studies were executed in a biosafety level 3 laboratory and were performed with twenty-four day old mice. Mouse infections with RRV were performed as described previously (235). Briefly, mice were anesthetized with isoflurane (Halocarbon Laboratories) prior to subcutaneous inoculation in the left rear footpad with 10^3 PFU of RRV in a 10 μl volume of phosphate-buffered saline (PBS)

diluent. Mock-infected animals were inoculated with PBS diluent alone. Mice were weighed daily and monitored for the development of clinical disease signs. Disease scores were assigned on a scale from 0 to 5 based on gripping ability, hind-limb weakness and altered gait as described previously (53, 235).

Viral titers. Viral titers of RRV-infected tissues were determined by plaque assay as described previously (235). Briefly, mice were anesthetized and sacrificed by exsanguination. Quadriceps tissues were removed and homogenized, and serum was extracted prior to freezing at -80°C until viral titers were determined. Viral tissues were thawed on ice and subsequently diluted 10-fold in PBS diluent. 200 µl of the diluted samples were pipetted in duplicate into each well of 70% confluent Vero cells in 6-well plates. The samples were incubated on the cells for 1 hour at 37°C in a CO_2 incubator and gently agitated every 15 minutes to ensure an even distribution of the inoculum on the cells. After incubation, the cells were overlayed with an agar overlay solution containing 50% of 2.5% CMC (Sigma), 50% 2X Modified Eagles Media, 3% FBS, 1% Pen/Strep, 1% L-glutamine and 1% 1M HEPES buffer (Mediatech), and incubated for 48-72 hours at 37°C in a CO_2 incubator. Cells were then fixed with 4% paraformaldehyde for >2 hours, counterstained with a 0.25% Crystal Violet solution, and viral plaques were counted.

Histological analysis. At 10 days post-infection, mice were sacrificed and perfused via cardiac puncture with 4% paraformaldehyde, pH 7.3. Excised tissues were paraffin-embedded, and 5-µm sections were prepared. To determine the extent of inflammation and tissue pathology, tissues were stained with hematoxylin and eosin (H & E) (53). Stained sections were blind-scored for overall inflammatory cell infiltration and tissue

damage as described (53, 235). Both scoring systems utilized a 10-point scale wherein 0-3 represents no to mild inflammation/damage, 4-6 represents moderate inflammation/damage, and 7-10 represents severe inflammation/damage.

Flow cytometry. At 7 and 10 days post-infection, mice were inoculated with RRV as described above, sacrificed by exsanguination and perfused extensively with 1X PBS. Quadriceps muscles were excised, minced, and incubated for 1.5-2 hours with vigorous shaking at 37°C in digestion buffer (RPMI, 10% fetal bovine serum, 15 mM HEPES, 2.5 mg/ml collagenase A [Worthington Biochemical Co.], 17 μg/ml DNase I [Roche]). Following digestions, tissue samples were pelleted, resuspended in HFA buffer (Hanks balanced salt solution [Gibco], 1% fetal bovine serum, 0.1% sodium azide), passed through a 70 μm cell strainer, and centrifuged for 8 min at 1,000 rpm. Cells were resuspended in HFA buffer, and viable cell counts were determined by trypan blue exclusion. Isolated cells were incubated with various antibodies, according to the associated staining panel, for 30 min to an hour at 4°C in fluorescence-activated cell sorter staining buffer (1x Hanks balanced salt solution, 1% fetal bovine serum, 2% normal rabbit serum). Cells were washed, fixed overnight in 2% paraformaldehyde and analyzed on a Cyan cytometer (DAKO-Cytomation) using Summit software. Isolated splenocytes from mock-infected animals were prepared similarly and used for single-color staining controls. The lymphocyte staining panel included the following antibodies: anti-NK1.1-phycoerythrin (PE) (eBioscience), anti-CD3-fluorescein isothiocyanate (FITC) (eBioscience), anti-B220-PE Texas Red (PETR) (Invitrogen), anti-LCA-PECy5 (eBioscience), anti-F4/80-PECy7 (eBioscience), anti-CD4-pacific blue (PB) (Caltag Laboratories), anti-CD8-pacific orange (PO) (Invitrogen) and anti-CD49b-

allophycocyanin (APC) (eBioscience). The monocyte staining panel included the following antibodies: anti-Ly6G-FITC (BD Pharmingen), anti-SigLecF-PE (BD Pharmingen), anti-CD11c-PETR (Invitrogen), anti-LCA-PECy5 (eBioscience), anti-F4/80-PECy7 (eBioscience), anti-CD11b-eF450 (eBioscience), anti-MHC class II-APC (eBioscience), and anti-B220-eF780 (eBioscience).

The gating strategies were described previously (235). Briefly, for the inflammatory leukocyte panel, CD11c+, LCA+ viable cells were displayed on a histogram of Gr-1 *versus* SigLecF. Neutrophils were defined as a distinct Gr-1 high, SigLecF+ cell population. The SigLecF+ subpopulation was then displayed on a histogram of CD11b *versus* CD11c, where eosinophils appeared as a CD11b high, CD11c low population, while resident macrophages were CD11b low and CD11c high. Excluding neutrophils and SigLecF high populations, the remaining CD11c+ cells were displayed on a plot of MHC class II *versus* B220. The B220 high, MHC class II low pDCs were excluded and the remaining cells were displayed on a plot of MHC class II *versus* CD11b; monocyte-derived DCs (or TIP-DCs) were the MHC class II low population, and inflammatory DCs (or CD11b high DCs) were MHC class II high and CD11b high. For the lymphocyte panel, viable lymphocytes (selected by forward/side scatter characteristics) were plotted on a histogram of CD3 *versus* autofluorescence, and the CD3+ cells were further displayed on a plot of CD4 versus CD8. B cells were defined as CD19+ and B220+ and NK cells were CD49b+ and NK1.1+.

Immunohistochemistry (IHC) staining. Mock- and RRV-infected animals were sacrificed at 10 days post-infection and perfused with 4% paraformaldehyde, pH 7.3. Excised quadriceps tissues were embedded in paraffin, and 5-µm sections were prepared.

To determine the extent of complement deposition in RRV-infected skeletal muscle, the tissues sections were deparaffinized in xylene, rehydrated through an ethanol gradient, and then probed with a goat anti-mouse C3 polyclonal antibody (1:500, Cappel) or a control goat IgG antibody using the Vectastain ABC-AP kit (Vector Labs, CA) and the Vector Blue alkaline phosphatase substrate kit (Vector Labs, CA) according to the manufacturers' instructions. Sections were then counterstained with Gill's hematoxylin. C3 deposition is indicated by a dark blue/violet stain within the tissues.

Macrophage co-culture experiments. To perform *in vitro* co-culture experiments, one day old WT pups were sacrificed by decapitation, and skeletal muscle was extracted from the murine limbs for myocyte culture preparation. Muscle tissue was minced in a petri dish with 1 ml of HBSS+ buffer containing Hanks balanced salt solution (Gibco), 1% L-glutamine (Mediatech) and 1/1000 Gentamicin (Sigma), and then 10 ml of 0.2% type II collagenase (Worthington Biochemicals) was added to the dish. The tissue samples were incubated in a 37ºC water bath for 30 min to 1 hour and vortexed every 10 min during the incubation period. The tissue samples were centrifuged at 3,000 rpm for 5 min, resuspended in warm DMEM (high glucose, Gibco) containing 6% FBS, 1/1000 gentamicin and 1% L-glutamine, and then passed through a 70 μm cell strainer. Cells were plated in 24-well plates and incubated at 37ºC for 48-72 hours, after which the media was aspirated and replaced with high glucose DMEM containing 3% FBS, 1% L-glutamine and 1/1000 gentamicin to induce tubule formation.

Following myocyte differentiation, myocyte cultures were infected with RRV (MOI: 20) and incubated for 2 hours at 37ºC in a CO_2 incubator. Bone-marrow macrophages obtained from WT and $TLR4^{-/-}$ adult mice were then added to the myocytes

in a 1:1 ratio according to the myocyte seeding density and co-cultured for 10-16 hours at 37ºC. At the indicated times post-infection, total RNA was isolated from the macrophages, reverse transcribed and analyzed for cytokine expression by quantitative Real-time PCR (RT-PCR) as described previously (235). Macrophage lysates were also examined for C3 activation by western blot analyses as described below.

Western blotting. At 10 days post-infection, mock-infected and RRV-infected mice were sacrificed and perfused with 1× PBS. Quadriceps muscles were excised and homogenized in radioimmunoprecipitation lysis buffer (RIPA; 50 μM Tris pH 8.0, 150 mM NaCl; 1% NP-40, 0.5% deoxycholate, 0.1% SDS and 1× complete protease inhibitor cocktail (Roche)). Protein concentration was determined by Bradford protein assay, and 25–30 μg of total protein was loaded onto a 10% SDS-PAGE gel. The protein was transferred onto a PVDF membrane, and the membranes were blocked in 5% milk, 0.1% Tween-20 in PBS. The membranes were probed with a goat anti-mouse C3 polyclonal antibody (1:500, Cappel) or a goat anti-mouse actin polyclonal antibody (1:500, SCBT), washed with PBS containing 0.1% Tween-20, and incubated with a rabbit anti-goat antibody conjugated to horseradish peroxidase (1:10,000, Sigma). Following the antibody incubations, the membranes were washed and then developed by an ECL reagent kit (Amersham) according to the manufacturer's instructions to visualize the proteins.

Statistical analyses. Data were analyzed using Prism software (GraphPad Software, Inc.). Comparisons of one-variable data were performed using a two-tailed unpaired Student's *t* test. Percent starting weight for WT and $TLR4^{-/-}$ mice was analyzed using a one-way ANOVA with multiple comparisons corrections ($P<0.01$ is considered significant). Clinical scores for WT and $TLR4^{-/-}$ mice were analyzed by Mann-Whitney

analysis with Bonferroni's correction ($P<0.01$ is considered significant). Bar graphs represent mean values ± standard deviation. Significant differences are represented by comparison (*) with the following legend: *P≤0.05, **P≤0.01, ***P≤0.001, ****P≤0.0001, unless otherwise indicated.

4.4 Results

TLR4 is required for RRV-induced disease

Macrophages and complement, in particular mannose binding lectin (MBL), are required for alphavirus-induced arthritis and myositis (51, 56-59, 175). Moreover, we have previously shown that toll-like receptor (TLR) 7 signaling through the TLR adaptor molecule myeloid differentiation primary response gene 88 (Myd88) is critical for inducing protection from severe Ross River virus-induced disease in mice (235). However, many of the host pathways that are involved in alphavirus pathogenesis, including the role of other TLRs in the infection process, remain poorly understood. Because TLR4 has been shown to influence innate and adaptive immune responses to viral infection, we evaluated the role of TLR4 in a mouse model of RRV-induced arthritis/myositis (103, 105-108, 279, 280). TLR4-deficient ($TLR4^{-/-}$) mice were highly resistant to RRV-induced disease, with $TLR4^{-/-}$ mice showing significantly reduced disease signs, as measured by weight loss and disease scores, compared to wild-type (WT) C57BL/6J animals over the course of infection (Figure 4.1). Consistent with previous studies, RRV-infected WT mice lost weight between days 6 and 10 post-

infection and reached peak disease scores (4.33 ± 0.29) at day 10 post-infection (Figure 4.1). In contrast, TLR4$^{-/-}$ mice continued to gain weight during the course of RRV infection, showing significantly increased weight gain at days 8, 9 and 10 days post-infection compared to WT mice (Figure 4.1A). Moreover, TLR4$^{-/-}$ mice showed a delayed onset of disease signs and showed significantly reduced disease throughout the course of infection compared with WT mice (Figure 4.1B). Mock-infected animals of both strains showed similar weight gain and failed to show disease signs (data not shown). These results suggest that TLR4 plays a pathologic role during RRV infection and is critical for arthritogenic alphavirus-induced disease pathogenesis.

Tissue damage during RRV infection is dependent on TLR4

To determine whether TLR4 functioned to protect mice from RRV-induced tissue damage, we performed a histological analysis of skeletal muscle tissue from RRV-infected WT and TLR4$^{-/-}$ mice. Because WT mice reach peak clinical disease at 10 days post-RRV infection (53, 235), mice were sacrificed at this timepoint, and quadriceps tissues were removed for histological preparation. As shown in Figure 4.1C, TLR4$^{-/-}$ mice showed significantly reduced skeletal muscle pathology compared to WT mice following RRV infection. While mock-infected animals of both strains showed similar levels of resident cellular infiltrates and intact muscle fibers, WT mice showed less intact muscle fibers and more overall tissue damage following RRV infection relative to TLR4$^{-/-}$ mice (Figure 4.1C).

To determine the degree of tissue damage present in the skeletal muscle at WT and TLR4$^{-/-}$ mice, histological slides of RRV-infected quadriceps tissues were blinded

and scored using a blind scoring method based on the overall tissue pathology present in the tissues (Figure 4.1D). As shown in Figure 4.1D, the skeletal muscle of RRV-infected TLR4$^{-/-}$ mice showed a drastic reduction in tissue damage compared with WT mice, with average damage scores in TLR4-deficient mice (2.5 ±1.0) significantly decreased relative to WT mice (6.8 ± 1.2) (Figure 4.1D). Therefore, these data suggest that TLR4 contributes significantly to the skeletal muscle damage incurred during RRV infection.

TLR4-deficient mice show reduced inflammatory leukocyte and NK cell recruitment at late times post-RRV infection

Evaluation of histology slides demonstrated that RRV infection resulted in a significant reduction in the levels of virus-induced pathology (Fig 4.1D). There also appeared to be a reduction in the overall levels of inflammatory cell infiltration into these tissues (Fig. 4.1C). Therefore, to further evaluate this observation using quantitative methods, we used our established flow cytometry protocols (60, 235) to isolate, phenotype, and quantify the inflammatory cell infiltrates within the muscle of RRV-infected TLR4$^{-/-}$ and WT mice at 7 and 10 days post-infection. WT and TLR4$^{-/-}$ mice showed no differences in the total numbers of LCA-positive cells in quadriceps tissues at both 7 and 10 days post-infection, indicating that the extent of tissue inflammation in WT and TLR4$^{-/-}$ mice is similar following RRV infection (Figure 4.2A and 4.2C). At 7 days post-infection, WT and TLR4$^{-/-}$ mice also showed similar levels of inflammatory leukocyte and lymphocyte cell populations, although TLR4$^{-/-}$ mice showed a slight increase in B cells compared to WT mice (Figure 4.2A and 4.2B). However, analyses of infiltrating leukocyte and lymphocyte populations at 10 days post-infection revealed a significant decrease in the total numbers of neutrophils, resident macrophages,

plasmacytoid dendritic cells (DC)s, monocyte DCs and NK cells in the quadriceps of TLR4$^{-/-}$ mice relative to WT mice (Figure 4.2C and 4.2D). These findings suggest that although WT and TLR4$^{-/-}$ mice showed similar degrees of overall inflammation by flow cytometry, TLR4 deficiency may affect the recruitment of specific leukocyte and lymphocyte populations into the skeletal muscle at later times during RRV infection.

Viral titers are similar between WT and TLR4-deficient mice following RRV infection

We have previously shown that mice deficient in TLR7 or Myd88 showed increased viral titers relative to WT mice at late times post-RRV infection, which correlated with enhanced disease (235). To determine whether TLR4 deficiency altered viral loads during RRV infection, we assessed viral burden in the skeletal muscle and serum of RRV-infected WT and TLR4$^{-/-}$ mice by plaque assay. As shown in Figure 4.3, WT and TLR4$^{-/-}$ mice showed similar viral titers in the quadriceps and serum throughout the course of infection. No differences in viral burden were detected in the quadriceps tissues of WT and TLR4$^{-/-}$ mice at 1, 2, 3, 5 and 7 days post-infection (Figure 4.3A). Moreover, WT and TLR4-deficient mice showed similar sera titers at 1, 2, and 3 days post-RRV infection (Figure 4.3B). Thus, RRV replication and clearance are similar in WT and TLR4$^{-/-}$ mice, suggesting that TLR4 deficiency does not affect the kinetics of RRV infection and that viral replication is not responsible for the differences in disease observed between WT and TLR4$^{-/-}$ mice.

Complement deposition and activation is decreased in RRV-targeted skeletal muscle of TLR4-deficient mice

Viral replication and inflammatory cell recruitment was similar in target tissues of WT and TLR4-deficient mice despite significant differences in disease outcome. Given the role of complement in driving RRV-induced disease, we hypothesized that complement activation may be decreased *in vivo* in $TLR4^{-/-}$ mice relative to WT mice during RRV infection. Therefore, we evaluated whether TLR4 was required for complement deposition in RRV-targeted skeletal muscle tissue by performing immunohistochemistry using a mouse-specific complement component 3 (C3) antibody. While mock-infected animals of both strains failed to show complement deposition, RRV-infected quadriceps tissues from $TLR4^{-/-}$ mice showed a substantial reduction in C3 deposition relative to WT mice at day 10 post-infection (Figure 4.4A). RRV-infected WT quadriceps tissue showed profuse C3 staining at areas of tissue damage following RRV infection, while the reduced complement deposition in $TLR4^{-/-}$ murine tissues correlated with the decreased tissue damage observed in these mice (Figure 4.4A). Tissue sections incubated with a control goat IgG antibody showed no IgG deposition (data not shown). These results indicate that TLR4 mediates complement deposition in RRV-targeted skeletal muscle tissue during RRV infection in mice.

Because TLR4-deficient mice exhibited decreased C3 deposition in quadriceps tissue compared to WT mice following RRV infection, we sought to determine whether the decreased complement deposition was leading to decreased complement activation in the knockout mice. Western blot analyses of quadriceps tissues from day 10-infected WT and TLR4-deficient mice indicated that C3 components, including the β chain of C3 and

the cleavage product iC3B, were reduced in the skeletal muscle of TLR4$^{-/-}$ mice compared to WT mice following RRV infection (Figure 4.4B). These results indicate that complement deposition and activation are reduced in TLR4-deficient mice following RRV infection, and TLR4 may be essential for complement –dependent RRV pathogenesis.

TLR4-deficient macrophages show reduced complement production following co-culture with RRV-infected myotubes

Several studies have demonstrated that inflammatory macrophages contribute to RRV-induced pathogenesis (51, 56, 57, 60, 175, 281), and macrophages have been shown to be a source of localized complement production (282, 283). Because TLR4-deficient mice showed reduced complement deposition and activation in skeletal muscle following RRV infection, we sought to determine whether TLR4 regulated complement production by macrophages in response to RRV infection. Therefore, we developed a novel co-culture assay in which primary myotube cultures derived from WT neonatal mice were infected with RRV and subsequently co-cultured with bone marrow-derived macrophages obtained from WT or TLR4$^{-/-}$ adult mice, as indicated in Materials and Methods. RNA was then isolated from the co-cultured macrophages and analyzed for C3 expression using quantitative real-time PCR (qRT-PCR). WT macrophages upregulated C3 expression in response to RRV-infected muscle cells (Figure 4.5A). Moreover, TLR4-deficient macrophages showed significantly reduced C3 mRNA expression compared to WT macrophages following co-culture with RRV-infected myotubes (Figure 4.5A). We also assessed the expression of a panel of other genes whose expression has previously been linked to C3-dependent signaling, including IL-6, S100A8 and S100A9, and the

expression of these genes was also decreased in the absence of TLR4 (Figure 4.5B). In contrast, IL-1β, which is induced independently of C3 during RRV infection, was unaffected in TLR4 -deficient macrophages (Figure 4.5B). Importantly, the induction of C3 and C3-dependent gene expression was dependent on infectious virus as cultures incubated with heat-inactivated RRV or mock-infected controls did not induce macrophage activation (data not shown).

To further assess whether TLR4 regulated C3 expression in response to RRV infection, we performed western blot analyses on the co-cultured WT and TLR4$^{-/-}$ macrophages to determine whether there were differences in downstream C3 activation. As shown in Figure 4.5C, complement activation components, including total C3, the α and β chains of C3, and iC3B, were all decreased in the TLR4-deficient macrophages compared to the WT macrophages following co-culture with RRV-infected myotubes (Figure 4.5C). Taken together, these findings demonstrate that complement activation in macrophages is dependent on TLR4 during RRV infection, suggesting that TLR4 contributes to complement-mediated disease during RRV infection.

4.5 Discussion

Arthritogenic alphaviruses are known to activate innate immune components such as complement and macrophages, which are critical mediators of alphavirus-induced arthritis/myositis (51, 56-60, 175, 281). However, the mechanisms underlying the immune-mediated disease that is induced by alphavirus infection are poorly understood.

Previous work in our laboratory demonstrated that TLR pathways are involved in arthritogenic alphavirus-induced disease, showing that the Myd88-dependent TLR7 signaling pathway mediates protection from severe RRV-induced disease and mortality in mice (235). The data presented in this work demonstrate that TLR4 is required for RRV pathogenesis in mice. Mice deficient in TLR4 exhibited decreased clinical morbidity and tissue damage compared to WT mice following RRV infection, despite showing similar levels of viral replication in target tissues. Furthermore, lack of TLR4 signaling resulted in a reduction in C3 production by macrophages within an *in vitro* myotube co-culture system, and TLR4 was also critical for complement deposition and activation in RRV-targeted skeletal muscle tissue during infection. Therefore, these results identify TLR4 as an essential mediator of RRV pathogenesis and suggest that TLR4 may be therapeutic target for the treatment of arthritogenic alphavirus-induced disease.

TLR4 has been implicated to play protective and pathologic roles during other viral infections (100, 103-108, 279). Additionally, TLR4 plays a pathologic role in multiple human and mouse models of inflammatory arthritis (119-126). However, we are not aware of any studies that have demonstrated a role for TLR4 in the development of alphavirus-induced disease. Therefore, our findings present a novel role for TLR4 in promoting arthritogenic alphavirus-induced disease. Furthermore, these results indicate that in the absence of TLR4 signaling, the expression and activation of complement is significantly reduced in RRV infected tissues. Given that complement activation plays a major role in driving RRV-induced disease, these results suggest that TLR4 affects the virus-induced disease process at least in part by regulating localized complement production in response to RRV infection. However, at this time, we cannot rule out the

possibility that TLR4 might contribute to the virus-induced disease process through other mechanisms.

Although we did not detect a role for viral replication in TLR4-dependent disease, we did detect slight but significant differences in cellular infiltration between WT and TLR4-deficient mice late during RRV infection (Fig. 4.2). The total numbers of specific cellular populations, including neutrophils, resident macrophages, plasmacytoid and monocytic DCs, and NK cells, were reduced in the skeletal muscle of TLR4-deficient mice at 10 days post-infection. Therefore, it is possible that TLR4 contributes to the inflammatory disease process in part by promoting the recruitment of inflammatory cells. However, it is important to note that at day 7 post-infection, which is a timepoint when we observed significantly decreased disease signs and tissue damage in the knockout mice, the TLR4-deficient mice did not exhibit any detectable alterations in inflammatory cell numbers. This suggests that TLR4 promotes disease through other mechanisms, such as inflammatory cell activation and subsequent induction of complement expression. This is supported by our *in vitro* assays, whereby we demonstrated that macrophages lacking TLR4 showed reduced expression of C3 following RRV infection (Fig 4.5). Moreover, complement activation was dependent on TLR4 *in vivo* in RRV-infected mice (Fig. 4.4). Previous studies have demonstrated that the expression of complement-dependent activation markers in human osteoarthritis patients is dependent on TLR4 (59, 60, 132, 133), suggesting that TLR4 may play a role in complement-mediated arthritis in humans. However, it is currently unclear how TLR4 deficiency is affecting downstream defects in complement-mediated disease during RRV infection.

TLR4 is known to bind bacterial lipopolysaccharide via the TLR4-MD2 complex (284). Additionally, TLR4 recognizes other microbial components, including viral envelope proteins and other bacterial elements, although the structural mechanisms behind these molecular interactions have not been demonstrated (284). TLR4 signaling has also been shown to be modulated in a monocytic cell line through a direct interaction with MBL, which mediates complement-dependent disease during RRV infection (60, 277, 278). Thus, it is possible that TLR4 is interacting with MBL during RRV infection, resulting in the downstream pathogenesis. Additionally, TLR4 has been shown to recognize the fusion (F) protein of respiratory syncytial virus (RSV), and the presence of the RSV F protein is necessary for TLR4-dependent inflammatory responses during RSV infection (99). Therefore, another possibility is that TLR4 is directly recognizing viral proteins during RRV infection to mediate downstream pathogenesis. Studies are ongoing in our laboratory to address the mechanism of TLR4-dependent activation during RRV infection.

Given the protective role of TLR7 signaling during RRV infection, it is notable that another TLR pathway to virus-induced pathology during the same viral infection. Because TLR7 signals exclusively through Myd88 within endosomes while TLR4 signals from the plasma membrane and endocytic vesicles through multiple adaptors and pathways, it is possible that different pathways are activated downstream of these two TLRs following RRV infection(284). Both TLR pathways are known to stimulate NFkB pathways, leading to pro-inflammatory cytokine expression. However, TLR7 signaling also leads to interferon-stimulated gene expression via IRF7 activation, while TLR4 can activate IRF3- and AP1-dependent pathways. Alternatively, the essential, protective

effects of TLR7 may mask the pathologic role of TLR4, where both molecules signal through Myd88, thereby highlighting the value of using TLR specific knockouts to dissect their role in disease processes, rather than drawing conclusions from studies where downstream adaptors have been knocked out. Additionally, it is possible that the roles of these TLRs are dependent on different cell types during RRV infection, such as B cells in the case of TLR7 and macrophages in the case of TLR4, and the kinetics of signaling through these TLRs may also differ during the course of RRV infection (93, 235). Thus, we are currently performing experiments to address the downstream targets of differential TLR signaling during RRV infection to better understand their roles in virally induced disease.

In summary, the results of this study demonstrate a pathologic role for TLR4 in the development of complement-mediated disease during RRV infection. These findings further elucidate the host inflammatory pathways that contribute to arthritogenic alphavirus-induced arthritis/myositis and identify TLR4 as a potential therapeutic target for the treatment of severe RRV-induced disease.

Figure 4.1

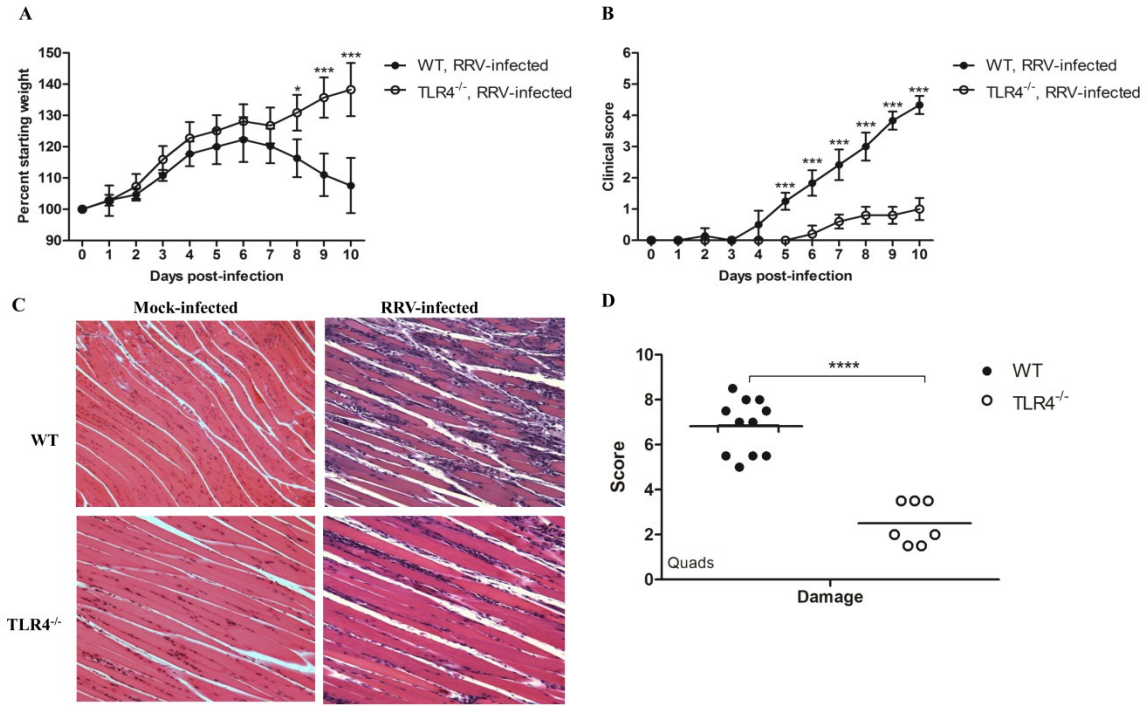

Figure 4.1: TLR4 contributes to the development of RRV-induced disease in mice.

Twenty-four day old C57BL/6J wild-type (WT), and TLR4$^{-/-}$ mice were subcutaneously infected in the left rear footpad with either PBS diluent (Mock) or 10^3 PFU of RRV and monitored for (A) weight loss and (B) clinical disease. N = 5-15 mice/strain/timepoint. *P<0.01, and *** P≤0.0001. Mice were sacrificed and perfused with 4% paraformaldehyde at 10 days post-infection. (C) & (D) Quadriceps muscles were excised and paraffin-embedded, and 5 µm tissue sections were stained with H&E. (C) Histological analysis of mock-infected and RRV-infected quadriceps muscles from WT and TLR4$^{-/-}$ mice at day 10 post-infection. Representative images are shown. (D) Blind scoring of overall damage observed in RRV-infected WT and TLR4$^{-/-}$ muscle tissue. N = 11 (WT) and 7 (TLR4$^{-/-}$). ****P≤5E-7.

Figure 4.2

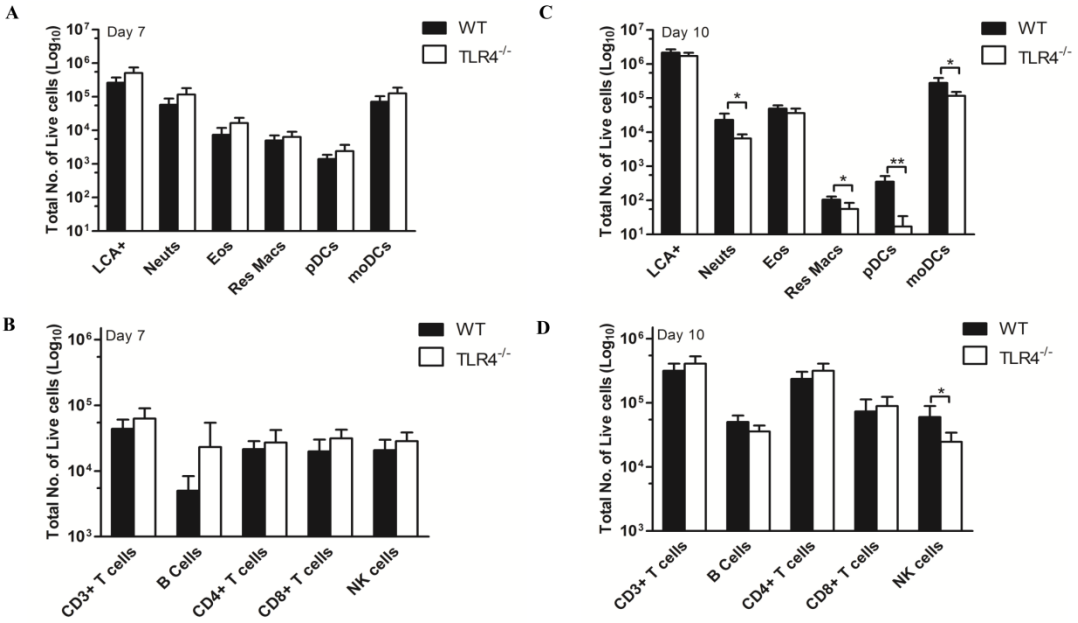

Figure 4.2: TLR4-deficient mice show reduced numbers of inflammatory leukocyte and NK cell populations in RRV-infected quadriceps at late times post-infection.

Twenty-four day old WT and TLR4$^{-/-}$ mice were subcutaneously infected in the left rear footpad with 10^3 PFU of RRV. At 7 and 10 days post-infection, mice were sacrificed and perfused with 1X PBS. Quadriceps muscles were excised, digested and prepared for flow cytometric analysis as described in Materials and Methods. (A) & (C) Total numbers of infiltrating inflammatory leukocyte cell populations isolated from RRV-infected WT and TLR4$^{-/-}$ quadriceps muscle tissue. (B) & (D) Total numbers of infiltrating lymphocyte cell populations isolated from RRV-infected quadriceps muscle tissue. N = 4-7 mice/strain/timepoint. *P≤0.01.

Figure 4.3

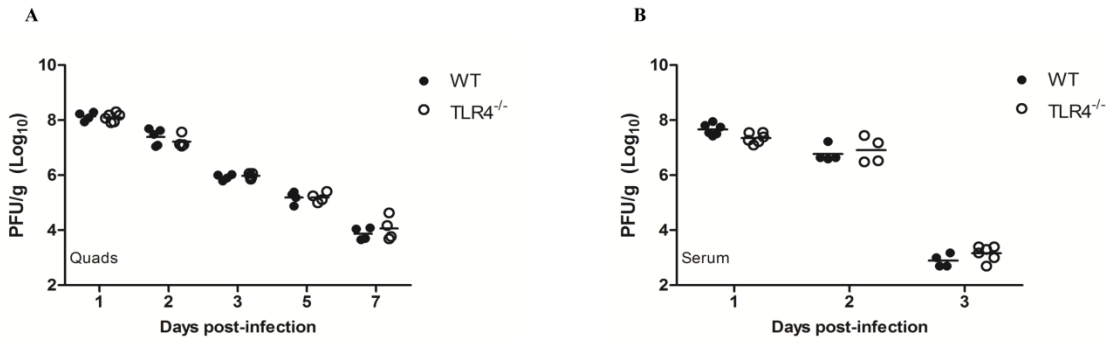

Figure 4.3: Viral titers are similar between WT and TLR4-deficient mice following RRV infection.

Twenty-four day old WT and TLR4$^{-/-}$ mice were subcutaneously infected in the left rear footpad with 10^3 PFU of RRV. At the indicated timepoints, mice were sacrificed by exsanguination and quadriceps tissues were dissected. Infectious virus present in (A) homogenized ipsilateral quadriceps tissue and (B) serum was quantified by plaque assay on Vero cells. N = 4-6 mice/strain/timepoint. *P≤0.05, **P≤0.01, ***P≤0.001.

Figure 4.4

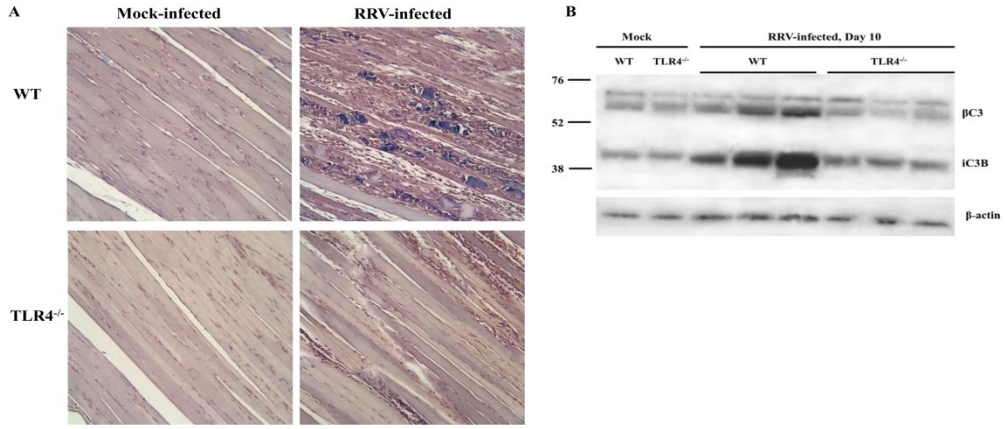

Figure 4.4: TLR4-deficient mice show reduced complement deposition and activation in RRV-infected muscle tissue.

Twenty-four day old WT and TLR4$^{-/-}$ mice were subcutaneously infected in the left rear footpad with either PBS diluent or 10^3 PFU of RRV. (A) Mice were sacrificed and perfused with 4% paraformaldehyde at 10 days post-infection. Quadriceps muscles were excised and paraffin-embedded, and unstained 5 μm tissue sections were obtained for immunohistochemistry (IHC) and counterstained with Gill's hemotoxylin as described in Materials and Methods. IHC staining for complement component 3 (C3) deposition in mock-infected and RRV-infected quadriceps muscles from WT and TLR4$^{-/-}$ mice at day 10 post-infection is indicated by dark blue/violet staining at areas of tissue damage. Representative images are shown. (B) Mice were sacrificed and perfused with 1X PBS at 10 days post-infection. Quadriceps muscles were excised, homogenized and prepared for Western Blot analysis as described in Materials and Methods. Samples were assessed for complement activation products using an anti-mouse C3 antibody, and each lane represents a single animal. Images are representative of three separate experiments.

Figure 4.5

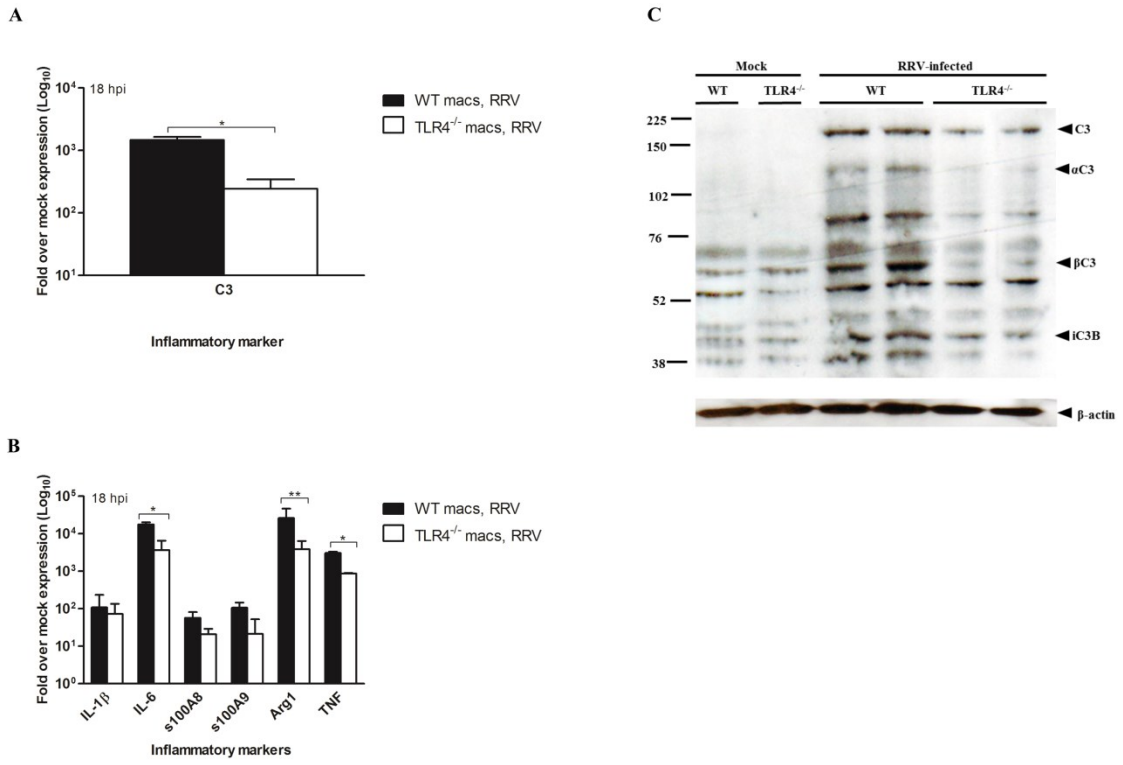

Figure 4.5: TLR4-deficient macrophages show reduced complement production compared to WT macrophages following co-culture with RRV-infected myotubes.

One day old WT mice were sacrificed by decapitation, and skeletal muscle was extracted for myocyte culture preparation as described in the Materials and Methods. Following myocyte differentiation, myotube cultures were infected with RRV (MOI: 20). At 2 hours post-infection, bone-marrow macrophages obtained from WT and TLR4$^{-/-}$ adult mice were added to the myotubes and co-cultured for 16 hours. (A) & (B) At 18 hours post-infection, total RNA was isolated from the WT and TLR4$^{-/-}$ macrophages, reverse transcribed, and analyzed for (A) C3 and (B) inflammatory marker expression by quantitative Real-time PCR as described in Materials and Methods. Inflammatory markers analyzed included IL-1β, IL-6, s100A8, s100A9, Arg1, and TNF. (C) At 18

hours post-infection, cell lysates were harvested from the WT and TLR4-deficient macrophages and prepared for western blot analysis as described in Materials and Methods. Samples were assessed for complement activation products using an anti-mouse C3 antibody, and each lane represents an individual sample. *P≤0.01, **P≤0.001.

CHAPTER FIVE:

DISCUSSION

5.1 TLR7 mediates protection from severe RRV-induced disease

TLR7 deficiency promotes antibody- and complement-mediated enhancement of RRV-induced disease

Using *in vitro* analyses and animal models, multiple studies demonstrate the critical roles that innate immune pathways play in the development of arthritogenic alphavirus-induced disease. The primary innate immune mechanism that mediates protection from alphavirus pathogenesis is the type I IFN response (136). IFN induction is essential for controlling alphavirus replication and limiting virus infectivity, and mice with severe deficiencies in IFN signaling succumb rapidly to alphavirus infection (135, 136). Furthermore, IRF3 and IRF7, which facilitate type I IFN and inflammatory cytokine production during viral infection, are required for protective IFN responses during lethal CHIKV and SINV infections, and ISGs induced through IFN signaling show potent antiviral effects during alphavirus infections (136, 148-151).

Less is known about the precise mechanisms through which IFN and other inflammatory mediators are induced during alphavirus infection, although several sensing pathways are implicated. Cytoplasmic PRR activity via RIG-I, MDA5, and PKR is

thought to be important in mediating IFN induction and other antiviral responses during alphavirus infections (165, 179, 181, 183, 184). Furthermore, evidence suggests that the CLRs, DC-SIGN and L-SIGN, may be utilized by SINV for cell entry, and the DC inhibitory receptor DCIR plays a protective role in regulating inflammatory responses to CHIKV infection (187, 188). However, many studies implicating the roles of these PRRs in alphavirus pathogenesis were not effectively demonstrated *in vivo*, and the evidence from these studies suggests that multiple PRRs regulate the host response to alphavirus infection.

The relative importance of TLRs to arthritogenic alphavirus infection is also poorly understood, although the TLR adaptors, Myd88 and TRIF show some role in protection from severe CHIKV dissemination and disease in mice (141, 150). Therefore, to determine whether TLR signaling played an essential role in arthritogenic alphavirus-induced disease, we initially examined the role of the central TLR adaptor, Myd88 in a mouse model of alphavirus-associated arthritis/myositis. The results of our initial study demonstrated that Myd88 signaling is a critical mediator of host defense during RRV infection and functioned to protect mice from severe RRV-induced skeletal muscle damage and mortality. Furthermore, we found that Myd88 signaling was dependent on TLR7 during RRV infection, and Myd88-dependent TLR7 signaling was required for the development of RRV-specific neutralizing antibody responses. Our findings were the first to establish the critical function of Myd88-dependent TLR7 signaling in mediating protective adaptive immune responses to arthritogenic alphavirus infection and revealed the importance of TLR pathways in the host defense against alphavirus-induced disease. Because Myd88-deficient mice were previously found to be more susceptible to CHIKV

dissemination but not CHIKV-induced mortality, these findings suggest that Myd88-dependent TLR signaling plays an important protective role in arthritogenic alphavirus infection, but the relative significance of this pathway may be contingent on the experimental approach or mouse model used (141).

As a follow-up to our previous study, we sought to determine the mechanism of RRV-induced disease exacerbation in the absence of Myd88-dependent TLR7 signaling. Because mice deficient in TLR7 produced high titers of low affinity, non-neutralizing RRV-specific antibodies, we assessed whether the antibodies produced in the absence of TLR7 were pathologic and found that TLR7- and Myd88-deficient mice were susceptible to severe antibody- and complement-dependent RRV-induced disease. This study was the first to demonstrate that Myd88-dependent TLR7 signaling protects mice from systemic complement-mediated immune complex disease during RRV infection. Further studies will be necessary to determine whether the mechanism of Myd88-mediated protection from CHIKV dissemination is also dependent on antibody responses to infection.

Insights into mechanisms of TLR7-mediated protection

The importance of TLR7 signaling to the development of RRV-specific neutralizing antibodies contributes to our insight into the mechanism of TLR7-mediated protection from RRV-induced disease. Although it is not currently known whether TLR7 signaling modulates B cell activity through a direct or indirect mechanism in our model, it is clear that TLR7 deficiency results in an inability to form splenic germinal centers and generates defective antibody responses during RRV infection. Because TLR7 signaling in DCs can regulate adaptive immune responses to viral infection via IFN production, we examined type I IFN levels in the sera of RRV-infected WT, TLR7- and

Myd88-deficient mice and found no differences in type I IFN expression across the infected strains (Figure 2.4) (202, 222, 224, 225). Furthermore, pDCs isolated from $TLR7^{-/-}$ mice showed no defect in type I IFN production in response to RRV infection (Figure 5.1). Thus, it is possible that TLR7 signaling may alter the function of DCs or other antigen-presenting cells by affecting their ability to activate B cells via antigen presentation and/or cytokine secretion, which could lead to defective B cell responses to RRV infection. Alternatively, because CD4+ T cells also express TLR7 and were significantly reduced in the skeletal muscle of TLR7-deficient mice late during RRV infection, TLR7 deficiency may affect CD4+ T cell activation and/or localization during infection, which can also modulate neutralizing antibody responses (82, 221).

However, evidence from other studies suggests that TLR7 signaling may function directly within B cells to modulate antibody maturation during viral infection (80). Recent studies demonstrated that Myd88-dependent TLR7 signaling is required for neutralizing antibody responses during vaccination and viral infections, and specific depletion of Myd88 in B cells results in the ablation of neutralizing antibody responses and a corresponding loss in protection from Friend virus infection (93, 96). Evidence suggests that B cell intrinsic TLR signaling can stimulate the development of germinal center B cells, which promote high-affinity, neutralizing antibody production, via two mechanisms (285). First, the combined activation of B cell receptors (BCR) and TLRs can induce germinal center differentiation in antigen-specific B cells. Second, the combination of BCR and TLR stimulation in germinal center B cells may function synergistically to promote somatic hypermutation and enhance the production of high-affinity IgG. Furthermore, TLR stimulation in activated B cells induces class switch

recombination through deaminase upregulation and may promote isotype switching from Th2-associated IgG1 to Th1-associated IgG2 (80, 285). The demonstration in our study that TLR7-deficient mice exhibited a skewed Th1/Th2 RRV-specific antibody response further supports the evidence that Myd88-dependent TLR7 signaling in B cells is required for efficient IgG class switching and protective antibody responses during infection. However, studies using tissue-specific depletions of Myd88 will be necessary to confirm whether intrinsic Myd88-dependent signaling in B cells is required for protection from severe RRV-induced disease.

In addition to its role in promoting protective antiviral antibody responses, our findings demonstrated that Myd88-dependent TLR7 signaling protects mice from myocardial tissue damage following RRV infection. Because Myd88- and TLR7-deficient animals also exhibited antibody and complement deposition in infected cardiac tissues, our results suggest that TLR7 deficiency promotes cardiac disease via antibody- and complement-mediated mechanisms. Previous studies have shown that Myd88 is essential for TLR-dependent anti-apoptotic signaling in myocardioctyes (286). Thus, it is also possible that deficiency in TLR7 signaling may result in cellular apoptosis of infected myocardial tissues, which can activate complement via damage-associated molecular patterns that are presented in apoptotic cells (234). However, the focal localization of the cardiac pathology, which corresponds to the focal staining of antibody and complement deposition, suggests that the cardiac damage incurred during RRV infection is associated with both antibody- and complement-dependent mechanisms of disease (Figures 3.3 and 3.4). Moreover, TLR7-deficient mice exhibited enhanced complement-associated pro-inflammatory marker expression in myocardial tissues

(Figure 3.3), and the expression of these markers is associated with cardiac suppression (244-248). To determine whether myocardial function is defective during RRV infection in the absence of TLR7 signaling, cardiomyocyte contractile function can be assessed by measuring cardiac ventricular pressures in RRV-infected WT, TLR7- and Myd88-deficient mice (287). Further investigation will be necessary to determine whether the cardiac injury induced in RRV-infected Myd88- and TLR7-deficient mice is sufficient to induce heart failure and/or decreased blood flow in these mice, which could lead to organ failure, or whether other factors are responsible for the mortality observed in these animals during RRV infection (288).

It is currently unclear from our study what PAMPs or signals regulate TLR7 signaling during alphavirus infection. Because TLR7 recognizes ssRNA, it is plausible that alphavirus genomic ssRNA exposed during viral uncoating in the endosome may trigger TLR7 responses upon infection (64). An alternative mechanism of TLR7 activation could be through RNA intermediates generated during viral replication, which could be trafficked to the endosome (via autophagy or other mechanisms) to stimulate TLR7. Follow-up studies will be necessary to determine which signals regulate TLR7 signaling during RRV infection.

Future directions

Myd88-deficient mice showed significant antibody and complement deposition and pathology in cardiac and renal tissues during RRV infection, and the enhancement of RRV-induced disease appears to be dependent on the C1q-dependent classical pathway of the complement cascade. However, we have not yet established whether Myd88- and TLR7-deficient mice exhibit enhanced C1q-bound immune complexes in the sera during

RRV infection, which could deposit systemically and is indicative of traditional serum sickness, or whether the antibody generated is deposited into tissues and results in local complement activation. To determine whether circulating immune complexes and/or complement activity is elevated in the sera in the absence of Myd88-dependent TLR7 signaling, sera from RRV-infected WT, Myd88$^{-/-}$, and TLR7$^{-/-}$ mice can be subjected to a C1q-binding assay, which is a quantitative method for measuring C1q binding to antibody-containing complexes, or a complement consumption assay, which measures total complement reactivity to the sera (289-291). Furthermore, because severe arthritogenic alphavirus-induced disease can be associated with autoantibody production, it would be interesting to determine whether the antibodies detected in non-RRV targeted cardiac and renal tissues of Myd88- and TLR7-deficient mice can cross-react with host antigens or whether they are only specific for RRV (48, 232, 249, 258, 292).

Levels of C3a, a marker of C3 cleavage and complement activation, are elevated in the synovial fluid of RRV-infected polyarthritis patients (58). Because RRV-induced disease in the context of normal TLR7 signaling is associated with MBL and the lectin pathway of complement activation, it would not be expected that human patients infected with RRV would suffer from complement-dependent immune complex disease (60). In fact, a study from our laboratory demonstrated that serum and synovial MBL levels correlated with the severity of disease in RRV-infected patients, while the levels of C1q-C4 complexes, which are indicative of classical complement activation, were similar in the synovial fluid of patients with severe and mild cases of RRV-induced disease (60, 290). However, the same study demonstrated that levels of the complement cleavage product, C4a, which can result from activation of the lectin or classical pathways, were

elevated in the synovial fluid of patients with severe RRV-induced polyarthritis compared to patients with mild disease, and it would be interesting to know whether levels of C1q-C4 complexes or IgG complexes are elevated in the sera of RRV-infected patients (60). Furthermore, our findings suggest that RRV-infected patients with defects in Myd88-dependent TLR7 signaling because of genetic polymorphisms in the genes associated with signal transduction may be at increased risk for developing C1q-associated immune complex disease, and targeted treatment of complement-induced disease via C3 or C1q inhibitors may provide therapeutic benefits to these patients (293). Larger human cohort studies will be necessary i) to determine whether immune complex disease can occur in RRV-infected patients and if so, ii) to evaluate the efficacy of complement-directed therapies in this subset of individuals.

In addition, studies have demonstrated that patients with severe rheumatoid arthritis have elevated levels of MBL and C1q-associated immune complexes (291, 294). Moreover, the inflammatory gene profiles of CHIKV- and RA-induced diseases are significantly similar, and evidence suggests that chronic CHIKV infection may lead to RA and autoantibody production in some patients (171, 295-297). Because prolonged alphavirus-induced arthropathy can lead to the development of autoantibodies and possibly rheumatic diseases, it would be beneficial to examine whether C1q-associated immune complexes are elevated in patients with chronic arthritogenic alphavirus-induced disease (292, 295, 297). Additionally, anti-rheumatic drugs (ARDs) such as sulfasalazine and methotrexate show considerable efficacy in treating patients with chronic CHIKV-induced polyarthritis (297). If patients with chronic arthritogenic alphavirus-induced disease also demonstrate enhanced C1q-associated immune complexes, combinatorial

treatments using ARDs and C1q inhibitors may provide therapeutic benefits in treating these patients.

5.2 TLR4 promotes RRV pathogenesis

TLR4 induces complement-mediated disease during RRV infection

Our studies evaluating the role of Myd88 and TLR7 in RRV-induced disease demonstrated that TLR signaling plays an essential role in arthritogenic alphavirus pathogenesis. However, it remained unclear whether other TLR pathways could be involved in alphavirus-induced disease. Thus, we directed our subsequent investigation to screen other TLR pathways using our mouse model of RRV-induced arthritis/myositis. Because TLR4 has shown important functions in a number of viral infections and in inflammatory arthritis, we evaluated the role of TLR4 during RRV infection and found that mice lacking TLR4 were resistant to RRV-induced disease. TLR4-deficient mice showed decreased complement activation and decreased skeletal muscle damage compared to WT mice following RRV infection, and TLR4-deficient macrophages showed deficiencies in complement activation following co-culture with RRV-infected muscle cells. Our findings are the first to demonstrate that i) TLR4 is required for the development of complement-mediated tissue damage during RRV infection, and ii) TLR4 signaling in macrophages regulates complement activation during RRV infection.

MBL, which is known to mediate RRV-induced inflammatory disease, has been shown to modulate TLR4 signaling in a macrophage cell line (60, 277, 278). Because these studies were investigated *in vitro* and have not been reported in the context of

infection, we sought to determine whether MBL could contribute to macrophage activation during RRV infection and if so, whether TLR4 signaling in macrophages was modulated by MBL following co-culture with RRV-infected muscle cells. Using our co-culture system, we demonstrated that macrophages lacking MBL showed decreased expression of C3 and other complement-associated pro-inflammatory markers compared to WT macrophages following co-culture with RRV-infected myotubes (Figure 5.2). Moreover, complement-associated activation markers were reduced in MBL- and TLR4-deficient macrophages, while levels of IL-1β expression were similar between WT, MBL$^{-/-}$, and TLR4$^{-/-}$ macrophages (Figure 5.2). In a follow-up study, we incubated co-cultured WT and TLR4-deficient macrophages with sera from WT or MBL-deficient mice and examined whether the sera (as a source of MBL) modulated C3 expression in macrophages during RRV infection. As shown in Figure 5.3, treatment with MBL-containing sera resulted in enhanced C3 expression in WT macrophages but did not affect C3 expression in TLR4-deficient macrophages following co-culture with RRV-infected myotubes (Figure 5.3). However, incubation with WT and MBL-deficient sera caused enhanced activation of WT and TLR4$^{-/-}$ macrophages that was independent of MBL (data not shown), and future studies should utilize purified MBL to avoid non-specific effects of the sera on macrophage activation. Taken together, these results suggest that MBL may modulate macrophages in a TLR4-dependent manner during RRV infection.

Previous studies demonstrated that the N-linked glycans on the RRV E1 and E2 glycoproteins contribute to type I IFN induction in DCs (40, 185). Additionally, evidence in our laboratory suggests that complement-mediated disease during RRV infection is dependent on the viral glycans because studies with RRV mutant viruses lacking the E1

and E2 envelope glycans showed reduced morbidity and complement activation in mice (Gunn and Heise, unpublished). Because complement activation was reduced in TLR4-deficient mice and macrophages during RRV infection, we hypothesized that the RRV envelope glycans may contribute to complement activation in a TLR4-dependent manner. Thus, we co-cultured macrophages from WT or TLR4$^{-/-}$ mice with primary myotubes that were infected with either RRV or an RRV mutant lacking the two glycans on the E2 glycoprotein (RRV-DM) (40). The results from the co-culture experiments revealed that the RRV-DM virus induced significantly less C3 and pro-inflammatory expression in WT macrophages than RRV (Figure 5.2). However, the expression of C3 and C3-associated inflammatory markers was similar between TLR4-deficient macrophages following infection with either RRV or RRV-DM, suggesting that glycan-mediated complement activity is dependent on TLR4 expression. Furthermore, because our previous studies indicated that TLR4-dependent macrophage activation may be modulated by MBL, we examined whether glycan-dependent macrophage activation was also dependent on MBL and found that MBL-deficient macrophages showed similar C3 and C3-associated pro-inflammatory marker expression following infection with either RRV or RRV-DM (Figure 5.2). These findings suggest that RRV-induced complement activation in macrophages is dependent on TLR4, MBL, and the viral envelope glycans.

Insights into mechanisms of TLR4-induced pathogenesis

Macrophages and complement contribute to arthritogenic alphavirus pathogenesis, and evidence suggests that macrophages may contribute to complement-mediated disease through localized complement production during RRV infection (51, 56, 57, 60, 175, 281). Additionally, the data derived from our in-vitro co-culture analyses

indicated that the expression of C3 and C3-associated pro-inflammatory markers in co-cultured macrophages were dependent on TLR4, MBL, and the viral envelope glycans, and complement expression in macrophages may be modulated by MBL in a TLR4-dependent manner during RRV infection. Using the data derived from co-culture system, we propose potential mechanisms of TLR4-induced disease during RRV infection. Firstly, MBL binds microbial carbohydrates, and evidence suggests that MBL may bind to the N-linked glycans on RRV glycoproteins to activate the lectin pathway of the complement cascade during RRV infection [(60, 234), and Gunn & Heise, unpublished]. Because MBL can directly interact with TLR4 and modulate macrophage activation, our data suggest that MBL may bind to TLR4 on macrophages and enhance TLR4 signaling during RRV infection, leading to increased complement activation and inflammation (277, 278). However, TLR4 can also be directly activated by viral glycoproteins, and it is possible that RRV envelope glycans interact with TLR4 through an MBL-independent mechanism to induce TLR4 activation (99-102). Further investigation will be necessary to determine whether MBL and/or the viral envelope glycans interact directly with TLR4 to mediate downstream pathogenesis during RRV infection.

Because TLR4 is known to signal through Myd88, it is noteworthy that $TLR4^{-/-}$ mice are resistant to RRV-induced disease, while $Myd88^{-/-}$ mice show enhanced susceptibility to RRV-induced morbidity and mortality. Because Myd88-dependent TLR7 signaling is critically important for protection from adaptive immune dysregulation during RRV infection, the role of Myd88-dependent TLR4 signaling during RRV infection may be less critical in comparison, and the cell types within which these TLR pathways function during RRV infection (i.e. B cells and macrophages, for example) may

also differ. However, it is also possible that the TLR4 signaling induced during RRV infection occurs independently of Myd88 via the TRAM-TRIF endosomal pathway of TLR4 activation (75). Interestingly, mice deficient in the other TLR4-associated adaptors, including $TRIF^{-/-}$, $TIRAP^{-/-}$, and $TRAM^{-/-}$ mice, showed a similar disease progression to WT mice following RRV infection (Neighbours, Long and Heise, unpublished). Thus, RRV-induced TLR4 signaling may be redundant through TRIF and TRAM, and future studies could address whether mice deficient in both TRIF and TRAM (TRIFxTRAM DKO mice) show a similar phenotype to TLR4-deficient mice following RRV infection.

Future directions

TLR4-deficient mice showed reduced complement deposition and activation in RRV-infected skeletal muscle tissue, and *in vitro* co-culture experiments demonstrated that complement activation in macrophages is dependent on TLR4 during RRV infection. However, our studies have not conclusively demonstrated that TLR4 signaling contributes to macrophage-dependent complement activation *in vivo*. It is possible that TLR4 deficiency in macrophages results in reduced expression of other pro-inflammatory markers, which we also observed *in vitro*, and the resulting decrease in macrophage cytokine secretion may reduce the activation of other effector cells that could mediate RRV-induced complement deposition and disease. Alternatively, TLR4 signaling may regulate complement deposition by macrophages during RRV infection, but other cell types such as NK cells may mediate the cytotoxicity that contributes to tissue damage during RRV infection (298). Our *in vitro* analyses suggested that TLR4 deficiency does not affect macrophage cytotoxicity as measured by nitric oxide and LDH release

following co-culture with RRV-infected myotubes (Figure 5.4), indicating that perhaps other cell types mediate cytotoxicity during RRV infection. However, because the *in vitro* co-culture system lacks the complexity of *in vivo* inflammatory processes and interactions, future studies should examine the impact of TLR4 signaling on macrophage cytotoxicity in RRV-infected mice. Moreover, follow-up studies will be necessary to confirm whether TLR4 deficiency affects complement activity in macrophages during *in vivo* RRV infection.

TLR4 activation is associated with pathologic outcomes in a number of chronic human inflammatory disorders, including arthritis (299). One of the therapeutic implications of our findings is that treating RRV-infected patients with pharmacological TLR4 antagonists may ameliorate RRV-induced disease. Eritoran is a synthetic lipid A that binds to MD2 within the TLR4 complex to antagonize TLR4 signaling, and administration of eritoran has shown efficacy in treating TLR4-induced inflammation (299). Alternatively, drugs that target reactive oxygen species or nitric oxides, which are induced by TLR4 signaling, may also reduce inflammation resulting from TLR4 activation. Future studies should examine whether treatment with drugs that directly or indirectly prevent TLR4 signaling reduces RRV-induced inflammatory disease. Additionally, because TLR4 signaling induces complement activation during RRV infection, drugs that directly target complement components or prevent complement activation may provide therapeutic benefits to RRV-infected patients.

5.3 Conclusions

In summary, host inflammatory pathways contribute to the development of arthritogenic alphavirus-induced disease, but many of the mechanisms underlying the

inflammation have not been elucidated. The work described in this dissertation demonstrates that TLR signaling significantly contributes to arthritogenic alphavirus pathogenesis, and TLR activation can lead to protective or pathologic outcomes during RRV infection. Our studies also demonstrate that TLR pathways regulate multiple components of RRV-induced disease, including complement activation. The role of Myd88-dependent TLR7 signaling in mediating protective antibody responses during RRV infection, other viral infections, and vaccinations suggests that targeting this pathway through TLR7 agonists may enhance therapeutic strategies designed to prevent or treat alphavirus infections. In contrast, specific strategies designed to block TLR4 signaling may prevent chronic inflammatory disease in RRV-infected patients. Further investigation will be necessary to determine whether TLR pathways contribute significantly to alphavirus-induced inflammatory arthritis in humans.

Figure 5.1

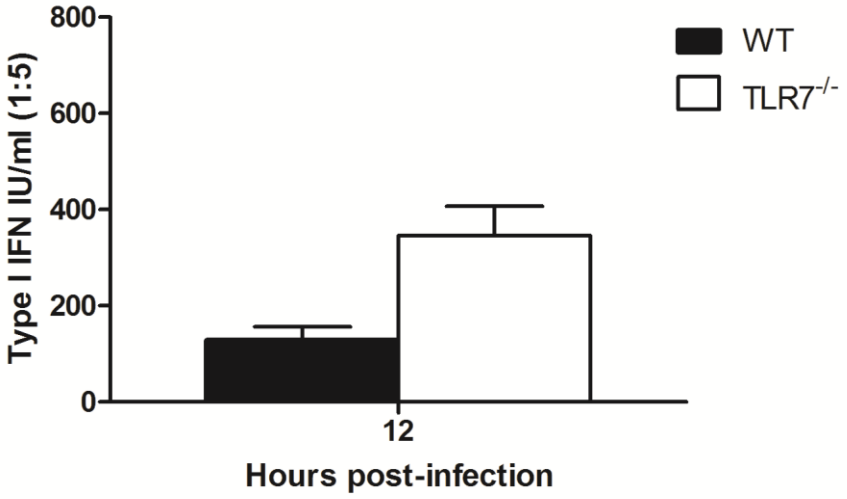

Figure 5.1: Plasmacytoid DCs from WT and TLR7$^{-/-}$ mice produce similar amounts of type I IFN following RRV infection.

Plasmacytoid DCs (pDCs) were isolated from adult WT and TLR7$^{-/-}$ mouse spleens using anti-mPDCA-1 microbeads (Miltenyi Biotec) and the autoMACS columns (Miltenyi Biotec), according to the manufacturer's instructions. Isolated pDCs were plated and infected with RRV (MOI: 20) for 12 hours, and supernatants were analyzed for type I IFN production by IFN Bioassay as described above (Chapter 2, Materials and Methods). N = 4 (WT) or 5 (TLR7$^{-/-}$) replicate samples per strain.

Figure 5.2

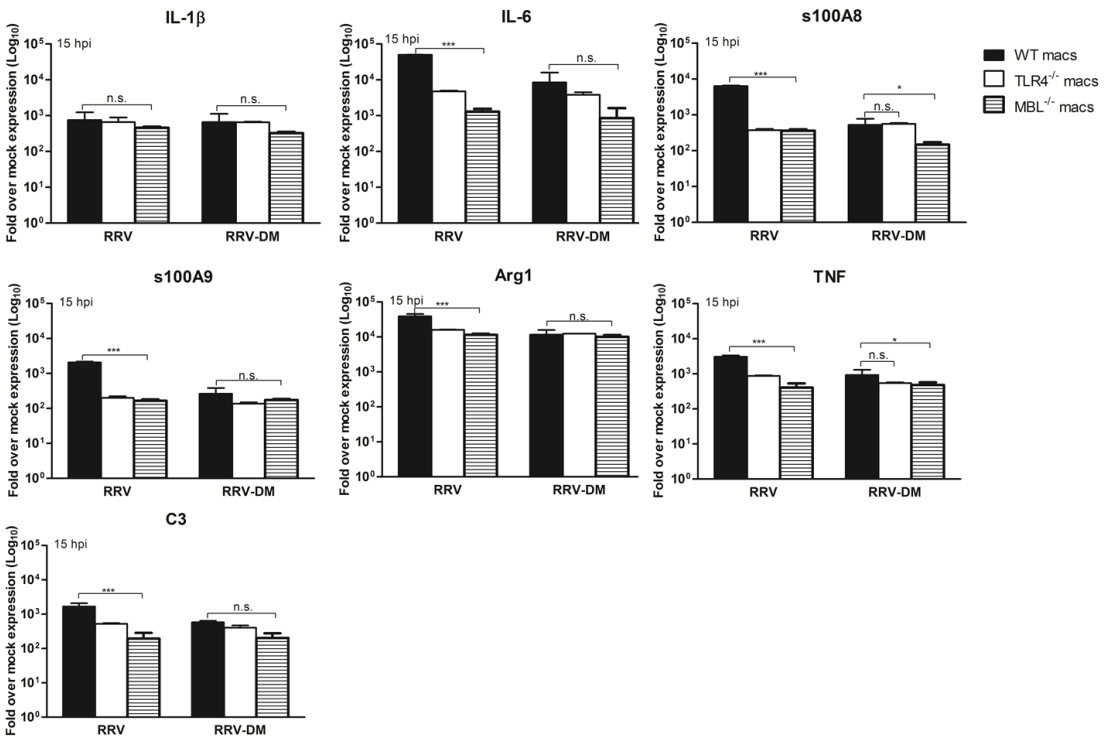

Figure 5.2: Expression of complement-associated inflammatory markers is reduced in TLR4- and MBL-deficient macrophages following co-culture with RRV-infected but not RRV-DM-infected myotubes.

One day old WT mice were sacrificed by decapitation, and skeletal muscle was extracted for myocyte culture preparation as described above (Chapter 4, Materials and Methods). Following myocyte differentiation, myotube cultures were infected with RRV or RRV-DM (MOI: 20). At 2 hours post-infection, bone-marrow macrophages obtained from WT, $TLR4^{-/-}$, and $MBL^{-/-}$ adult mice were added to the myotubes and co-cultured for 16 hours. Total RNA was isolated from the macrophages, reverse transcribed, and analyzed for C3 and inflammatory marker expression by quantitative Real-time PCR. Inflammatory markers analyzed included IL-1β, IL-6, s100A8, s100A9, Arg1, and TNF.

Figure 5.3

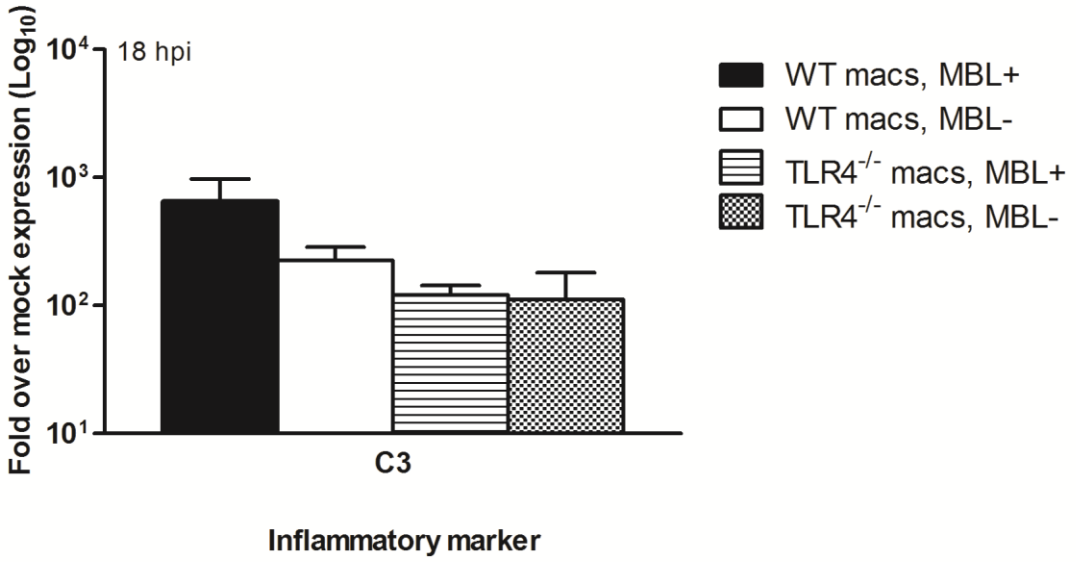

Figure 5.3: MBL treatment enhances C3 expression in WT macrophages but not TLR4-deficient macrophages following co-culture with RRV-infected myotubes.

One day old WT mice were sacrificed by decapitation, and skeletal muscle was extracted for myocyte culture preparation as described above (Chapter 4, Materials and Methods). Following myocyte differentiation, myotube cultures were infected with RRV (MOI: 20). At 2 hours post-infection, bone-marrow macrophages obtained from WT and $TLR4^{-/-}$ adult mice were added to the myotubes and co-cultured for 14 hours. At 16 hours post-infection, sera from WT or $MBL^{-/-}$ mice were diluted 1:10 in media and incubated on the cultures for 2 hours. Total RNA was isolated from the macrophages, reverse transcribed, and analyzed for C3 expression by quantitative Real-time PCR. N = 3 replicate samples/strain/treatment.

Figure 5.4

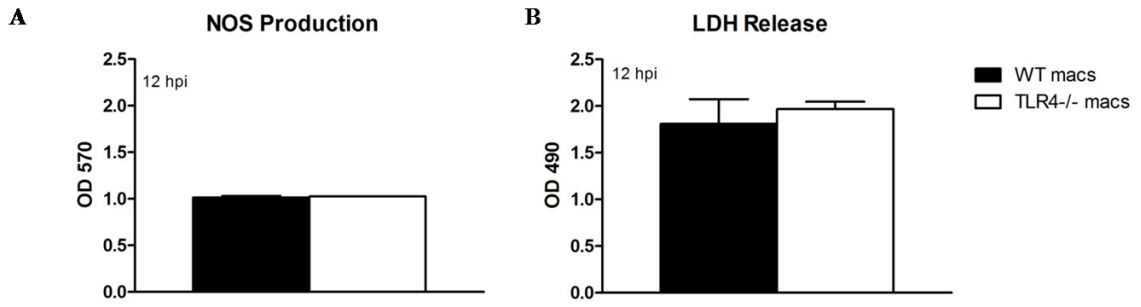

Figure 5.4: Macrophage cytotoxicity is not impacted by TLR4 signaling following co-culture with RRV-infected myotubes.

One day old WT mice were sacrificed by decapitation, and skeletal muscle was extracted for myocyte culture preparation as described in the Materials and Methods. Following myocyte differentiation, myotube cultures were infected with RRV (MOI: 20). At 2 hours post-infection, bone-marrow macrophages obtained from WT and $TLR4^{-/-}$ adult mice were added to the myotubes and co-cultured for 10 hours. (A) & (B) At 12 hours post-infection, cytotoxicity of the macrophage-myotube co-cultures was determined by ELISA using (A) NOS production and (B) LDH release in the infected supernatants as measures of cytotoxicity. Data is expressed over mock-infected cultures.

REFERENCES

1. Weaver, S. C., R. Winegar, I. D. Manger, and N. L. Forrester. 2012. Alphaviruses: population genetics and determinants of emergence. Antiviral Res. 94:242-257. doi: 10.1016/j.antiviral.2012.04.002; 10.1016/j.antiviral.2012.04.002.

2. Tauraso, N. M., and A. Shelokov. 1967. Arboviruses--a problem in classification. Arch. Gesamte Virusforsch. 22:273-279.

3. Powers, A. M., A. C. Brault, Y. Shirako, E. G. Strauss, W. Kang, J. H. Strauss, and S. C. Weaver. 2001. Evolutionary relationships and systematics of the alphaviruses. J. Virol. 75:10118-10131. doi: 10.1128/JVI.75.21.10118-10131.2001.

4. Simpson, D. I. 1972. Arbovirus diseases. Br. Med. Bull. 28:10-15.

5. Zacks, M. A., and S. Paessler. 2010. Encephalitic alphaviruses. Vet. Microbiol. 140:281-286. doi: 10.1016/j.vetmic.2009.08.023.

6. Krastinova, E., I. Quatresous, and A. Tarantola. 2006. Imported cases of chikungunya in metropolitan France: update to June 2006. Euro Surveill. 11:E060824.1.

7. Lanciotti, R. S., O. L. Kosoy, J. J. Laven, A. J. Panella, J. O. Velez, A. J. Lambert, and G. L. Campbell. 2007. Chikungunya virus in US travelers returning from India, 2006. Emerg. Infect. Dis. 13:764-767. doi: 10.3201/eid1305.070015.

8. Rezza, G., L. Nicoletti, R. Angelini, R. Romi, A. C. Finarelli, M. Panning, P. Cordioli, C. Fortuna, S. Boros, F. Magurano, G. Silvi, P. Angelini, M. Dottori, M. G. Ciufolini, G. C. Majori, A. Cassone, and CHIKV study group. 2007. Infection with chikungunya virus in Italy: an outbreak in a temperate region. Lancet. 370:1840-1846. doi: 10.1016/S0140-6736(07)61779-6.

9. Staples, J. E., R. F. Breiman, and A. M. Powers. 2009. Chikungunya fever: an epidemiological review of a re-emerging infectious disease. Clin. Infect. Dis. 49:942-948. doi: 10.1086/605496; 10.1086/605496.

10. Powers, A. M., A. C. Brault, R. B. Tesh, and S. C. Weaver. 2000. Re-emergence of Chikungunya and O'nyong-nyong viruses: evidence for distinct geographical lineages and distant evolutionary relationships. J. Gen. Virol. 81:471-479.

11. Anonymous 2007. Outbreak and spread of chikungunya. Wkly. Epidemiol. Rec. 82:409-415.

12. Staples, J. E., R. F. Breiman, and A. M. Powers. 2009. Chikungunya fever: an epidemiological review of a re-emerging infectious disease. Clin. Infect. Dis. 49:942-948. doi: 10.1086/605496; 10.1086/605496.

13. Carey, D. E. 1971. Chikungunya and dengue: a case of mistaken identity? J. Hist. Med. Allied Sci. 26:243-262.

14. Jacups, S. P., P. I. Whelan, and B. J. Currie. 2008. Ross River virus and Barmah Forest virus infections: a review of history, ecology, and predictive models, with implications for tropical northern Australia. Vector Borne Zoonotic Dis. 8:283-297. doi: 10.1089/vbz.2007.0152; 10.1089/vbz.2007.0152.

15. Suhrbier, A., M. C. Jaffar-Bandjee, and P. Gasque. 2012. Arthritogenic alphaviruses--an overview. Nat. Rev. Rheumatol. 8:420-429. doi: 10.1038/nrrheum.2012.64; 10.1038/nrrheum.2012.64.

16. Harley, D., A. Sleigh, and S. Ritchie. 2001. Ross River virus transmission, infection, and disease: a cross-disciplinary review. Clin. Microbiol. Rev. 14:909-32, table of contents. doi: 10.1128/CMR.14.4.909-932.2001.

17. Naish, S., W. Hu, K. Mengersen, and S. Tong. 2011. Spatio-temporal patterns of Barmah Forest virus disease in Queensland, Australia. PLoS One. 6:e25688. doi: 10.1371/journal.pone.0025688; 10.1371/journal.pone.0025688.

18. Russell, R. C. 1998. Mosquito-borne arboviruses in Australia: the current scene and implications of climate change for human health. Int. J. Parasitol. 28:955-969.

19. MORGAN, C., C. HOWE, and H. M. ROSE. 1961. Structure and development of viruses as observed in the electron microscope. V. Western equine encephalomyelitis virus. J. Exp. Med. 113:219-234.

20. Fuller, S. D. 1987. The T=4 envelope of Sindbis virus is organized by interactions with a complementary T=3 capsid. Cell. 48:923-934.

21. Mancini, E. J., M. Clarke, B. E. Gowen, T. Rutten, and S. D. Fuller. 2000. Cryo-electron microscopy reveals the functional organization of an enveloped virus, Semliki Forest virus. Mol. Cell. 5:255-266.

22. Jose, J., J. E. Snyder, and R. J. Kuhn. 2009. A structural and functional perspective of alphavirus replication and assembly. Future Microbiol. 4:837-856. doi: 10.2217/fmb.09.59; 10.2217/fmb.09.59.

23. Leung, J. Y., M. M. Ng, and J. J. Chu. 2011. Replication of alphaviruses: a review on the entry process of alphaviruses into cells. Adv. Virol. 2011:249640. doi: 10.1155/2011/249640; 10.1155/2011/249640.

24. Glanville, N., M. Ranki, J. Morser, L. Kaariainen, and A. E. Smith. 1976. Initiation of translation directed by 42S and 26S RNAs from Semliki Forest virus in vitro. Proc. Natl. Acad. Sci. U. S. A. 73:3059-3063.

25. Owen, K. E., and R. J. Kuhn. 1996. Identification of a region in the Sindbis virus nucleocapsid protein that is involved in specificity of RNA encapsidation. J. Virol. 70:2757-2763.

26. de Curtis, I., and K. Simons. 1988. Dissection of Semliki Forest virus glycoprotein delivery from the trans-Golgi network to the cell surface in permeabilized BHK cells. Proc. Natl. Acad. Sci. U. S. A. 85:8052-8056.

27. Jupille, H. J., L. Oko, K. A. Stoermer, M. T. Heise, S. Mahalingam, B. M. Gunn, and T. E. Morrison. 2011. Mutations in nsP1 and PE2 are critical determinants of Ross River virus-induced musculoskeletal inflammatory disease in a mouse model. Virology. 410:216-227. doi: 10.1016/j.virol.2010.11.012.

28. Cruz, C. C., M. S. Suthar, S. A. Montgomery, R. Shabman, J. Simmons, R. E. Johnston, T. E. Morrison, and M. T. Heise. 2010. Modulation of type I IFN induction by a virulence determinant within the alphavirus nsP1 protein. Virology. 399:1-10. doi: 10.1016/j.virol.2009.12.031.

29. Simmons, J. D., A. C. Wollish, and M. T. Heise. 2010. A determinant of Sindbis virus neurovirulence enables efficient disruption of Jak/STAT signaling. J. Virol. 84:11429-11439. doi: 10.1128/JVI.00577-10; 10.1128/JVI.00577-10.

30. Mayuri, T. W. Geders, J. L. Smith, and R. J. Kuhn. 2008. Role for conserved residues of sindbis virus nonstructural protein 2 methyltransferase-like domain in regulation of minus-strand synthesis and development of cytopathic infection. J. Virol. 82:7284-7297. doi: 10.1128/JVI.00224-08; 10.1128/JVI.00224-08.

31. Garmashova, N., R. Gorchakov, E. Volkova, S. Paessler, E. Frolova, and I. Frolov. 2007. The Old World and New World alphaviruses use different virus-specific proteins for induction of transcriptional shutoff. J. Virol. 81:2472-2484. doi: 10.1128/JVI.02073-06.

32. Fros, J. J., W. J. Liu, N. A. Prow, C. Geertsema, M. Ligtenberg, D. L. Vanlandingham, E. Schnettler, J. M. Vlak, A. Suhrbier, A. A. Khromykh, and G. P. Pijlman. 2010. Chikungunya virus nonstructural protein 2 inhibits type I/II interferon-stimulated JAK-STAT signaling. J. Virol. 84:10877-10887. doi: 10.1128/JVI.00949-10; 10.1128/JVI.00949-10.

33. Breakwell, L., P. Dosenovic, G. B. Karlsson Hedestam, M. D'Amato, P. Liljestrom, J. Fazakerley, and G. M. McInerney. 2007. Semliki Forest virus nonstructural protein 2 is involved in suppression of the type I interferon response. J. Virol. 81:8677-8684. doi: 10.1128/JVI.02411-06.

34. Bao, H., A. A. Ramanathan, O. Kawalakar, S. G. Sundaram, C. Tingey, C. B. Bian, N. Muruganandam, P. Vijayachari, N. Y. Sardesai, D. B. Weiner, K. E. Ugen, and K. Muthumani. 2013. Nonstructural Protein 2 (nsP2) of Chikungunya Virus (CHIKV) Enhances Protective Immunity Mediated by a CHIKV Envelope Protein Expressing DNA Vaccine. Viral Immunol. 26:75-83. doi: 10.1089/vim.2012.0061; 10.1089/vim.2012.0061.

35. Tuittila, M., and A. E. Hinkkanen. 2003. Amino acid mutations in the replicase protein nsP3 of Semliki Forest virus cumulatively affect neurovirulence. J. Gen. Virol. 84:1525-1533.

36. Park, E., and D. E. Griffin. 2009. The nsP3 macro domain is important for Sindbis virus replication in neurons and neurovirulence in mice. Virology. 388:305-314. doi: 10.1016/j.virol.2009.03.031; 10.1016/j.virol.2009.03.031.

37. Fros, J. J., N. E. Domeradzka, J. Baggen, C. Geertsema, J. Flipse, J. M. Vlak, and G. P. Pijlman. 2012. Chikungunya virus nsP3 blocks stress granule assembly by recruitment of G3BP into cytoplasmic foci. J. Virol. 86:10873-10879. doi: 10.1128/JVI.01506-12; 10.1128/JVI.01506-12.

38. Saxton-Shaw, K. D., J. P. Ledermann, E. M. Borland, J. L. Stovall, E. C. Mossel, A. J. Singh, J. Wilusz, and A. M. Powers. 2013. O'nyong nyong Virus Molecular Determinants of Unique Vector Specificity Reside in Non-Structural Protein 3. PLoS Negl Trop. Dis. 7:e1931. doi: 10.1371/journal.pntd.0001931; 10.1371/journal.pntd.0001931.

39. Rathore, A. P., M. L. Ng, and S. G. Vasudevan. 2013. Differential unfolded protein response during Chikungunya and Sindbis virus infection: CHIKV nsP4 suppresses eIF2alpha phosphorylation. Virol. J. 10:36. doi: 10.1186/1743-422X-10-36.

40. Shabman, R. S., K. M. Rogers, and M. T. Heise. 2008. Ross River virus envelope glycans contribute to type I interferon production in myeloid dendritic cells. J. Virol. 82:12374-12383. doi: 10.1128/JVI.00985-08.

41. Suhrbier, A., and M. La Linn. 2004. Clinical and pathologic aspects of arthritis due to Ross River virus and other alphaviruses. Curr. Opin. Rheumatol. 16:374-379.

42. Jaffar-Bandjee, M. C., D. Ramful, B. A. Gauzere, J. J. Hoarau, P. Krejbich-Trotot, S. Robin, A. Ribera, J. Selambarom, and P. Gasque. 2010. Emergence and clinical insights into the pathology of Chikungunya virus infection. Expert Rev. Anti Infect. Ther. 8:987-996. doi: 10.1586/eri.10.92.

43. Couderc, T., and M. Lecuit. 2009. Focus on Chikungunya pathophysiology in human and animal models. Microbes Infect. 11:1197-1205. doi: 10.1016/j.micinf.2009.09.002; 10.1016/j.micinf.2009.09.002.

44. de Andrade, D. C., S. Jean, P. Clavelou, R. Dallel, and D. Bouhassira. 2010. Chronic pain associated with the Chikungunya Fever: long lasting burden of an acute illness. BMC Infect. Dis. 10:31-2334-10-31. doi: 10.1186/1471-2334-10-31; 10.1186/1471-2334-10-31.

45. Fraser, J. R. 1986. Epidemic polyarthritis and Ross River virus disease. Clin. Rheum. Dis. 12:369-388.

46. Hoarau, J. J., M. C. Jaffar Bandjee, P. Krejbich Trotot, T. Das, G. Li-Pat-Yuen, B. Dassa, M. Denizot, E. Guichard, A. Ribera, T. Henni, F. Tallet, M. P. Moiton, B. A. Gauzere, S. Bruniquet, Z. Jaffar Bandjee, P. Morbidelli, G. Martigny, M. Jolivet, F. Gay, M. Grandadam, H. Tolou, V. Vieillard, P. Debre, B. Autran, and P. Gasque. 2010. Persistent chronic inflammation and infection by Chikungunya arthritogenic alphavirus in spite of a robust host immune response. J. Immunol. 184:5914-5927. doi: 10.4049/jimmunol.0900255; 10.4049/jimmunol.0900255.

47. Gerardin, P., G. Barau, A. Michault, M. Bintner, H. Randrianaivo, G. Choker, Y. Lenglet, Y. Touret, A. Bouveret, P. Grivard, K. Le Roux, S. Blanc, I. Schuffenecker, T. Couderc, F. Arenzana-Seisdedos, M. Lecuit, and P. Y. Robillard. 2008. Multidisciplinary prospective study of mother-to-child chikungunya virus infections on the island of La Reunion. PLoS Med. 5:e60. doi: 10.1371/journal.pmed.0050060; 10.1371/journal.pmed.0050060.

48. Bouquillard, E., and B. Combe. 2009. Rheumatoid arthritis after Chikungunya fever: a prospective follow-up study of 21 cases. Ann. Rheum. Dis. 68:1505-1506. doi: 10.1136/ard.2008.097626; 10.1136/ard.2008.097626.

49. Teo, T. H., F. M. Lum, W. W. Lee, and L. F. Ng. 2012. Mouse models for Chikungunya virus: deciphering immune mechanisms responsible for disease and pathology. Immunol. Res. 53:136-147. doi: 10.1007/s12026-012-8266-x; 10.1007/s12026-012-8266-x.

50. Heise, M. T., D. A. Simpson, and R. E. Johnston. 2000. Sindbis-group alphavirus replication in periosteum and endosteum of long bones in adult mice. J. Virol. 74:9294-9299.

51. Lidbury, B. A., C. Simeonovic, G. E. Maxwell, I. D. Marshall, and A. J. Hapel. 2000. Macrophage-induced muscle pathology results in morbidity and mortality for Ross River virus-infected mice. J. Infect. Dis. 181:27-34. doi: 10.1086/315164.

52. Gardner, J., I. Anraku, T. T. Le, T. Larcher, L. Major, P. Roques, W. A. Schroder, S. Higgs, and A. Suhrbier. 2010. Chikungunya virus arthritis in adult wild-type mice. J. Virol. 84:8021-8032. doi: 10.1128/JVI.02603-09; 10.1128/JVI.02603-09.

53. Morrison, T. E., A. C. Whitmore, R. S. Shabman, B. A. Lidbury, S. Mahalingam, and M. T. Heise. 2006. Characterization of Ross River virus tropism and virus-induced inflammation in a mouse model of viral arthritis and myositis. J. Virol. 80:737-749. doi: 10.1128/JVI.80.2.737-749.2006.

54. Morrison, T. E., L. Oko, S. A. Montgomery, A. C. Whitmore, A. R. Lotstein, B. M. Gunn, S. A. Elmore, and M. T. Heise. 2011. A mouse model of chikungunya virus-induced musculoskeletal inflammatory disease: evidence of arthritis, tenosynovitis, myositis, and persistence. Am. J. Pathol. 178:32-40. doi: 10.1016/j.ajpath.2010.11.018; 10.1016/j.ajpath.2010.11.018.

55. Kuhn, R. J., H. G. Niesters, Z. Hong, and J. H. Strauss. 1991. Infectious RNA transcripts from Ross River virus cDNA clones and the construction and characterization of defined chimeras with Sindbis virus. Virology. 182:430-441.

56. Lidbury, B. A., and S. Mahalingam. 2000. Specific ablation of antiviral gene expression in macrophages by antibody-dependent enhancement of Ross River virus infection. J. Virol. 74:8376-8381.

57. Lidbury, B. A., N. E. Rulli, A. Suhrbier, P. N. Smith, S. R. McColl, A. L. Cunningham, A. Tarkowski, N. van Rooijen, R. J. Fraser, and S. Mahalingam. 2008. Macrophage-derived proinflammatory factors contribute to the development of arthritis and myositis after infection with an arthrogenic alphavirus. J. Infect. Dis. 197:1585-1593. doi: 10.1086/587841.

58. Morrison, T. E., R. J. Fraser, P. N. Smith, S. Mahalingam, and M. T. Heise. 2007. Complement contributes to inflammatory tissue destruction in a mouse model of Ross River virus-induced disease. J. Virol. 81:5132-5143. doi: 10.1128/JVI.02799-06.

59. Morrison, T. E., J. D. Simmons, and M. T. Heise. 2008. Complement receptor 3 promotes severe ross river virus-induced disease. J. Virol. 82:11263-11272. doi: 10.1128/JVI.01352-08.

60. Gunn, B. M., T. E. Morrison, A. C. Whitmore, L. K. Blevins, L. Hueston, R. J. Fraser, L. J. Herrero, R. Ramirez, P. N. Smith, S. Mahalingam, and M. T. Heise. 2012. Mannose binding lectin is required for alphavirus-induced arthritis/myositis. PLoS Pathog. 8:e1002586. doi: 10.1371/journal.ppat.1002586; 10.1371/journal.ppat.1002586.

61. Rulli, N. E., A. Guglielmotti, G. Mangano, M. S. Rolph, C. Apicella, A. Zaid, A. Suhrbier, and S. Mahalingam. 2009. Amelioration of alphavirus-induced arthritis and myositis in a mouse model by treatment with bindarit, an inhibitor of monocyte chemotactic proteins. Arthritis Rheum. 60:2513-2523. doi: 10.1002/art.24682; 10.1002/art.24682.

62. Wang, D., A. Suhrbier, A. Penn-Nicholson, J. Woraratanadharm, J. Gardner, M. Luo, T. T. Le, I. Anraku, M. Sakalian, D. Einfeld, and J. Y. Dong. 2011. A complex adenovirus vaccine against chikungunya virus provides complete protection against viraemia and arthritis. Vaccine. 29:2803-2809. doi: 10.1016/j.vaccine.2011.01.108; 10.1016/j.vaccine.2011.01.108.

63. Mallilankaraman, K., D. J. Shedlock, H. Bao, O. U. Kawalekar, P. Fagone, A. A. Ramanathan, B. Ferraro, J. Stabenow, P. Vijayachari, S. G. Sundaram, N. Muruganandam, G. Sarangan, P. Srikanth, A. S. Khan, M. G. Lewis, J. J. Kim, N. Y. Sardesai, K. Muthumani, and D. B. Weiner. 2011. A DNA vaccine against chikungunya virus is protective in mice and induces neutralizing antibodies in mice and nonhuman primates. PLoS Negl Trop. Dis. 5:e928. doi: 10.1371/journal.pntd.0000928; 10.1371/journal.pntd.0000928.

64. Kawai, T., and S. Akira. 2010. The role of pattern-recognition receptors in innate immunity: update on Toll-like receptors. Nat. Immunol. 11:373-384. doi: 10.1038/ni.1863.

65. Akira, S., S. Uematsu, and O. Takeuchi. 2006. Pathogen recognition and innate immunity. Cell. 124:783-801. doi: 10.1016/j.cell.2006.02.015.

66. Song, D. H., and J. O. Lee. 2012. Sensing of microbial molecular patterns by Toll-like receptors. Immunol. Rev. 250:216-229. doi: 10.1111/j.1600-065X.2012.01167.x; 10.1111/j.1600-065X.2012.01167.x.

67. Lin, S. C., Y. C. Lo, and H. Wu. 2010. Helical assembly in the MyD88-IRAK4-IRAK2 complex in TLR/IL-1R signalling. Nature. 465:885-890. doi: 10.1038/nature09121; 10.1038/nature09121.

68. Luo, J., G. Obmolova, T. J. Malia, S. J. Wu, K. E. Duffy, J. D. Marion, J. K. Bell, P. Ge, Z. H. Zhou, A. Teplyakov, Y. Zhao, R. J. Lamb, J. L. Jordan, L. R. San Mateo, R. W. Sweet, and G. L. Gilliland. 2012. Lateral clustering of TLR3:dsRNA signaling units revealed by TLR3ecd:3Fabs quaternary structure. J. Mol. Biol. 421:112-124. doi: 10.1016/j.jmb.2012.05.006; 10.1016/j.jmb.2012.05.006.

69. Kawai, T., and S. Akira. 2011. Toll-like receptors and their crosstalk with other innate receptors in infection and immunity. Immunity. 34:637-650. doi: 10.1016/j.immuni.2011.05.006; 10.1016/j.immuni.2011.05.006.

70. Oldenburg, M., A. Kruger, R. Ferstl, A. Kaufmann, G. Nees, A. Sigmund, B. Bathke, H. Lauterbach, M. Suter, S. Dreher, U. Koedel, S. Akira, T. Kawai, J. Buer, H. Wagner, S. Bauer, H. Hochrein, and C. J. Kirschning. 2012. TLR13 recognizes bacterial 23S rRNA devoid of erythromycin resistance-forming modification. Science. 337:1111-1115. doi: 10.1126/science.1220363; 10.1126/science.1220363.

71. Li, M., Y. Zhou, G. Feng, and S. B. Su. 2009. The critical role of Toll-like receptor signaling pathways in the induction and progression of autoimmune diseases. Curr. Mol. Med. 9:365-374.

72. Weller, S., M. Bonnet, H. Delagreverie, L. Israel, M. Chrabieh, L. Marodi, C. Rodriguez-Gallego, B. Z. Garty, C. Roifman, A. C. Issekutz, S. E. Zitnik, C. Hoarau, Y. Camcioglu, J. Vasconcelos, C. Rodrigo, P. D. Arkwright, A. Cerutti, E. Meffre, S. Y. Zhang, A. Alcais, A. Puel, J. L. Casanova, C. Picard, J. C. Weill, and C. A. Reynaud. 2012. IgM+IgD+CD27+ B cells are markedly reduced in IRAK-4-, MyD88-, and TIRAP- but not UNC-93B-deficient patients. Blood. 120:4992-5001. doi: 10.1182/blood-2012-07-440776; 10.1182/blood-2012-07-440776.

73. Guan, Y., D. R. Ranoa, S. Jiang, S. K. Mutha, X. Li, J. Baudry, and R. I. Tapping. 2010. Human TLRs 10 and 1 share common mechanisms of innate immune sensing but not signaling. J. Immunol. 184:5094-5103. doi: 10.4049/jimmunol.0901888; 10.4049/jimmunol.0901888.

74. Andrade, W. A., C. Souza Mdo, E. Ramos-Martinez, K. Nagpal, M. S. Dutra, M. B. Melo, D. C. Bartholomeu, S. Ghosh, D. T. Golenbock, and R. T. Gazzinelli. 2013. Combined action of nucleic acid-sensing Toll-like receptors and TLR11/TLR12 heterodimers imparts resistance to Toxoplasma gondii in mice. Cell. Host Microbe. 13:42-53. doi: 10.1016/j.chom.2012.12.003; 10.1016/j.chom.2012.12.003.

75. Jeong, E., and J. Y. Lee. 2011. Intrinsic and extrinsic regulation of innate immune receptors. Yonsei Med. J. 52:379-392. doi: 10.3349/ymj.2011.52.3.429; 10.3349/ymj.2011.52.3.379.

76. Figueiredo, R. T., V. C. Bittencourt, L. C. Lopes, G. Sassaki, and E. Barreto-Bergter. 2012. Toll-like receptors (TLR2 and TLR4) recognize polysaccharides of Pseudallescheria boydii cell wall. Carbohydr. Res. 356:260-264. doi: 10.1016/j.carres.2012.02.028; 10.1016/j.carres.2012.02.028.

77. Figueiredo, R. T., P. L. Fernandez, F. F. Dutra, Y. Gonzalez, L. C. Lopes, V. C. Bittencourt, G. L. Sassaki, E. Barreto-Bergter, and M. T. Bozza. 2010. TLR4 recognizes Pseudallescheria boydii conidia and purified rhamnomannans. J. Biol. Chem. 285:40714-40723. doi: 10.1074/jbc.M110.181255; 10.1074/jbc.M110.181255.

78. Bonizzi, G., and M. Karin. 2004. The two NF-kappaB activation pathways and their role in innate and adaptive immunity. Trends Immunol. 25:280-288. doi: 10.1016/j.it.2004.03.008.

79. Taniguchi, T., K. Ogasawara, A. Takaoka, and N. Tanaka. 2001. IRF family of transcription factors as regulators of host defense. Annu. Rev. Immunol. 19:623-655. doi: 10.1146/annurev.immunol.19.1.623.

80. Browne, E. P. 2012. Regulation of B-cell responses by Toll-like receptors. Immunology. 136:370-379. doi: 10.1111/j.1365-2567.2012.03587.x; 10.1111/j.1365-2567.2012.03587.x.

81. Prince, L. R., M. K. Whyte, I. Sabroe, and L. C. Parker. 2011. The role of TLRs in neutrophil activation. Curr. Opin. Pharmacol. 11:397-403. doi: 10.1016/j.coph.2011.06.007; 10.1016/j.coph.2011.06.007.

82. Kulkarni, R., S. Behboudi, and S. Sharif. 2011. Insights into the role of Toll-like receptors in modulation of T cell responses. Cell Tissue Res. 343:141-152. doi: 10.1007/s00441-010-1017-1; 10.1007/s00441-010-1017-1.

83. Kvarnhammar, A. M., and L. O. Cardell. 2012. Pattern-recognition receptors in human eosinophils. Immunology. 136:11-20. doi: 10.1111/j.1365-2567.2012.03556.x; 10.1111/j.1365-2567.2012.03556.x.

84. Rao, K. N., and M. A. Brown. 2008. Mast cells: multifaceted immune cells with diverse roles in health and disease. Ann. N. Y. Acad. Sci. 1143:83-104. doi: 10.1196/annals.1443.023; 10.1196/annals.1443.023.

85. Brinkmann, M. M., E. Spooner, K. Hoebe, B. Beutler, H. L. Ploegh, and Y. M. Kim. 2007. The interaction between the ER membrane protein UNC93B and TLR3, 7, and 9 is crucial for TLR signaling. J. Cell Biol. 177:265-275. doi: 10.1083/jcb.200612056.

86. Akira, S. 2009. Pathogen recognition by innate immunity and its signaling. Proc. Jpn. Acad. Ser. B. Phys. Biol. Sci. 85:143-156.

87. Tang, F., Q. Du, and Y. J. Liu. 2010. Plasmacytoid dendritic cells in antiviral immunity and autoimmunity. Sci. China Life. Sci. 53:172-182. doi: 10.1007/s11427-010-0045-0; 10.1007/s11427-010-0045-0.

88. Arpaia, N., and G. M. Barton. 2011. Toll-like receptors: key players in antiviral immunity. Curr. Opin. Virol. 1:447-454. doi: 10.1016/j.coviro.2011.10.006; 10.1016/j.coviro.2011.10.006.

89. Diebold, S. S., T. Kaisho, H. Hemmi, S. Akira, and C. Reis e Sousa. 2004. Innate antiviral responses by means of TLR7-mediated recognition of single-stranded RNA. Science. 303:1529-1531. doi: 10.1126/science.1093616.

90. Lund, J. M., L. Alexopoulou, A. Sato, M. Karow, N. C. Adams, N. W. Gale, A. Iwasaki, and R. A. Flavell. 2004. Recognition of single-stranded RNA viruses by Toll-like receptor 7. Proc. Natl. Acad. Sci. U. S. A. 101:5598-5603. doi: 10.1073/pnas.0400937101.

91. Mandl, J. N., R. Akondy, B. Lawson, N. Kozyr, S. I. Staprans, R. Ahmed, and M. B. Feinberg. 2011. Distinctive TLR7 signaling, type I IFN production, and attenuated innate and adaptive immune responses to yellow fever virus in a primate reservoir host. J. Immunol. 186:6406-6416. doi: 10.4049/jimmunol.1001191; 10.4049/jimmunol.1001191.

92. Schlaepfer, E., A. Audige, H. Joller, and R. F. Speck. 2006. TLR7/8 triggering exerts opposing effects in acute versus latent HIV infection. J. Immunol. 176:2888-2895.

93. Browne, E. P. 2011. Toll-like receptor 7 controls the anti-retroviral germinal center response. PLoS Pathog. 7:e1002293. doi: 10.1371/journal.ppat.1002293.

94. Davidson, S., G. Kaiko, Z. Loh, A. Lalwani, V. Zhang, K. Spann, S. Y. Foo, N. Hansbro, S. Uematsu, S. Akira, K. I. Matthaei, H. F. Rosenberg, P. S. Foster, and S. Phipps. 2011. Plasmacytoid dendritic cells promote host defense against acute pneumovirus infection via the TLR7-MyD88-dependent signaling pathway. J. Immunol. 186:5938-5948. doi: 10.4049/jimmunol.1002635; 10.4049/jimmunol.1002635.

95. Town, T., F. Bai, T. Wang, A. T. Kaplan, F. Qian, R. R. Montgomery, J. F. Anderson, R. A. Flavell, and E. Fikrig. 2009. Toll-like receptor 7 mitigates lethal West Nile encephalitis via interleukin 23-dependent immune cell infiltration and homing. Immunity. 30:242-253. doi: 10.1016/j.immuni.2008.11.012; 10.1016/j.immuni.2008.11.012.

96. Kasturi, S. P., I. Skountzou, R. A. Albrecht, D. Koutsonanos, T. Hua, H. I. Nakaya, R. Ravindran, S. Stewart, M. Alam, M. Kwissa, F. Villinger, N. Murthy, J. Steel, J. Jacob, R. J. Hogan, A. Garcia-Sastre, R. Compans, and B. Pulendran. 2011. Programming the magnitude and persistence of antibody responses with innate immunity. Nature. 470:543-547. doi: 10.1038/nature09737.

97. Miller, R. L., T. C. Meng, and M. A. Tomai. 2008. The antiviral activity of Toll-like receptor 7 and 7/8 agonists. Drug News. Perspect. 21:69-87.

98. Tal, G., A. Mandelberg, I. Dalal, K. Cesar, E. Somekh, A. Tal, A. Oron, S. Itskovich, A. Ballin, S. Houri, A. Beigelman, O. Lider, G. Rechavi, and N. Amariglio. 2004. Association between common Toll-like receptor 4 mutations and severe respiratory syncytial virus disease. J. Infect. Dis. 189:2057-2063. doi: 10.1086/420830.

99. Kurt-Jones, E. A., L. Popova, L. Kwinn, L. M. Haynes, L. P. Jones, R. A. Tripp, E. E. Walsh, M. W. Freeman, D. T. Golenbock, L. J. Anderson, and R. W. Finberg. 2000. Pattern recognition receptors TLR4 and CD14 mediate response to respiratory syncytial virus. Nat. Immunol. 1:398-401. doi: 10.1038/80833.

100. Jude, B. A., Y. Pobezinskaya, J. Bishop, S. Parke, R. M. Medzhitov, A. V. Chervonsky, and T. V. Golovkina. 2003. Subversion of the innate immune system by a retrovirus. Nat. Immunol. 4:573-578. doi: 10.1038/ni926.

101. Burzyn, D., J. C. Rassa, D. Kim, I. Nepomnaschy, S. R. Ross, and I. Piazzon. 2004. Toll-like receptor 4-dependent activation of dendritic cells by a retrovirus. J. Virol. 78:576-584.

102. Rassa, J. C., J. L. Meyers, Y. Zhang, R. Kudaravalli, and S. R. Ross. 2002. Murine retroviruses activate B cells via interaction with toll-like receptor 4. Proc. Natl. Acad. Sci. U. S. A. 99:2281-2286. doi: 10.1073/pnas.042355399.

103. Berzsenyi, M. D., S. K. Roberts, S. Preiss, D. J. Woollard, M. R. Beard, N. A. Skinner, D. S. Bowden, and K. Visvanathan. 2011. Hepatic TLR2 & TLR4 expression correlates with hepatic inflammation and TNF-alpha in HCV & HCV/HIV infection. J. Viral Hepat. 18:852-860. doi: 10.1111/j.1365-2893.2010.01390.x; 10.1111/j.1365-2893.2010.01390.x.

104. Imai, Y., K. Kuba, G. G. Neely, R. Yaghubian-Malhami, T. Perkmann, G. van Loo, M. Ermolaeva, R. Veldhuizen, Y. H. Leung, H. Wang, H. Liu, Y. Sun, M. Pasparakis, M. Kopf, C. Mech, S. Bavari, J. S. Peiris, A. S. Slutsky, S. Akira, M. Hultqvist, R. Holmdahl, J. Nicholls, C. Jiang, C. J. Binder, and J. M. Penninger. 2008. Identification of oxidative stress and Toll-like receptor 4 signaling as a key pathway of acute lung injury. Cell. 133:235-249. doi: 10.1016/j.cell.2008.02.043; 10.1016/j.cell.2008.02.043.

105. Lagos, D., R. J. Vart, F. Gratrix, S. J. Westrop, V. Emuss, P. P. Wong, R. Robey, N. Imami, M. Bower, F. Gotch, and C. Boshoff. 2008. Toll-like receptor 4 mediates innate immunity to Kaposi sarcoma herpesvirus. Cell. Host Microbe. 4:470-483. doi: 10.1016/j.chom.2008.09.012.

106. Lin, Y., L. Yu, H. Yan, W. Yang, L. Tang, H. L. Zhang, Q. Liu, S. S. Zou, Y. Q. He, C. Wang, M. C. Wu, and H. Y. Wang. 2012. Gut-derived Lipopolysaccharide Promotes T Cell-mediated Hepatitis in Mice through Toll-like Receptor 4. Cancer. Prev. Res. (Phila). . doi: 10.1158/1940-6207.CAPR-11-0364.

107. Yu, H. T., H. Jiang, Y. Zhang, X. P. Nan, Y. Li, W. Wang, W. Jiang, D. Q. Yang, W. J. Su, J. P. Wang, P. Z. Wang, and X. F. Bai. 2012. Hantaan Virus Triggers TLR4-Dependent Innate Immune Responses. Viral Immunol. . doi: 10.1089/vim.2012.0005.

108. Anukumar, B., and P. Shahir. 2012. Chandipura Virus infection in mice: the role of toll like receptor 4 in pathogenesis. BMC Infect. Dis. 12:125. doi: 10.1186/1471-2334-12-125.

109. Abdelsadik, A., and A. Trad. 2011. Toll-like receptors on the fork roads between innate and adaptive immunity. Hum. Immunol. 72:1188-1193. doi: 10.1016/j.humimm.2011.08.015; 10.1016/j.humimm.2011.08.015.

110. Pradhan, V. D., S. Das, P. Surve, and K. Ghosh. 2012. Toll-like receptors in autoimmunity with special reference to systemic lupus erythematosus. Indian. J. Hum. Genet. 18:155-160. doi: 10.4103/0971-6866.100750; 10.4103/0971-6866.100750.

111. Asea, A., M. Rehli, E. Kabingu, J. A. Boch, O. Bare, P. E. Auron, M. A. Stevenson, and S. K. Calderwood. 2002. Novel signal transduction pathway utilized by extracellular HSP70: role of toll-like receptor (TLR) 2 and TLR4. J. Biol. Chem. 277:15028-15034. doi: 10.1074/jbc.M200497200.

112. Ohashi, K., V. Burkart, S. Flohe, and H. Kolb. 2000. Cutting edge: heat shock protein 60 is a putative endogenous ligand of the toll-like receptor-4 complex. J. Immunol. 164:558-561.

113. Vabulas, R. M., S. Braedel, N. Hilf, H. Singh-Jasuja, S. Herter, P. Ahmad-Nejad, C. J. Kirschning, C. Da Costa, H. G. Rammensee, H. Wagner, and H. Schild. 2002. The endoplasmic reticulum-resident heat shock protein Gp96 activates dendritic cells via the Toll-like receptor 2/4 pathway. J. Biol. Chem. 277:20847-20853. doi: 10.1074/jbc.M200425200.

114. Johnson, G. B., G. J. Brunn, and J. L. Platt. 2004. Cutting edge: an endogenous pathway to systemic inflammatory response syndrome (SIRS)-like reactions through Toll-like receptor 4. J. Immunol. 172:20-24.

115. Termeer, C., F. Benedix, J. Sleeman, C. Fieber, U. Voith, T. Ahrens, K. Miyake, M. Freudenberg, C. Galanos, and J. C. Simon. 2002. Oligosaccharides of Hyaluronan activate dendritic cells via toll-like receptor 4. J. Exp. Med. 195:99-111.

116. Lee, J. Y., K. H. Sohn, S. H. Rhee, and D. Hwang. 2001. Saturated fatty acids, but not unsaturated fatty acids, induce the expression of cyclooxygenase-2 mediated through Toll-like receptor 4. J. Biol. Chem. 276:16683-16689. doi: 10.1074/jbc.M011695200.

117. Smiley, S. T., J. A. King, and W. W. Hancock. 2001. Fibrinogen stimulates macrophage chemokine secretion through toll-like receptor 4. J. Immunol. 167:2887-2894.

118. Miller, Y. I., S. Viriyakosol, D. S. Worrall, A. Boullier, S. Butler, and J. L. Witztum. 2005. Toll-like receptor 4-dependent and -independent cytokine secretion induced by minimally oxidized low-density lipoprotein in macrophages. Arterioscler. Thromb. Vasc. Biol. 25:1213-1219. doi: 10.1161/01.ATV.0000159891.73193.31.

119. Goh, F. G., and K. S. Midwood. 2012. Intrinsic danger: activation of Toll-like receptors in rheumatoid arthritis. Rheumatology (Oxford). 51:7-23. doi: 10.1093/rheumatology/ker257; 10.1093/rheumatology/ker257.

120. Kim, H. S., and D. H. Chung. 2012. TLR4-mediated IL-12 production enhances IFN-gamma and IL-1beta production, which inhibits TGF-beta production and promotes antibody-induced joint inflammation. Arthritis Res. Ther. 14:R210. doi: 10.1186/ar4048.

121. Kim, J. H., H. S. Kim, H. Y. Kim, S. J. Oh, and D. H. Chung. 2012. Direct engagement of TLR4 in invariant NKT cells regulates immune diseases by differential IL-4 and IFN-gamma production in mice. PLoS One. 7:e45348. doi: 10.1371/journal.pone.0045348; 10.1371/journal.pone.0045348.

122. Ospelt, C., F. Brentano, Y. Rengel, J. Stanczyk, C. Kolling, P. P. Tak, R. E. Gay, S. Gay, and D. Kyburz. 2008. Overexpression of toll-like receptors 3 and 4 in synovial tissue from patients with early rheumatoid arthritis: toll-like receptor expression in early and longstanding arthritis. Arthritis Rheum. 58:3684-3692. doi: 10.1002/art.24140; 10.1002/art.24140.

123. Sohn, D. H., J. Sokolove, O. Sharpe, J. C. Erhart, P. E. Chandra, L. J. Lahey, T. M. Lindstrom, I. Hwang, K. A. Boyer, T. P. Andriacchi, and W. H. Robinson. 2012. Plasma proteins present in osteoarthritic synovial fluid can stimulate cytokine production via Toll-like receptor 4. Arthritis Res. Ther. 14:R7. doi: 10.1186/ar3555; 10.1186/ar3555.

124. van den Brand, B. T., S. Abdollahi-Roodsaz, M. B. Bennink, J. Bussink, O. J. Arntz, W. B. van den Berg, and F. A. van de Loo. 2013. Toll-like receptor 4 in bone marrow-derived cells as well as tissue-resident cells participate in aggravating autoimmune destructive arthritis. Ann. Rheum. Dis. . doi: 10.1136/annrheumdis-2012-202467.

125. Abdollahi-Roodsaz, S., L. A. Joosten, M. M. Helsen, B. Walgreen, P. L. van Lent, L. A. van den Bersselaar, M. I. Koenders, and W. B. van den Berg. 2008. Shift from toll-like receptor 2 (TLR-2) toward TLR-4 dependency in the erosive stage of chronic streptococcal cell wall arthritis coincident with TLR-4-mediated interleukin-17 production. Arthritis Rheum. 58:3753-3764. doi: 10.1002/art.24127; 10.1002/art.24127.

126. Abdollahi-Roodsaz, S., L. A. Joosten, M. F. Roelofs, T. R. Radstake, G. Matera, C. Popa, J. W. van der Meer, M. G. Netea, and W. B. van den Berg. 2007. Inhibition of Toll-like receptor 4 breaks the inflammatory loop in autoimmune destructive arthritis. Arthritis Rheum. 56:2957-2967. doi: 10.1002/art.22848.

127. Papadimitraki, E. D., G. K. Bertsias, and D. T. Boumpas. 2007. Toll like receptors and autoimmunity: a critical appraisal. J. Autoimmun. 29:310-318. doi: 10.1016/j.jaut.2007.09.001.

128. Hennessy, E. J., A. E. Parker, and L. A. O'Neill. 2010. Targeting Toll-like receptors: emerging therapeutics? Nat. Rev. Drug Discov. 9:293-307. doi: 10.1038/nrd3203; 10.1038/nrd3203.

129. Vogl, T., K. Tenbrock, S. Ludwig, N. Leukert, C. Ehrhardt, M. A. van Zoelen, W. Nacken, D. Foell, T. van der Poll, C. Sorg, and J. Roth. 2007. Mrp8 and Mrp14 are endogenous activators of Toll-like receptor 4, promoting lethal, endotoxin-induced shock. Nat. Med. 13:1042-1049. doi: 10.1038/nm1638.

130. Holzinger, D., M. Frosch, A. Kastrup, F. H. Prince, M. H. Otten, L. W. Van Suijlekom-Smit, R. ten Cate, E. P. Hoppenreijs, S. Hansmann, H. Moncrieffe, S. Ursu, L. R. Wedderburn, J. Roth, D. Foell, and H. Wittkowski. 2012. The Toll-like receptor 4 agonist MRP8/14 protein complex is a sensitive indicator for disease activity and predicts relapses in systemic-onset juvenile idiopathic arthritis. Ann. Rheum. Dis. 71:974-980. doi: 10.1136/annrheumdis-2011-200598; 10.1136/annrheumdis-2011-200598.

131. Loser, K., T. Vogl, M. Voskort, A. Lueken, V. Kupas, W. Nacken, L. Klenner, A. Kuhn, D. Foell, L. Sorokin, T. A. Luger, J. Roth, and S. Beissert. 2010. The Toll-like receptor 4 ligands Mrp8 and Mrp14 are crucial in the development of autoreactive CD8+ T cells. Nat. Med. 16:713-717. doi: 10.1038/nm.2150; 10.1038/nm.2150.

132. Schelbergen, R. F., A. B. Blom, M. H. van den Bosch, A. Sloetjes, S. Abdollahi-Roodsaz, B. W. Schreurs, J. S. Mort, T. Vogl, J. Roth, W. B. van den Berg, and P. L. van Lent. 2012. Alarmins S100A8 and S100A9 elicit a catabolic effect in human osteoarthritic chondrocytes that is dependent on Toll-like receptor 4. Arthritis Rheum. 64:1477-1487. doi: 10.1002/art.33495; 10.1002/art.33495.

133. Zreiqat, H., D. Belluoccio, M. M. Smith, R. Wilson, L. A. Rowley, K. Jones, Y. Ramaswamy, T. Vogl, J. Roth, J. F. Bateman, and C. B. Little. 2010. S100A8 and S100A9 in experimental osteoarthritis. Arthritis Res. Ther. 12:R16. doi: 10.1186/ar2917; 10.1186/ar2917.

134. Roelofs, M. F., L. A. Joosten, S. Abdollahi-Roodsaz, A. W. van Lieshout, T. Sprong, F. H. van den Hoogen, W. B. van den Berg, and T. R. Radstake. 2005. The expression of toll-like receptors 3 and 7 in rheumatoid arthritis synovium is increased and costimulation of toll-like receptors 3, 4, and 7/8 results in synergistic cytokine production by dendritic cells. Arthritis Rheum. 52:2313-2322. doi: 10.1002/art.21278.

135. Frolov, I., M. Akhrymuk, I. Akhrymuk, S. Atasheva, and E. I. Frolova. 2012. Early events in alphavirus replication determine the outcome of infection. J. Virol. 86:5055-5066. doi: 10.1128/JVI.07223-11; 10.1128/JVI.07223-11.

136. Ryman, K. D., and W. B. Klimstra. 2008. Host responses to alphavirus infection. Immunol. Rev. 225:27-45. doi: 10.1111/j.1600-065X.2008.00670.x.

137. Ryman, K. D., W. B. Klimstra, K. B. Nguyen, C. A. Biron, and R. E. Johnston. 2000. Alpha/beta interferon protects adult mice from fatal Sindbis virus infection and is an important determinant of cell and tissue tropism. J. Virol. 74:3366-3378.

138. White, L. J., J. G. Wang, N. L. Davis, and R. E. Johnston. 2001. Role of alpha/beta interferon in Venezuelan equine encephalitis virus pathogenesis: effect of an attenuating mutation in the 5' untranslated region. J. Virol. 75:3706-3718. doi: 10.1128/JVI.75.8.3706-3718.2001.

139. Couderc, T., F. Chretien, C. Schilte, O. Disson, M. Brigitte, F. Guivel-Benhassine, Y. Touret, G. Barau, N. Cayet, I. Schuffenecker, P. Despres, F. Arenzana-Seisdedos, A. Michault, M. L. Albert, and M. Lecuit. 2008. A mouse model for Chikungunya: young age and inefficient type-I interferon signaling are risk factors for severe disease. PLoS Pathog. 4:e29. doi: 10.1371/journal.ppat.0040029.

140. Alsharifi, M., M. Lobigs, M. Regner, E. Lee, A. Koskinen, and A. Mullbacher. 2005. Type I interferons trigger systemic, partial lymphocyte activation in response to viral infection. J. Immunol. 175:4635-4640.

141. Schilte, C., T. Couderc, F. Chretien, M. Sourisseau, N. Gangneux, F. Guivel-Benhassine, A. Kraxner, J. Tschopp, S. Higgs, A. Michault, F. Arenzana-Seisdedos, M. Colonna, L. Peduto, O. Schwartz, M. Lecuit, and M. L. Albert. 2010. Type I IFN controls chikungunya virus via its action on nonhematopoietic cells. J. Exp. Med. 207:429-442. doi: 10.1084/jem.20090851.

142. Sun, B., I. Skjaeveland, T. Svingerud, J. Zou, J. Jorgensen, and B. Robertsen. 2011. Antiviral activity of salmonid gamma interferon against infectious pancreatic necrosis virus and salmonid alphavirus and its dependency on type I interferon. J. Virol. 85:9188-9198. doi: 10.1128/JVI.00319-11.

143. Grieder, F. B., and S. N. Vogel. 1999. Role of interferon and interferon regulatory factors in early protection against Venezuelan equine encephalitis virus infection. Virology. 257:106-118. doi: 10.1006/viro.1999.9662.

144. Tseng, J. C., Y. Zheng, H. Yee, D. E. Levy, and D. Meruelo. 2007. Restricted tissue tropism and acquired resistance to Sindbis viral vector expression in the absence of innate and adaptive immunity. Gene Ther. 14:1166-1174. doi: 10.1038/sj.gt.3302973.

145. Gardner, C. L., C. W. Burke, S. T. Higgs, W. B. Klimstra, and K. D. Ryman. 2012. Interferon-alpha/beta deficiency greatly exacerbates arthritogenic disease in mice infected with wild-type chikungunya virus but not with the cell culture-adapted live-attenuated 181/25 vaccine candidate. Virology. 425:103-112. doi: 10.1016/j.virol.2011.12.020; 10.1016/j.virol.2011.12.020.

146. Furuya, Y., J. Chan, E. C. Wan, A. Koskinen, K. R. Diener, J. D. Hayball, M. Regner, A. Mullbacher, and M. Alsharifi. 2011. Gamma-irradiated influenza virus uniquely induces IFN-I mediated lymphocyte activation independent of the TLR7/MyD88 pathway. PLoS One. 6:e25765. doi: 10.1371/journal.pone.0025765; 10.1371/journal.pone.0025765.

147. Alsharifi, M., M. Lobigs, M. M. Simon, A. Kersten, K. Muller, A. Koskinen, E. Lee, and A. Mullbacher. 2006. NK cell-mediated immunopathology during an acute viral infection of the CNS. Eur. J. Immunol. 36:887-896. doi: 10.1002/eji.200535342.

148. Sato, M., H. Suemori, N. Hata, M. Asagiri, K. Ogasawara, K. Nakao, T. Nakaya, M. Katsuki, S. Noguchi, N. Tanaka, and T. Taniguchi. 2000. Distinct and essential roles of transcription factors IRF-3 and IRF-7 in response to viruses for IFN-alpha/beta gene induction. Immunity. 13:539-548.

149. Schilte, C., M. R. Buckwalter, M. E. Laird, M. S. Diamond, O. Schwartz, and M. L. Albert. 2012. Cutting edge: independent roles for IRF-3 and IRF-7 in hematopoietic and nonhematopoietic cells during host response to Chikungunya infection. J. Immunol. 188:2967-2971. doi: 10.4049/jimmunol.1103185; 10.4049/jimmunol.1103185.

150. Rudd, P. A., J. Wilson, J. Gardner, T. Larcher, C. Babarit, T. T. Le, I. Anraku, Y. Kumagai, Y. M. Loo, M. Gale Jr, S. Akira, A. A. Khromykh, and A. Suhrbier. 2012. Interferon response factors 3 and 7 protect against Chikungunya virus hemorrhagic fever and shock. J. Virol. 86:9888-9898. doi: 10.1128/JVI.00956-12; 10.1128/JVI.00956-12.

151. Esen, N., P. K. Blakely, E. K. Rainey-Barger, and D. N. Irani. 2012. Complexity of the microglial activation pathways that drive innate host responses during lethal alphavirus encephalitis in mice. ASN Neuro. 4:207-221. doi: 10.1042/AN20120016; 10.1042/AN20120016.

152. Peltier, D. C., H. M. Lazear, J. R. Farmer, M. S. Diamond, and D. J. Miller. 2013. Neurotropic arboviruses induce interferon regulatory factor 3-mediated neuronal responses that are cytoprotective, interferon independent, and inhibited by Western equine encephalitis virus capsid. J. Virol. 87:1821-1833. doi: 10.1128/JVI.02858-12; 10.1128/JVI.02858-12.

153. Koterski, J., N. Twenhafel, A. Porter, D. S. Reed, S. Martino-Catt, B. Sobral, O. Crasta, T. Downey, and L. DaSilva. 2007. Gene expression profiling of nonhuman

primates exposed to aerosolized Venezuelan equine encephalitis virus. FEMS Immunol. Med. Microbiol. 51:462-472. doi: 10.1111/j.1574-695X.2007.00319.x.

154. Patil, D. R., S. L. Hundekar, and V. A. Arankalle. 2012. Expression profile of immune response genes during acute myopathy induced by chikungunya virus in a mouse model. Microbes Infect. 14:457-469. doi: 10.1016/j.micinf.2011.12.008; 10.1016/j.micinf.2011.12.008.

155. Schoggins, J. W., S. J. Wilson, M. Panis, M. Y. Murphy, C. T. Jones, P. Bieniasz, and C. M. Rice. 2011. A diverse range of gene products are effectors of the type I interferon antiviral response. Nature. 472:481-485. doi: 10.1038/nature09907; 10.1038/nature09907.

156. Zhang, Y., C. W. Burke, K. D. Ryman, and W. B. Klimstra. 2007. Identification and characterization of interferon-induced proteins that inhibit alphavirus replication. J. Virol. 81:11246-11255. doi: 10.1128/JVI.01282-07.

157. Lenschow, D. J., C. Lai, N. Frias-Staheli, N. V. Giannakopoulos, A. Lutz, T. Wolff, A. Osiak, B. Levine, R. E. Schmidt, A. Garcia-Sastre, D. A. Leib, A. Pekosz, K. P. Knobeloch, I. Horak, and H. W. Virgin 4th. 2007. IFN-stimulated gene 15 functions as a critical antiviral molecule against influenza, herpes, and Sindbis viruses. Proc. Natl. Acad. Sci. U. S. A. 104:1371-1376. doi: 10.1073/pnas.0607038104.

158. Werneke, S. W., C. Schilte, A. Rohatgi, K. J. Monte, A. Michault, F. Arenzana-Seisdedos, D. L. Vanlandingham, S. Higgs, A. Fontanet, M. L. Albert, and D. J. Lenschow. 2011. ISG15 is critical in the control of Chikungunya virus infection independent of UbE1L mediated conjugation. PLoS Pathog. 7:e1002322. doi: 10.1371/journal.ppat.1002322; 10.1371/journal.ppat.1002322.

159. Giannakopoulos, N. V., E. Arutyunova, C. Lai, D. J. Lenschow, A. L. Haas, and H. W. Virgin. 2009. ISG15 Arg151 and the ISG15-conjugating enzyme UbE1L are important for innate immune control of Sindbis virus. J. Virol. 83:1602-1610. doi: 10.1128/JVI.01590-08; 10.1128/JVI.01590-08.

160. Teng, T. S., S. S. Foo, D. Simamarta, F. M. Lum, T. H. Teo, A. Lulla, N. K. Yeo, E. G. Koh, A. Chow, Y. S. Leo, A. Merits, K. C. Chin, and L. F. Ng. 2012. Viperin restricts chikungunya virus replication and pathology. J. Clin. Invest. 122:4447-4460. doi: 10.1172/JCI63120; 10.1172/JCI63120.

161. Jones, P. H., M. Maric, M. N. Madison, W. Maury, R. J. Roller, and C. M. Okeoma. 2013. BST-2/tetherin-mediated restriction of chikungunya (CHIKV) VLP budding is counteracted by CHIKV non-structural protein 1 (nsP1). Virology. 438:37-49. doi: 10.1016/j.virol.2013.01.010; 10.1016/j.virol.2013.01.010.

162. Landis, H., A. Simon-Jodicke, A. Kloti, C. Di Paolo, J. J. Schnorr, S. Schneider-Schaulies, H. P. Hefti, and J. Pavlovic. 1998. Human MxA protein confers resistance

to Semliki Forest virus and inhibits the amplification of a Semliki Forest virus-based replicon in the absence of viral structural proteins. J. Virol. 72:1516-1522.

163. Atasheva, S., M. Akhrymuk, E. I. Frolova, and I. Frolov. 2012. New PARP gene with an anti-alphavirus function. J. Virol. 86:8147-8160. doi: 10.1128/JVI.00733-12; 10.1128/JVI.00733-12.

164. Brehin, A. C., I. Casademont, M. P. Frenkiel, C. Julier, A. Sakuntabhai, and P. Despres. 2009. The large form of human 2',5'-Oligoadenylate Synthetase (OAS3) exerts antiviral effect against Chikungunya virus. Virology. 384:216-222. doi: 10.1016/j.virol.2008.10.021; 10.1016/j.virol.2008.10.021.

165. Karki, S., M. M. Li, J. W. Schoggins, S. Tian, C. M. Rice, and M. R. MacDonald. 2012. Multiple interferon stimulated genes synergize with the zinc finger antiviral protein to mediate anti-alphavirus activity. PLoS One. 7:e37398. doi: 10.1371/journal.pone.0037398; 10.1371/journal.pone.0037398.

166. Burke, C. W., C. L. Gardner, J. J. Steffan, K. D. Ryman, and W. B. Klimstra. 2009. Characteristics of alpha/beta interferon induction after infection of murine fibroblasts with wild-type and mutant alphaviruses. Virology. 395:121-132. doi: 10.1016/j.virol.2009.08.039.

167. Akhrymuk, I., S. V. Kulemzin, and E. I. Frolova. 2012. Evasion of the innate immune response: the Old World alphavirus nsP2 protein induces rapid degradation of Rpb1, a catalytic subunit of RNA polymerase II. J. Virol. 86:7180-7191. doi: 10.1128/JVI.00541-12; 10.1128/JVI.00541-12.

168. Simmons, J. D., L. J. White, T. E. Morrison, S. A. Montgomery, A. C. Whitmore, R. E. Johnston, and M. T. Heise. 2009. Venezuelan equine encephalitis virus disrupts STAT1 signaling by distinct mechanisms independent of host shutoff. J. Virol. 83:10571-10581. doi: 10.1128/JVI.01041-09; 10.1128/JVI.01041-09.

169. Yin, J., C. L. Gardner, C. W. Burke, K. D. Ryman, and W. B. Klimstra. 2009. Similarities and differences in antagonism of neuron alpha/beta interferon responses by Venezuelan equine encephalitis and Sindbis alphaviruses. J. Virol. 83:10036-10047. doi: 10.1128/JVI.01209-09; 10.1128/JVI.01209-09.

170. Rulli, N. E., A. Suhrbier, L. Hueston, M. T. Heise, D. Tupanceska, A. Zaid, A. Wilmes, K. Gilmore, B. A. Lidbury, and S. Mahalingam. 2005. Ross River virus: molecular and cellular aspects of disease pathogenesis. Pharmacol. Ther. 107:329-342. doi: 10.1016/j.pharmthera.2005.03.006.

171. Nakaya, H. I., J. Gardner, Y. S. Poo, L. Major, B. Pulendran, and A. Suhrbier. 2012. Gene profiling of Chikungunya virus arthritis in a mouse model reveals significant overlap with rheumatoid arthritis. Arthritis Rheum. 64:3553-3563. doi: 10.1002/art.34631; 10.1002/art.34631.

172. Morrison, T. E., and M. T. Heise. 2008. The host complement system and arbovirus pathogenesis. Curr. Drug Targets. 9:165-172.

173. Brooke, C. B., A. Schafer, G. K. Matsushima, L. J. White, and R. E. Johnston. 2012. Early activation of the host complement system is required to restrict central nervous system invasion and limit neuropathology during Venezuelan equine encephalitis virus infection. J. Gen. Virol. 93:797-806. doi: 10.1099/vir.0.038281-0; 10.1099/vir.0.038281-0.

174. Boere, W. A., B. J. Benaissa-Trouw, T. Harmsen, T. Erich, C. A. Kraaijeveld, and H. Snippe. 1986. The role of complement in monoclonal antibody-mediated protection against virulent Semliki Forest virus. Immunology. 58:553-559.

175. Herrero, L. J., M. Nelson, A. Srikiatkhachorn, R. Gu, S. Anantapreecha, G. Fingerle-Rowson, R. Bucala, E. Morand, L. L. Santos, and S. Mahalingam. 2011. Critical role for macrophage migration inhibitory factor (MIF) in Ross River virus-induced arthritis and myositis. Proc. Natl. Acad. Sci. U. S. A. 108:12048-12053. doi: 10.1073/pnas.1101089108.

176. Rulli, N. E., M. S. Rolph, A. Srikiatkhachorn, S. Anantapreecha, A. Guglielmotti, and S. Mahalingam. 2011. Protection from arthritis and myositis in a mouse model of acute chikungunya virus disease by bindarit, an inhibitor of monocyte chemotactic protein-1 synthesis. J. Infect. Dis. 204:1026-1030. doi: 10.1093/infdis/jir470; 10.1093/infdis/jir470.

177. Chang, M., B. Collet, P. Nie, K. Lester, S. Campbell, C. J. Secombes, and J. Zou. 2011. Expression and functional characterization of the RIG-I-like receptors MDA5 and LGP2 in Rainbow trout (Oncorhynchus mykiss). J. Virol. 85:8403-8412. doi: 10.1128/JVI.00445-10; 10.1128/JVI.00445-10.

178. Thon-Hon, V. G., M. Denizot, G. Li-Pat-Yuen, C. Giry, M. C. Jaffar-Bandjee, and P. Gasque. 2012. Deciphering the differential response of two human fibroblast cell lines following Chikungunya virus infection. Virol. J. 9:213-422X-9-213. doi: 10.1186/1743-422X-9-213; 10.1186/1743-422X-9-213.

179. Gitlin, L., W. Barchet, S. Gilfillan, M. Cella, B. Beutler, R. A. Flavell, M. S. Diamond, and M. Colonna. 2006. Essential role of mda-5 in type I IFN responses to polyriboinosinic:polyribocytidylic acid and encephalomyocarditis picornavirus. Proc. Natl. Acad. Sci. U. S. A. 103:8459-8464. doi: 10.1073/pnas.0603082103.

180. Kato, H., S. Sato, M. Yoneyama, M. Yamamoto, S. Uematsu, K. Matsui, T. Tsujimura, K. Takeda, T. Fujita, O. Takeuchi, and S. Akira. 2005. Cell type-specific involvement of RIG-I in antiviral response. Immunity. 23:19-28. doi: 10.1016/j.immuni.2005.04.010.

181. White, L. K., T. Sali, D. Alvarado, E. Gatti, P. Pierre, D. Streblow, and V. R. Defilippis. 2011. Chikungunya virus induces IPS-1-dependent innate immune activation and protein kinase R-independent translational shutoff. J. Virol. 85:606-620. doi: 10.1128/JVI.00767-10; 10.1128/JVI.00767-10.

182. Wollish, A. C., M. T. Ferris, L. K. Blevins, Y. M. Loo, M. Gale Jr, and M. T. Heise. 2013. An attenuating mutation in a neurovirulent Sindbis virus strain interacts with the IPS-1 signaling pathway in vivo. Virology. 435:269-280. doi: 10.1016/j.virol.2012.09.008; 10.1016/j.virol.2012.09.008.

183. Schulz, O., A. Pichlmair, J. Rehwinkel, N. C. Rogers, D. Scheuner, H. Kato, O. Takeuchi, S. Akira, R. J. Kaufman, and C. Reis e Sousa. 2010. Protein kinase R contributes to immunity against specific viruses by regulating interferon mRNA integrity. Cell. Host Microbe. 7:354-361. doi: 10.1016/j.chom.2010.04.007; 10.1016/j.chom.2010.04.007.

184. Gorchakov, R., E. Frolova, B. R. Williams, C. M. Rice, and I. Frolov. 2004. PKR-dependent and -independent mechanisms are involved in translational shutoff during Sindbis virus infection. J. Virol. 78:8455-8467. doi: 10.1128/JVI.78.16.8455-8467.2004.

185. Shabman, R. S., T. E. Morrison, C. Moore, L. White, M. S. Suthar, L. Hueston, N. Rulli, B. Lidbury, J. P. Ting, S. Mahalingam, and M. T. Heise. 2007. Differential induction of type I interferon responses in myeloid dendritic cells by mosquito and mammalian-cell-derived alphaviruses. J. Virol. 81:237-247. doi: 10.1128/JVI.01590-06.

186. Knight, R. L., K. L. Schultz, R. J. Kent, M. Venkatesan, and D. E. Griffin. 2009. Role of N-linked glycosylation for sindbis virus infection and replication in vertebrate and invertebrate systems. J. Virol. 83:5640-5647. doi: 10.1128/JVI.02427-08; 10.1128/JVI.02427-08.

187. Klimstra, W. B., E. M. Nangle, M. S. Smith, A. D. Yurochko, and K. D. Ryman. 2003. DC-SIGN and L-SIGN can act as attachment receptors for alphaviruses and distinguish between mosquito cell- and mammalian cell-derived viruses. J. Virol. 77:12022-12032.

188. Long, K. M., A. C. Whitmore, M. T. Ferris, G. D. Sempowski, C. McGee, B. Trollinger, B. Gunn, and M. Heise. 2013. Dendritic cell immune receptor (DCIR) regulates Chikungunya virus pathogenesis in mice. J. Virol. . doi: 10.1128/JVI.01611-12.

189. Li, Y. G., U. Siripanyaphinyo, U. Tumkosit, N. Noranate, A. A-Nuegoonpipat, Y. Pan, M. Kameoka, T. Kurosu, K. Ikuta, N. Takeda, and S. Anantapreecha. 2012. Poly (I:C), an agonist of toll-like receptor-3, inhibits replication of the Chikungunya

virus in BEAS-2B cells. Virol. J. 9:114-422X-9-114. doi: 10.1186/1743-422X-9-114; 10.1186/1743-422X-9-114.

190. Laine, M., R. Luukkainen, and A. Toivanen. 2004. Sindbis viruses and other alphaviruses as cause of human arthritic disease. J. Intern. Med. 256:457-471. doi: 10.1111/j.1365-2796.2004.01413.x.

191. Staples, J. E., R. F. Breiman, and A. M. Powers. 2009. Chikungunya fever: an epidemiological review of a re-emerging infectious disease. Clin. Infect. Dis. 49:942-948. doi: 10.1086/605496.

192. Gould, E. A., B. Coutard, H. Malet, B. Morin, S. Jamal, S. Weaver, A. Gorbalenya, G. Moureau, C. Baronti, I. Delogu, N. Forrester, M. Khasnatinov, T. Gritsun, X. de Lamballerie, and B. Canard. 2010. Understanding the alphaviruses: recent research on important emerging pathogens and progress towards their control. Antiviral Res. 87:111-124. doi: 10.1016/j.antiviral.2009.07.007.

193. Morrison, T. E., A. C. Whitmore, R. S. Shabman, B. A. Lidbury, S. Mahalingam, and M. T. Heise. 2006. Characterization of Ross River virus tropism and virus-induced inflammation in a mouse model of viral arthritis and myositis. J. Virol. 80:737-749. doi: 10.1128/JVI.80.2.737-749.2006.

194. Yamamoto, M., and S. Akira. 2005. TIR domain-containing adaptors regulate TLR signaling pathways. Adv. Exp. Med. Biol. 560:1-9. doi: 10.1007/0-387-24180-9_1.

195. McKimmie, C. S., and J. K. Fazakerley. 2005. In response to pathogens, glial cells dynamically and differentially regulate Toll-like receptor gene expression. J. Neuroimmunol. 169:116-125. doi: 10.1016/j.jneuroim.2005.08.006.

196. McKimmie, C. S., N. Johnson, A. R. Fooks, and J. K. Fazakerley. 2005. Viruses selectively upregulate Toll-like receptors in the central nervous system. Biochem. Biophys. Res. Commun. 336:925-933. doi: 10.1016/j.bbrc.2005.08.209.

197. Takeda, K. 2005. Evolution and integration of innate immune recognition systems: the Toll-like receptors. J. Endotoxin Res. 11:51-55. doi: 10.1179/096805105225006687.

198. Oda, K., and H. Kitano. 2006. A comprehensive map of the toll-like receptor signaling network. Mol. Syst. Biol. 2:2006.0015. doi: 10.1038/msb4100057.

199. Watters, T. M., E. F. Kenny, and L. A. O'Neill. 2007. Structure, function and regulation of the Toll/IL-1 receptor adaptor proteins. Immunol. Cell Biol. 85:411-419. doi: 10.1038/sj.icb.7100095.

200. Burns, K., F. Martinon, C. Esslinger, H. Pahl, P. Schneider, J. L. Bodmer, F. Di Marco, L. French, and J. Tschopp. 1998. MyD88, an adapter protein involved in interleukin-1 signaling. J. Biol. Chem. 273:12203-12209.

201. Boraschi, D., and A. Tagliabue. 2006. The interleukin-1 receptor family. Vitam. Horm. 74:229-254. doi: 10.1016/S0083-6729(06)74009-2.

202. Davidson, S., G. Kaiko, Z. Loh, A. Lalwani, V. Zhang, K. Spann, S. Y. Foo, N. Hansbro, S. Uematsu, S. Akira, K. I. Matthaei, H. F. Rosenberg, P. S. Foster, and S. Phipps. 2011. Plasmacytoid dendritic cells promote host defense against acute pneumovirus infection via the TLR7-MyD88-dependent signaling pathway. J. Immunol. 186:5938-5948. doi: 10.4049/jimmunol.1002635.

203. Yang, K., A. Puel, S. Zhang, C. Eidenschenk, C. L. Ku, A. Casrouge, C. Picard, H. von Bernuth, B. Senechal, S. Plancoulaine, S. Al-Hajjar, A. Al-Ghonaium, L. Marodi, D. Davidson, D. Speert, C. Roifman, B. Z. Garty, A. Ozinsky, F. J. Barrat, R. L. Coffman, R. L. Miller, X. Li, P. Lebon, C. Rodriguez-Gallego, H. Chapel, F. Geissmann, E. Jouanguy, and J. L. Casanova. 2005. Human TLR-7-, -8-, and -9-mediated induction of IFN-alpha/beta and -lambda Is IRAK-4 dependent and redundant for protective immunity to viruses. Immunity. 23:465-478. doi: 10.1016/j.immuni.2005.09.016.

204. Simone, O., C. Tortorella, B. Zaccaro, N. Napoli, and S. Antonaci. 2010. Impairment of TLR7-dependent signaling in dendritic cells from chronic hepatitis C virus (HCV)-infected non-responders to interferon/ribavirin therapy. J. Clin. Immunol. 30:556-565. doi: 10.1007/s10875-010-9387-4.

205. Mandl, J. N., R. Akondy, B. Lawson, N. Kozyr, S. I. Staprans, R. Ahmed, and M. B. Feinberg. 2011. Distinctive TLR7 signaling, type I IFN production, and attenuated innate and adaptive immune responses to yellow fever virus in a primate reservoir host. J. Immunol. 186:6406-6416. doi: 10.4049/jimmunol.1001191.

206. Stewart, C. R., A. Bagnaud-Baule, A. J. Karpala, S. Lowther, P. G. Mohr, T. G. Wise, J. W. Lowenthal, and A. G. Bean. 2011. Toll-Like Receptor 7 Ligands Inhibit Influenza A Infection in Chickens. J. Interferon Cytokine Res. . doi: 10.1089/jir.2011.0036.

207. Cervantes-Barragan, L., R. Zust, F. Weber, M. Spiegel, K. S. Lang, S. Akira, V. Thiel, and B. Ludewig. 2007. Control of coronavirus infection through plasmacytoid dendritic-cell-derived type I interferon. Blood. 109:1131-1137. doi: 10.1182/blood-2006-05-023770.

208. Takahashi, K., S. Asabe, S. Wieland, U. Garaigorta, P. Gastaminza, M. Isogawa, and F. V. Chisari. 2010. Plasmacytoid dendritic cells sense hepatitis C virus-infected cells, produce interferon, and inhibit infection. Proc. Natl. Acad. Sci. U. S. A. 107:7431-7436. doi: 10.1073/pnas.1002301107.

209. Wang, K., R. Liu, J. Li, J. Mao, Y. Lei, J. Wu, J. Zeng, T. Zhang, H. Wu, L. Chen, C. Huang, and Y. Wei. 2011. Quercetin induces protective autophagy in gastric cancer cells: Involvement of Akt-mTOR- and hypoxia-induced factor 1alpha-mediated signaling. Autophagy. 7:.

210. Yoneyama, H., K. Matsuno, E. Toda, T. Nishiwaki, N. Matsuo, A. Nakano, S. Narumi, B. Lu, C. Gerard, S. Ishikawa, and K. Matsushima. 2005. Plasmacytoid DCs help lymph node DCs to induce anti-HSV CTLs. J. Exp. Med. 202:425-435. doi: 10.1084/jem.20041961.

211. Zucchini, N., G. Bessou, S. Traub, S. H. Robbins, S. Uematsu, S. Akira, L. Alexopoulou, and M. Dalod. 2008. Cutting edge: Overlapping functions of TLR7 and TLR9 for innate defense against a herpesvirus infection. J. Immunol. 180:5799-5803.

212. Burdeinick-Kerr, R., J. Wind, and D. E. Griffin. 2007. Synergistic roles of antibody and interferon in noncytolytic clearance of Sindbis virus from different regions of the central nervous system. J. Virol. 81:5628-5636. doi: 10.1128/JVI.01152-06.

213. Fragkoudis, R., L. Breakwell, C. McKimmie, A. Boyd, G. Barry, A. Kohl, A. Merits, and J. K. Fazakerley. 2007. The type I interferon system protects mice from Semliki Forest virus by preventing widespread virus dissemination in extraneural tissues, but does not mediate the restricted replication of avirulent virus in central nervous system neurons. J. Gen. Virol. 88:3373-3384. doi: 10.1099/vir.0.83191-0.

214. Mosmann, T. R., and R. L. Coffman. 1989. TH1 and TH2 cells: different patterns of lymphokine secretion lead to different functional properties. Annu. Rev. Immunol. 7:145-173. doi: 10.1146/annurev.iy.07.040189.001045.

215. Romagnani, S. 1995. Biology of human TH1 and TH2 cells. J. Clin. Immunol. 15:121-129.

216. Mosmann, T. R., H. Cherwinski, M. W. Bond, M. A. Giedlin, and R. L. Coffman. 2005. Two types of murine helper T cell clone. I. Definition according to profiles of lymphokine activities and secreted proteins. 1986. J. Immunol. 175:5-14.

217. Aydar, Y., S. Sukumar, A. K. Szakal, and J. G. Tew. 2005. The influence of immune complex-bearing follicular dendritic cells on the IgM response, Ig class switching, and production of high affinity IgG. J. Immunol. 174:5358-5366.

218. Barry, G., L. Breakwell, R. Fragkoudis, G. Attarzadeh-Yazdi, J. Rodriguez-Andres, A. Kohl, and J. K. Fazakerley. 2009. PKR acts early in infection to suppress Semliki Forest virus production and strongly enhances the type I interferon response. J. Gen. Virol. 90:1382-1391. doi: 10.1099/vir.0.007336-0.

219. Ryman, K. D., and W. B. Klimstra. 2008. Host responses to alphavirus infection. Immunol. Rev. 225:27-45. doi: 10.1111/j.1600-065X.2008.00670.x.

220. Ryman, K. D., L. J. White, R. E. Johnston, and W. B. Klimstra. 2002. Effects of PKR/RNase L-dependent and alternative antiviral pathways on alphavirus replication and pathogenesis. Viral Immunol. 15:53-76. doi: 10.1089/088282402317340233.

221. McHeyzer-Williams, L. J., N. Pelletier, L. Mark, N. Fazilleau, and M. G. McHeyzer-Williams. 2009. Follicular helper T cells as cognate regulators of B cell immunity. Curr. Opin. Immunol. 21:266-273. doi: 10.1016/j.coi.2009.05.010.

222. Chen, M., C. Barnfield, T. I. Naslund, M. N. Fleeton, and P. Liljestrom. 2005. MyD88 expression is required for efficient cross-presentation of viral antigens from infected cells. J. Virol. 79:2964-2972. doi: 10.1128/JVI.79.5.2964-2972.2005.

223. Diebold, S. S., M. Montoya, H. Unger, L. Alexopoulou, P. Roy, L. E. Haswell, A. Al-Shamkhani, R. Flavell, P. Borrow, and C. Reis e Sousa. 2003. Viral infection switches non-plasmacytoid dendritic cells into high interferon producers. Nature. 424:324-328. doi: 10.1038/nature01783.

224. Gilliet, M., W. Cao, and Y. J. Liu. 2008. Plasmacytoid dendritic cells: sensing nucleic acids in viral infection and autoimmune diseases. Nat. Rev. Immunol. 8:594-606. doi: 10.1038/nri2358.

225. Colonna, M., G. Trinchieri, and Y. J. Liu. 2004. Plasmacytoid dendritic cells in immunity. Nat. Immunol. 5:1219-1226. doi: 10.1038/ni1141.

226. Delgado, M. F., S. Coviello, A. C. Monsalvo, G. A. Melendi, J. Z. Hernandez, J. P. Batalle, L. Diaz, A. Trento, H. Y. Chang, W. Mitzner, J. Ravetch, J. A. Melero, P. M. Irusta, and F. P. Polack. 2009. Lack of antibody affinity maturation due to poor Toll-like receptor stimulation leads to enhanced respiratory syncytial virus disease. Nat. Med. 15:34-41. doi: 10.1038/nm.1894.

227. Walport, M. J. 2001. Complement. First of two parts. N. Engl. J. Med. 344:1058-1066. doi: 10.1056/NEJM200104053441406.

228. Trouw, L. A., and M. R. Daha. 2011. Role of complement in innate immunity and host defense. Immunol. Lett. 138:35-37. doi: 10.1016/j.imlet.2011.02.014.

229. Hietala, M. A., I. M. Jonsson, A. Tarkowski, S. Kleinau, and M. Pekna. 2002. Complement deficiency ameliorates collagen-induced arthritis in mice. J. Immunol. 169:454-459.

230. Ji, H., K. Ohmura, U. Mahmood, D. M. Lee, F. M. Hofhuis, S. A. Boackle, K. Takahashi, V. M. Holers, M. Walport, C. Gerard, A. Ezekowitz, M. C. Carroll, M.

Brenner, R. Weissleder, J. S. Verbeek, V. Duchatelle, C. Degott, C. Benoist, and D. Mathis. 2002. Arthritis critically dependent on innate immune system players. Immunity. 16:157-168.

231. Takada, A., and Y. Kawaoka. 2003. Antibody-dependent enhancement of viral infection: molecular mechanisms and in vivo implications. Rev. Med. Virol. 13:387-398. doi: 10.1002/rmv.405.

232. Ganu, M. A., and A. S. Ganu. 2011. Post-chikungunya chronic arthritis--our experience with DMARDs over two year follow up. J. Assoc. Physicians India. 59:83-86.

233. Manimunda, S. P., P. Vijayachari, R. Uppoor, A. P. Sugunan, S. S. Singh, S. K. Rai, A. B. Sudeep, N. Muruganandam, I. K. Chaitanya, and D. R. Guruprasad. 2010. Clinical progression of chikungunya fever during acute and chronic arthritic stages and the changes in joint morphology as revealed by imaging. Trans. R. Soc. Trop. Med. Hyg. 104:392-399. doi: 10.1016/j.trstmh.2010.01.011; 10.1016/j.trstmh.2010.01.011.

234. Ricklin, D., G. Hajishengallis, K. Yang, and J. D. Lambris. 2010. Complement: a key system for immune surveillance and homeostasis. Nat. Immunol. 11:785-797. doi: 10.1038/ni.1923; 10.1038/ni.1923.

235. Neighbours, L. M., K. Long, A. C. Whitmore, and M. T. Heise. 2012. Myd88-dependent TLR7 signaling mediates protection from severe Ross River virus-induced disease in mice. J. Virol. . doi: 10.1128/JVI.00601-12.

236. Hansel, T. T., H. Kropshofer, T. Singer, J. A. Mitchell, and A. J. George. 2010. The safety and side effects of monoclonal antibodies. Nat. Rev. Drug Discov. 9:325-338. doi: 10.1038/nrd3003; 10.1038/nrd3003.

237. Sacks, S. H., W. Zhou, and N. S. Sheerin. 1996. Complement synthesis in the injured kidney: does it have a role in immune complex glomerulonephritis? J. Am. Soc. Nephrol. 7:2314-2319.

238. Schellekens, H. 2005. Factors influencing the immunogenicity of therapeutic proteins. Nephrol. Dial. Transplant. 20 Suppl 6:vi3-9. doi: 10.1093/ndt/gfh1092.

239. Schernthaner, G. 1993. Immunogenicity and allergenic potential of animal and human insulins. Diabetes Care. 16 Suppl 3:155-165.

240. Nangaku, M., and W. G. Couser. 2005. Mechanisms of immune-deposit formation and the mediation of immune renal injury. Clin. Exp. Nephrol. 9:183-191. doi: 10.1007/s10157-005-0357-8.

241. Dennert, R., H. J. Crijns, and S. Heymans. 2008. Acute viral myocarditis. Eur. Heart J. 29:2073-2082. doi: 10.1093/eurheartj/ehn296; 10.1093/eurheartj/ehn296.

242. Corsten, M. F., B. Schroen, and S. Heymans. 2012. Inflammation in viral myocarditis: friend or foe? Trends Mol. Med. 18:426-437. doi: 10.1016/j.molmed.2012.05.005; 10.1016/j.molmed.2012.05.005.

243. Girn, J., M. Kavoosi, and J. Chantler. 2002. Enhancement of coxsackievirus B3 infection by antibody to a different coxsackievirus strain. J. Gen. Virol. 83:351-358.

244. Atefi, G., F. S. Zetoune, T. J. Herron, J. Jalife, M. Bosmann, R. Al-Aref, J. V. Sarma, and P. A. Ward. 2011. Complement dependency of cardiomyocyte release of mediators during sepsis. FASEB J. 25:2500-2508. doi: 10.1096/fj.11-183236; 10.1096/fj.11-183236.

245. Cain, B. S., D. R. Meldrum, C. A. Dinarello, X. Meng, K. S. Joo, A. Banerjee, and A. H. Harken. 1999. Tumor necrosis factor-alpha and interleukin-1beta synergistically depress human myocardial function. Crit. Care Med. 27:1309-1318.

246. Janssen, S. P., G. Gayan-Ramirez, A. Van den Bergh, P. Herijgers, K. Maes, E. Verbeken, and M. Decramer. 2005. Interleukin-6 causes myocardial failure and skeletal muscle atrophy in rats. Circulation. 111:996-1005. doi: 10.1161/01.CIR.0000156469.96135.0D.

247. Kumar, A., V. Thota, L. Dee, J. Olson, E. Uretz, and J. E. Parrillo. 1996. Tumor necrosis factor alpha and interleukin 1beta are responsible for in vitro myocardial cell depression induced by human septic shock serum. J. Exp. Med. 183:949-958.

248. Maass, D. L., J. White, and J. W. Horton. 2002. IL-1beta and IL-6 act synergistically with TNF-alpha to alter cardiac contractile function after burn trauma. Shock. 18:360-366.

249. Rose, N. R., and S. L. Hill. 1996. Autoimmune myocarditis. Int. J. Cardiol. 54:171-175.

250. Welch, T. R., and L. W. Blystone. 2005. C3 is central to the interstitial component of experimental immune complex glomerulonephritis. Clin. Immunol. 115:80-84. doi: 10.1016/j.clim.2004.10.008.

251. Sam, I. C., A. Kamarulzaman, G. S. Ong, R. S. Veriah, S. Ponnampalavanar, Y. F. Chan, and S. AbuBakar. 2010. Chikungunya virus-associated death in Malaysia. Trop. Biomed. 27:343-347.

252. Menon, P. R., K. C, J. Sankar, K. M. Gopinathan, and G. Mohan. 2010. A child with serious Chikungunya virus (CHIKV) infection requiring intensive care, after

an outbreak. Indian J. Pediatr. 77:1326-1328. doi: 10.1007/s12098-010-0174-2; 10.1007/s12098-010-0174-2.

253. Tandale, B. V., P. S. Sathe, V. A. Arankalle, R. S. Wadia, R. Kulkarni, S. V. Shah, S. K. Shah, J. K. Sheth, A. B. Sudeep, A. S. Tripathy, and A. C. Mishra. 2009. Systemic involvements and fatalities during Chikungunya epidemic in India, 2006. J. Clin. Virol. 46:145-149. doi: 10.1016/j.jcv.2009.06.027; 10.1016/j.jcv.2009.06.027.

254. Fuse, K., G. Chan, Y. Liu, P. Gudgeon, M. Husain, M. Chen, W. C. Yeh, S. Akira, and P. P. Liu. 2005. Myeloid differentiation factor-88 plays a crucial role in the pathogenesis of Coxsackievirus B3-induced myocarditis and influences type I interferon production. Circulation. 112:2276-2285. doi: 10.1161/CIRCULATIONAHA.105.536433.

255. Molina, K. M., X. Garcia, S. W. Denfield, Y. Fan, W. R. Morrow, J. A. Towbin, E. A. Frazier, and D. P. Nelson. 2013. Parvovirus b19 myocarditis causes significant morbidity and mortality in children. Pediatr. Cardiol. 34:390-397. doi: 10.1007/s00246-012-0468-4; 10.1007/s00246-012-0468-4.

256. Miller, S. D., Y. Katz-Levy, K. L. Neville, and C. L. Vanderlugt. 2001. Virus-induced autoimmunity: epitope spreading to myelin autoepitopes in Theiler's virus infection of the central nervous system. Adv. Virus Res. 56:199-217.

257. Kyu, B., A. Matsumori, Y. Sato, I. Okada, N. M. Chapman, and S. Tracy. 1992. Cardiac persistence of cardioviral RNA detected by polymerase chain reaction in a murine model of dilated cardiomyopathy. Circulation. 86:522-530.

258. Neu, N., K. W. Beisel, M. D. Traystman, N. R. Rose, and S. W. Craig. 1987. Autoantibodies specific for the cardiac myosin isoform are found in mice susceptible to Coxsackievirus B3-induced myocarditis. J. Immunol. 138:2488-2492.

259. Hanten, J. A., J. P. Vasilakos, C. L. Riter, L. Neys, K. E. Lipson, S. S. Alkan, and W. Birmachu. 2008. Comparison of human B cell activation by TLR7 and TLR9 agonists. BMC Immunol. 9:39-2172-9-39. doi: 10.1186/1471-2172-9-39; 10.1186/1471-2172-9-39.

260. Jeisy-Scott, V., J. H. Kim, W. G. Davis, W. Cao, J. M. Katz, and S. Sambhara. 2012. TLR7 Recognition Is Dispensable for Influenza Virus A Infection but Important for the Induction of Hemagglutinin-Specific Antibodies in Response to the 2009 Pandemic Split Vaccine in Mice. J. Virol. 86:10988-10998. doi: 10.1128/JVI.01064-12.

261. Seo, S. U., H. J. Kwon, J. H. Song, Y. H. Byun, B. L. Seong, T. Kawai, S. Akira, and M. N. Kweon. 2010. MyD88 signaling is indispensable for primary influenza A virus infection but dispensable for secondary infection. J. Virol. 84:12713-12722. doi: 10.1128/JVI.01675-10; 10.1128/JVI.01675-10.

262. Rezza, G., L. Nicoletti, R. Angelini, R. Romi, A. C. Finarelli, M. Panning, P. Cordioli, C. Fortuna, S. Boros, F. Magurano, G. Silvi, P. Angelini, M. Dottori, M. G. Ciufolini, G. C. Majori, A. Cassone, and CHIKV study group. 2007. Infection with chikungunya virus in Italy: an outbreak in a temperate region. Lancet. 370:1840-1846. doi: 10.1016/S0140-6736(07)61779-6.

263. Weaver, S. C., and W. K. Reisen. 2010. Present and future arboviral threats. Antiviral Res. 85:328-345. doi: 10.1016/j.antiviral.2009.10.008; 10.1016/j.antiviral.2009.10.008.

264. Grandadam, M., V. Caro, S. Plumet, J. M. Thiberge, Y. Souares, A. B. Failloux, H. J. Tolou, M. Budelot, D. Cosserat, I. Leparc-Goffart, and P. Despres. 2011. Chikungunya virus, southeastern France. Emerg. Infect. Dis. 17:910-913. doi: 10.3201/eid1705.101873; 10.3201/eid1705.101873.

265. Dupont-Rouzeyrol, M., V. Caro, L. Guillaumot, M. Vazeille, E. D'Ortenzio, J. M. Thiberge, N. Baroux, A. C. Gourinat, M. Grandadam, and A. B. Failloux. 2012. Chikungunya Virus and the Mosquito Vector Aedes aegypti in New Caledonia (South Pacific Region). Vector Borne Zoonotic Dis. 12:1036-1041. doi: 10.1089/vbz.2011.0937; 10.1089/vbz.2011.0937.

266. Daffis, S., M. A. Samuel, M. S. Suthar, M. Gale Jr, and M. S. Diamond. 2008. Toll-like receptor 3 has a protective role against West Nile virus infection. J. Virol. 82:10349-10358. doi: 10.1128/JVI.00935-08; 10.1128/JVI.00935-08.

267. Kurt-Jones, E. A., M. Chan, S. Zhou, J. Wang, G. Reed, R. Bronson, M. M. Arnold, D. M. Knipe, and R. W. Finberg. 2004. Herpes simplex virus 1 interaction with Toll-like receptor 2 contributes to lethal encephalitis. Proc. Natl. Acad. Sci. U. S. A. 101:1315-1320. doi: 10.1073/pnas.0308057100.

268. Le Goffic, R., V. Balloy, M. Lagranderie, L. Alexopoulou, N. Escriou, R. Flavell, M. Chignard, and M. Si-Tahar. 2006. Detrimental contribution of the Toll-like receptor (TLR)3 to influenza A virus-induced acute pneumonia. PLoS Pathog. 2:e53. doi: 10.1371/journal.ppat.0020053.

269. Murawski, M. R., G. N. Bowen, A. M. Cerny, L. J. Anderson, L. M. Haynes, R. A. Tripp, E. A. Kurt-Jones, and R. W. Finberg. 2009. Respiratory syncytial virus activates innate immunity through Toll-like receptor 2. J. Virol. 83:1492-1500. doi: 10.1128/JVI.00671-08; 10.1128/JVI.00671-08.

270. Samuelsson, C., J. Hausmann, H. Lauterbach, M. Schmidt, S. Akira, H. Wagner, P. Chaplin, M. Suter, M. O'Keeffe, and H. Hochrein. 2008. Survival of lethal poxvirus infection in mice depends on TLR9, and therapeutic vaccination provides protection. J. Clin. Invest. 118:1776-1784. doi: 10.1172/JCI33940; 10.1172/JCI33940.

271. Szomolanyi-Tsuda, E., X. Liang, R. M. Welsh, E. A. Kurt-Jones, and R. W. Finberg. 2006. Role for TLR2 in NK cell-mediated control of murine cytomegalovirus in vivo. J. Virol. 80:4286-4291. doi: 10.1128/JVI.80.9.4286-4291.2006.

272. Walsh, K. B., J. R. Teijaro, E. I. Zuniga, M. J. Welch, D. M. Fremgen, S. D. Blackburn, K. F. von Tiehl, E. J. Wherry, R. A. Flavell, and M. B. Oldstone. 2012. Toll-like receptor 7 is required for effective adaptive immune responses that prevent persistent virus infection. Cell. Host Microbe. 11:643-653. doi: 10.1016/j.chom.2012.04.016; 10.1016/j.chom.2012.04.016.

273. Zhu, J., X. Huang, and Y. Yang. 2007. Innate immune response to adenoviral vectors is mediated by both Toll-like receptor-dependent and -independent pathways. J. Virol. 81:3170-3180. doi: 10.1128/JVI.02192-06.

274. Wang, T., T. Town, L. Alexopoulou, J. F. Anderson, E. Fikrig, and R. A. Flavell. 2004. Toll-like receptor 3 mediates West Nile virus entry into the brain causing lethal encephalitis. Nat. Med. 10:1366-1373. doi: 10.1038/nm1140.

275. Zucchini, N., G. Bessou, S. Traub, S. H. Robbins, S. Uematsu, S. Akira, L. Alexopoulou, and M. Dalod. 2008. Cutting edge: Overlapping functions of TLR7 and TLR9 for innate defense against a herpesvirus infection. J. Immunol. 180:5799-5803.

276. Klein Klouwenberg, P., L. Tan, W. Werkman, G. M. van Bleek, and F. Coenjaerts. 2009. The role of Toll-like receptors in regulating the immune response against respiratory syncytial virus. Crit. Rev. Immunol. 29:531-550.

277. Shimizu, T., C. Nishitani, H. Mitsuzawa, S. Ariki, M. Takahashi, K. Ohtani, N. Wakamiya, and Y. Kuroki. 2009. Mannose binding lectin and lung collectins interact with Toll-like receptor 4 and MD-2 by different mechanisms. Biochim. Biophys. Acta. 1790:1705-1710. doi: 10.1016/j.bbagen.2009.10.006; 10.1016/j.bbagen.2009.10.006.

278. Wang, M., Y. Chen, Y. Zhang, L. Zhang, X. Lu, and Z. Chen. 2011. Mannan-binding lectin directly interacts with Toll-like receptor 4 and suppresses lipopolysaccharide-induced inflammatory cytokine secretion from THP-1 cells. Cell. Mol. Immunol. 8:265-275. doi: 10.1038/cmi.2011.1; 10.1038/cmi.2011.1.

279. Haynes, L. M., D. D. Moore, E. A. Kurt-Jones, R. W. Finberg, L. J. Anderson, and R. A. Tripp. 2001. Involvement of toll-like receptor 4 in innate immunity to respiratory syncytial virus. J. Virol. 75:10730-10737. doi: 10.1128/JVI.75.22.10730-10737.2001.

280. Mosoian, A., A. Teixeira, C. S. Burns, L. E. Sander, G. L. Gusella, C. He, J. M. Blander, P. Klotman, and M. E. Klotman. 2010. Prothymosin-alpha inhibits HIV-1

via Toll-like receptor 4-mediated type I interferon induction. Proc. Natl. Acad. Sci. U. S. A. 107:10178-10183. doi: 10.1073/pnas.0914870107.

281. Stoermer, K. A., A. Burrack, L. Oko, S. A. Montgomery, L. B. Borst, R. G. Gill, and T. E. Morrison. 2012. Genetic ablation of arginase 1 in macrophages and neutrophils enhances clearance of an arthritogenic alphavirus. J. Immunol. 189:4047-4059. doi: 10.4049/jimmunol.1201240; 10.4049/jimmunol.1201240.

282. Fischer, M. B., M. Ma, N. C. Hsu, and M. C. Carroll. 1998. Local synthesis of C3 within the splenic lymphoid compartment can reconstitute the impaired immune response in C3-deficient mice. J. Immunol. 160:2619-2625.

283. Verschoor, A., M. A. Brockman, D. M. Knipe, and M. C. Carroll. 2001. Cutting edge: myeloid complement C3 enhances the humoral response to peripheral viral infection. J. Immunol. 167:2446-2451.

284. Kawai, T., and S. Akira. 2010. The role of pattern-recognition receptors in innate immunity: update on Toll-like receptors. Nat. Immunol. 11:373-384. doi: 10.1038/ni.1863; 10.1038/ni.1863.

285. DeFranco, A. L., D. C. Rookhuizen, and B. Hou. 2012. Contribution of Toll-like receptor signaling to germinal center antibody responses. Immunol. Rev. 247:64-72. doi: 10.1111/j.1600-065X.2012.01115.x; 10.1111/j.1600-065X.2012.01115.x.

286. Chao, W. 2009. Toll-like receptor signaling: a critical modulator of cell survival and ischemic injury in the heart. Am. J. Physiol. Heart Circ. Physiol. 296:H1-12. doi: 10.1152/ajpheart.00995.2008; 10.1152/ajpheart.00995.2008.

287. Niederbichler, A. D., L. M. Hoesel, M. V. Westfall, H. Gao, K. R. Ipaktchi, L. Sun, F. S. Zetoune, G. L. Su, S. Arbabi, J. V. Sarma, S. C. Wang, M. R. Hemmila, and P. A. Ward. 2006. An essential role for complement C5a in the pathogenesis of septic cardiac dysfunction. J. Exp. Med. 203:53-61. doi: 10.1084/jem.20051207.

288. Brutsaert, D. L. 2006. Cardiac dysfunction in heart failure: the cardiologist's love affair with time. Prog. Cardiovasc. Dis. 49:157-181. doi: 10.1016/j.pcad.2006.08.010.

289. Nielsen, H., H. Sorensen, V. Faber, and S. E. Svehag. 1978. Circulating immune complexes, complement activation kinetics and serum sickness following treatment with heterologous anti-snake venom globulin. Scand. J. Immunol. 7:25-33.

290. Wouters, D., A. E. Voskuyl, E. T. Molenaar, B. A. Dijkmans, and C. E. Hack. 2006. Evaluation of classical complement pathway activation in rheumatoid arthritis: measurement of C1q-C4 complexes as novel activation products. Arthritis Rheum. 54:1143-1150. doi: 10.1002/art.21729.

291. Zubler, R. H., U. Nydegger, L. H. Perrin, K. Fehr, J. McCormick, P. H. Lambert, and P. A. Miescher. 1976. Circulating and intra-articular immune complexes in patients with rheumatoid arthritis. Correlation of 125I-Clq binding activity with clinical and biological features of the disease. J. Clin. Invest. 57:1308-1319. doi: 10.1172/JCI108399.

292. Sane, J., S. Kurkela, M. L. Lokki, A. Miettinen, T. Helve, A. Vaheri, and O. Vapalahti. 2012. Clinical Sindbis alphavirus infection is associated with HLA-DRB1*01 allele and production of autoantibodies. Clin. Infect. Dis. 55:358-363. doi: 10.1093/cid/cis405; 10.1093/cid/cis405.

293. Castelli, R., A. Zanichelli, M. Cicardi, and M. Cugno. 2013. Acquired C1-inhibitor deficiency and lymphoproliferative disorders: A tight relationship. Crit. Rev. Oncol. Hematol. . doi: 10.1016/j.critrevonc.2013.02.004; 10.1016/j.critrevonc.2013.02.004.

294. Troelsen, L. N., P. Garred, and S. Jacobsen. 2010. Mortality and predictors of mortality in rheumatoid arthritis--a role for mannose-binding lectin? J. Rheumatol. 37:536-543. doi: 10.3899/jrheum.090812; 10.3899/jrheum.090812.

295. Bouquillard, E., and B. Combe. 2009. A report of 21 cases of rheumatoid arthritis following Chikungunya fever. A mean follow-up of two years. Joint Bone Spine. 76:654-657. doi: 10.1016/j.jbspin.2009.08.005; 10.1016/j.jbspin.2009.08.005.

296. Chopra, A., V. Anuradha, V. Lagoo-Joshi, V. Kunjir, S. Salvi, and M. Saluja. 2008. Chikungunya virus aches and pains: an emerging challenge. Arthritis Rheum. 58:2921-2922. doi: 10.1002/art.23753; 10.1002/art.23753.

297. Ganu, M. A., and A. S. Ganu. 2011. Post-chikungunya chronic arthritis--our experience with DMARDs over two year follow up. J. Assoc. Physicians India. 59:83-86.

298. Qing, X., G. C. Koo, and J. E. Salmon. 2012. Complement regulates conventional DC-mediated NK-cell activation by inducing TGF-beta1 in Gr-1+ myeloid cells. Eur. J. Immunol. 42:1723-1734. doi: 10.1002/eji.201142290; 10.1002/eji.201142290.

299. Lucas, K., and M. Maes. 2013. Role of the Toll Like Receptor (TLR) Radical Cycle in Chronic Inflammation: Possible Treatments Targeting the TLR4 Pathway. Mol. Neurobiol. . doi: 10.1007/s12035-013-8425-7.